SAN BRUNO MOUNTAIN WIND INVESTIGATION--
A WIND-TUNNEL MODEL STUDY

by

J. A. Garrison, Assistant Civil Engineer

and

J. E. Cermak, Professor-in-Charge
Fluid Mechanics Program

FLUID MECHANICS PROGRAM
ENGINEERING RESEARCH CENTER
COLLEGE OF ENGINEERING

COLORADO STATE UNIVERSITY
FORT COLLINS, COLORADO

SAN BRUNO MOUNTAIN WIND INVESTIGATION--
A WIND-TUNNEL MODEL STUDY

by

J. A. Garrison, Assistant Civil Engineer

and

J. E. Cermak, Professor-in-Charge
Fluid Mechanics Program

Prepared under contract
with

Metronics Associates, Inc.
3201 Porter Drive
Stanford Industrial Park
Palo Alto, California 94304

for

Wilsey and Ham

Consulting Engineers
1035 East Hillsdale Blvd.
San Mateo, California 94404

Fluid Mechanics Program
Fluid Dynamics and Diffusion Laboratory
College of Engineering
Colorado State University
Fort Collins, Colorado 80521

April 1968 CER67-68JEC-JAG58

ACKNOWLEDGMENTS

The authors wish to acknowledge the many helpful suggestions of Dr. William A. Perkins and Spencer Duckworth.

To Montie Orgill for his patient hours of data reduction, the authors also express their grateful thanks.

TABLE OF CONTENTS

LIST OF TABLES

LIST OF FIGURES

LIST OF OVERLAYS

Note: Overlays to a 1:6000 scale and measuring 2½ x 3 ft are furnished separately with this report - one copy each. Copies 8½ x 11 in. will be bound and issued as a supplement.

LIST OF OVERLAYS - Continued:

Number	Model	Scale	Wind Direction
0-29	E	1:3000	180°
0-30	I	1:3000	180°
0-31	4.0	1:3000	135°
0-32	I	1:3000	135°

SAN BRUNO MOUNTAIN WIND INVESTIGATION --
A WIND TUNNEL STUDY

I. INTRODUCTION

The wind tunnel study of San Bruno Mountain had as its aim the determination of the effect of major topographic modifications on the existing pattern of wind flow and velocities for both winter and summer typical conditions.

San Bruno Mountain is largely undeveloped and is a rugged and largely inaccessible mountain, 1300 feet high, lying to the south and west of the Guadalupe Valley. A spur of the mountain runs along the north side of the valley, (see Fig. 1). At present, the mountain shelters the valley from the cool, moist, marine air which flows in from the ocean in the summer under inversion conditions and significantly moderates summer weather conditions in the valley. The proposed modifications include excavation of the north and northwest facing slope and/or the south slope of the mountain, (See Figs. 2 and 3). Concern has been expressed about the effects of these major modifications upon the present tractable climate in the valley, including the town of Brisbane. Additionally, since the excavated area is to be developed for building sites, the most favorable conditions within the modified areas are to be sought.

During the week of 16 October, Mr. Victor Cromie spent some time observing flows over various structural models mounted in the 1:3000 scale E model excavation. This effort was an attempt to visualize the effect these rather large structures would have on flow structure in the excavation under inversion conditions. The results were qualitative but extremely informative for general planning purposes. No attempt is made to describe these observations in this report.

II. SIMILITUDE REQUIREMENTS

The dominant requirements for similarity of air flow over a topographic complex and a small scale model of the topography must be determined for each specific situation. Considerations which determine the best approximation to exact similarity for the wind are based on the type of topography involved, the model scale (closely related to extent of area to be studied and the wind-tunnel dimensions), the significant thermal regimes encountered in nature, and the types of wind data important to the problem. For the San Bruno Mountain wind investigation, the following significant characteristics must be considered:

1. Topography -- Sharp, well-defined features leading to dominant effects of geometry on flow.
2. Model scale -- Area of importance to be reduced to an area approximately 4 x 4 ft is approximately 24,000 x 24,000 ft giving an optimum scale of 1:6000.
3. Thermal regimes -- Strong neutral flows in winter and elevated inversion-layer flows of marine air in summer are important.
4. Wind data -- The basic data required are the distribution of mean winds.

Requirements for similarity of atmospheric motion in the atmospheric surface layer are established and given in a report by staff of the Fluid Dynamics and Diffusion Laboratory.[1] Specific

---

1 Cermak, J. E., et al: Simulation of Atmospheric Motion by Wind-Tunnel Flows, Task Report, U.S. Army Grant DA-AMC-28-043-G20, Fluid Dynamics and Diffusion Laboratory, Colorado State University, May 1966.

requirements for this study of San Bruno Mountain consistent with the foregoing characteristics are discussed in the following paragraphs.

The fundamental consideration of flow similarity, based on an inspectional analysis of the governing conservation equations (mass, momentum and energy), reveal four categories of similarity which must be accounted for. These categories are usually referred to as follows:

1. Geometrical similarity
2. Dynamic similarity
3. Thermal similarity
4. Boundary condition similarity

A. <u>Geometrical Similarity</u>

Complete geometrical similarity of the model and prototype is assured if a scale model is constructed in which the horizontal and vertical scales are equal. For small scale modeling where the Reynolds numbers cannot be made equal for model and prototype, the vertical scale is sometimes slightly enlarged to produce layer local pressure difference to compensate for the relatively larger viscous forces in the model. The appropriate amount of vertical stretching cannot be determined without comparisons between model and prototype (this is the usual practice in hydraulic modeling of a river system). For a topographic model, the correct degree of distortion would probably be different for different parts of the model. In the San Bruno Mountain, for basic scales of 1:6000 and 1:3000, the difference in elevation (1300 ft maximum in the prototype) greatly exceeds the laminar sub-layer thickness for a turbulent flow over the model; therefore, no vertical exaggeration of the model appears to be necessary. Nevertheless, a slight vertical exaggeration occurred for each model scale used. This resulted from the convenience of using standard thicknesses of plastic sheet to represent actual contour intervals shown on the topographic maps in constructing the model. This distortion resulted in a vertical scale of 1:4800 and a horizontal scale of 1:6000 for the complete model. The partial model had a vertical scale of 1:2400 and a horizontal scale of 1:3000. The exact effect of these distortions is not known; however, the effect on mean velocity distribution should be favorable since the ratio of model Reynolds number to prototype Reynolds number is approximately 1:5000 for the complete model and 1:2500 for the partial model.

B. Dynamic Similarity

The criteria for dynamic similarity are best established by expressing the equation of motion in a non-dimensional form. For our purposes, the following form in which the forces due to density difference produced by thermal stratification and an approximation to the forces produced by turbulent mixing are included is very useful:

$$\overline{U}_j \frac{\partial \overline{U}_i}{\partial X_j} = - \left[\frac{g_o L \overline{\Delta T}_o}{\overline{U}_o^2 \, \overline{T}_o}\right] \frac{\overline{\Delta T}}{\overline{T}_o} g_i + \left[\frac{\nu}{L\overline{U}_o}\right] \frac{\partial^2 \overline{U}_i}{\partial X_j^2} + \left[\frac{K}{L\overline{U}_o}\right] \frac{\partial^2 \overline{U}_i}{\partial X_j^2}$$

In the formulation, the scaling is as follows:

Mean velocity -- $\overline{U}_i = \overline{U}_j'/\overline{U}_o$

Mean temperature -- $\overline{\Delta T} = \overline{\Delta T'}/\overline{T}_o$

Space coordinates -- $X_i = X_i'/L$

Gravitational acceleration -- $g_i = g_i'/g_o$

where a prime denotes dimensional quantities, and an over bar indicates a time average.

From this formulation three criteria for dynamic similarity emerge --

i) Reynolds number $= \dfrac{LU_o}{\nu}$

ii) Turbulent Reynolds number $= \dfrac{LU_o}{K}$

iii) Richardson number $= \dfrac{g_o}{\overline{T}_o} \dfrac{\overline{\Delta T_o}\ L}{\overline{U_o^2}}$

Because of the limited extent of the area, approximately 5 miles in length, Coriolis accelerations were neglected, so that the Rossby number does not appear as a coefficient.

The significance of these criteria relative to the San Bruno Mountain are now considered for the neutral flow regime and the stably stratified regime.

1. Neutral Flow -- For neutral flows, dynamic similarity appears to require equality of the two Reynolds numbers for model and prototype. Of course, the Richardson number will be zero for both model and prototype. Fortunately, the Reynolds number equality for geometry such as San Bruno Mountain (sharp featured geometry) is not an important condition, provided the Reynolds number is in excess of about 10^4. This is because the flow pattern in such cases is dominated by the geometry with the result that forces due to inertia and local pressure differences control rather than the viscous forces. Using a wind speed of 30 ft/sec, a Reynolds number for the 1:6000 scale model is approximately (using the mountain height as L):

$$\frac{\overline{U}_o L}{\nu} = \frac{30}{1.5 \times 10^{-4}} \left(\frac{3}{12} \right) = 5 \times 10^4$$

In this case, the air flowing over the model is turbulent, and the mean flow pattern is dominated by the topographic geometry.

2. Stably Stratified Flow -- For this flow to be dynamically similar, both the Richardson number and the Reynolds number should be equal for model and prototype flows. Examination of the Richardson number reveals that if the model and prototype values are to be essentially equal it is necessary to adjust the model temperature difference and mean reference velocity so that

$$\left(\frac{\overline{\Delta T_o}}{\overline{U_o^2}}\right)_{model} = \left(\frac{\overline{\Delta T_o}}{\overline{U_o^2}}\right)_{prototype} \qquad \frac{L_{prototype}}{L_{model}}$$

or for the 1:6000 scale model

$$\left(\frac{\overline{\Delta T_o}}{\overline{U_o^2}}\right)_{model} = \left(\frac{\overline{\Delta T_o}}{\overline{U_o^2}}\right)_{prototype} \qquad X\ 6000$$

To achieve this relationship, it is, of course, necessary to make $\overline{\Delta T_o}$ between the model as large as possible and $\overline{U_o^2}$ as small as possible. A set of values common to the wind tunnel conditions is $\overline{\Delta T_o} = 30^oC$ and $\overline{U_o^2} = 1\ ft^2/sec^2$.

When the foregoing values of $\overline{\Delta T_o}$ and $\overline{U_o^2}$ are used to achieve near equality of the Richardson number, flow in the wind tunnel becomes laminar while flow over the prototype is turbulent. Under such apparently different flow conditions, what is the degree of similarity for mean wind velocities? Similarity can be approximately achieved, and this may be demonstrated by arguing from the dimensionless form of the equations of motion previously stated. For a laminar flow over the model,

$K=0$, while for a turbulent prototype flow $\nu << K$ and may be neglected; therefore, the appropriate equation for the model is

$$\overline{U_j} \frac{\partial \overline{U_i}}{\partial X_j} = - \left[\frac{g_o L \overline{\Delta T_o}}{\overline{U_o^2} \, \overline{T_o}} \right] \frac{\overline{\Delta T}}{\overline{T_o}} g_i + \left(\frac{\nu}{L\overline{U_o}} \right) \frac{\partial^2 \overline{U_i}}{\partial X^2_j}$$

while for the prototype it is

$$\overline{U_j} \frac{\partial \overline{U_i}}{\partial X_j} = - \left[\frac{g_o L \overline{\Delta T_o}}{\overline{U_o^2} \, \overline{T_o}} \right] \frac{\overline{\Delta T}}{\overline{T_o}} g_i + \left(\frac{k}{L\overline{U_o}} \right) \frac{\partial^2 U_i}{\partial X^2_j}$$

Accordingly, with the two Richardson numbers approximately equal, the mean velocity fields will be approximately equal if

$$\left(\frac{L\overline{U_o}}{\nu} \right)_{model} = \left(\frac{L\overline{U_o}}{K} \right)_{prototype}$$

Thus, the ratio of eddy viscosity, K , to molecular viscosity, ν , for the 1:6000 scale model should be approximately

$$\frac{k}{\nu} = \frac{(L\ \overline{U}_o)_p}{(L\ \overline{U}_o)_m} = 6000 \frac{(\overline{U}_o)_p}{(\overline{U}_o)_m}$$

if the two Reynolds numbers are to be equal. The range of k/ν has been found to vary from 10^3 to 10^5 under different circumstances; therefore, the necessary condition does exist. Probably the best way to understand this correspondence of mean velocity field for a laminar and a turbulent flow is to think of the prototype fluid as being a "sticky" fluid with an average viscosity of K .

C. Thermal Similarity

Criteria for thermal similarity may be derived from examination of the appropriate dimensionless form of the conservation of energy equation. If this is done in the same manner as was done for the equations of motion, while considering that no condensation or evaporation occurs and that all velocities are small compared to the velocity of sound, only two criteria are required from similarity. These are the following:

$$\left(\frac{g_o}{\overline{T}_o} \frac{\overline{\Delta T}_o L}{\overline{U}_o^2}\right)_{model} = \left(\frac{g_o}{\overline{T}_o} \frac{\overline{\Delta T}_o L}{\overline{U}_o^2}\right)_{prototype}$$

and

$$\left(\frac{C_p \nu}{k}\right)_{model} = \left(\frac{C_p \nu}{k}\right)_{prototype}$$

where C_p is the specific heat at constant pressure, ν is the dynamic viscosity and k is the thermal conductivity of the fluid. In other words, the Richardson numbers should be equal in model and prototype, and the Prandtl numbers should be equal for model and prototype. This can be achieved, since the possibility for Richardson number equality has already been demonstrated in the preceding section, and the Prandtl numbers will be equal if air is used for the model flow.

D. Boundary Condition Similarity

For similarity of the mean velocity field, two important conditions of similarity must be placed upon the gross flow field submerging the topography. These boundary conditions are as follows:

a. Flows approaching the topographic area should have similar distributions of velocity and density.

b. The pressure gradient of the ambient flows should be similar.

Similarity of the approach flows is discussed in the following paragraph for the two thermal regimes of interest. The second condition of similarity is met if the pressure gradient of the gross wind-tunnel flow is maintained near zero; i.e., $dp/dx = 0$. This is best accomplished by adjusting the contour of the wind-tunnel ceiling.

For neutral flows, similarity of the approach flow requires that the approaching shear flow have a similar vertical distribution of mean velocity. The best approximation to matching the wind-tunnel approach flow with the prototype approach flow is to develop a turbulent boundary layer which is several times thicker than the height of the topographic features. This can be accomplished easily by using a long test section, roughening the approach surface and/or placing non-uniform grids at the test-section entrance. In this study, the boundary layer thickness for neutral flows of 30 ft/sec was developed "naturally" to a depth of 12 in. over the 18 ft of approach surface.

For stably-stratified flows, the mean velocity distribution and density distribution with height should be made approximately similar for the laboratory and field flows. In the San Bruno Mountain area, summer approach flows of marine air exhibit a characteristic elevated inversion layer. Therefore, a first approximation to similarity for this approach flow requires specification of a height to the bottom of the layer and a representative gross Richardson number to characterize the layer stability. The particular method used in this study to generate the approach flow (generation of a ground based stable shear layer by passing the air over a dry-ice bed and subsequently over an electrically heated surface) resulted in an approach flow with the following gross characteristics:

a. Elevation of inversion base -- 1600 ft (scaled to prototype)

b. Richardson number for a layer above the base equal to the San Bruno Mountain elevation --

$$\frac{g_o}{\overline{T}_o} \frac{\overline{\Delta T}_o}{\overline{U^2_o}} L = \frac{32}{274} \frac{10}{1^2} \frac{1300}{4800} = 0.32$$

From observation of actual flow over San Bruno Mountain and the available data, the foregoing inversion-base elevation and Richardson number appear to represent a typical prototype flow.

In summary, the similarity requirements for neutral flow and stably stratified flow with an elevated inversion base are realizable for a 1:6000 scale model of San Bruno Mountain. The neutral flow modeling for this type of topography is well established and has been successfully used to study flow over such obstacles as Bayview Park hill[1] and the Rock of Gibraltar. The elevated inversion flow has not been simulated in previous model studies; therefore, the simulation techniques developed in this study represent an advance in modeling technique. Modeling of a ground based inversion flow over Pt. Arguello[2] with a laminar flow (scale of 1:12,000) is the only previous successful attempt closely related to the present problem.

---

1 Cermak, J. E., Malhotra, R. C., and Plate, E. J.: Investigation of the Candlestick Park Wind Problem, July 1963, Colorado State University.

2 Cermak, J. E., and Peterka, Jon: Simulation of Wind Fields over Point Arguello, California, by Wind-Tunnel Flow over a Topographic Model, Colorado State University, November 1966.

III. MODELING TECHNIQUES

A. Models

As mentioned above, models were constructed to a scale of 1:6000 horizontally (with a vertical scale of 1:4800) and 1:3000 (with a vertical scale of 1:2400). Areas included in the two models are indicated in Fig. 4. Topographic maps made from recent photogrammetric surveys to a scale of 1:6000 covering all of the San Bruno Mountain and Guadalupe Valley and much of the rest of the area to be modeled were furnished by Wilsey & Ham, Consulting Engineers. To fill in the remainder, the appropriate portions of the USGS San Francisco South Quadrangle, 7.5 minute series topographic map, revision of 1956, was enlarged by using a precision pantograph. Generally good agreement was found at the intersections of the two mappings.

Once the master topographic map of the entire area was made, tracings of each 100 foot contour (each 50 foot contour in the case of the 1:3000 model) were made on regular tracing paper. This paper was fastened to a 1/4 in. thick sheet of styrofoam plastic and guided past a hot wire, cutting both plastic and paper. (A certain amount of skill must be developed with this technique as the plastic tends to shrink away from the hot wire with time and so the cutting must proceed at as nearly a constant speed as possible). These "lifts" were then glued together with a white glue and the whole structure mounted on a 68 in. diameter 1/2 in. plywood disc, cut into equal semi-circular discs for ease in handling. Once the contours were mounted, their edges were shaped with sandpaper until the desired finished surface was produced. The models were built with sections that can be removed and replaced with other sections representing other possible configurations. The models were painted with a black styrofoam paint, and reference lines were marked on their surfaces with 1/16 in. pressure sensitive white tape. A ground plane, representing sea level, was made of 1/2 in. plywood having a 68 in. diameter hole cut in it to permit rotation of the model for differing wind orientation and with the leading edge feathered down to the tunnel floor to afford minimum disturbance to the boundary layer flow. When placed in the tunnel, the ground plane was screwed to the tunnel floor and the leading edge taped with 3/4 in. masking tape to provide a smoother transition. After installation in the tunnel, joints in the model itself were closed with modeling clay.

B. Description of Facility

The testing was done in the Colorado State University low speed wind tunnel which has a test section of 6 ft x 6 ft and 32 ft long. The contraction ratio is 4:1, and air flow powered by a 75 hp variable pitch vaneaxial fan. A 10 ft section of the floor can be heated by individually controlable electric elements beneath the aluminum base, permitting heating of any portion of the plate. Four ft of roughness was placed in the start of the test section to help generate the boundary layer. The center of rotation of the model was placed 21 ft downstream of the start of the test section. A window centered approximately over the model in the ceiling of the tunnel was used in making photographs during testing.

C. Instrumentation

An Equibar Pressure Meter, model 120A, manufactured by Trans-Sonics Inc. of Burlington Mass., was used in conjunction with a United Sensors PBA-12-F-H-K Pitot-Static tube for determining the velocities of the non-density flows in the tunnel. The output from the pressure meter was fed into the "Y" input of an 8 1/2 x 11 in. Moseley "Autograph" X-Y-Y' recorder, Model 136A, and the vertical position of the pitot tube was fed into the "X" input to obtain the vertical velocity distributions above selected points. When a second pressure meter was available, a second pitot tube placed at the beginning of the test section in the free stream, was used simultaneously to monitor the tunnel velocity during the actual taking of the profiles. The second pitot tube was always used to set the tunnel velocity. The probe was positioned with the tunnel carriage which allows traversing vertically or horizontally and which has electrical position readout provisions.

D. Flow Conditioning

It was observed in the first instance of the 1:6000 model being tested in the tunnel with tufts scattered freely about the surface, that while the flow on the upstream slopes was closely similar to observer field conditions, a separation was seen along the crest of the ridge, giving upslope winds on the lee side of the ridge which were not observed on site. While this could be eliminated by reducing the velocity to about 1/3 ft/sec, it was then found that quantitative measurements of these low speeds was very difficult. Some time was spent in an attempt to develop a reliable method of measuring these low velocities by observing the frequencies of the vortex streets shed by cylinders, but it was found that this method was much too lengthy to be of practical use for this study and it was abandoned. In addition, when smoke was injected into the tunnel at these low velocities, some instabilities in the flow were observed, principally a side-to-side meander which would come and go irregularly. This was seen with both the oil smoke which was injected from tubing at higher velocities than the ambient tunnel air and with smoke from $TiCl_4$ which imparted no velocity to the tunnel air.

An attempt was made to simulate an inversion about 100 ft above the crest of the mountain by placing a 4 x 6 ft sheet of clear acrylic plastic in the tunnel supported horizontally by legs along the sides and by a cord in the center, running to the top of the tunnel. Use of this "invisible shield" did improve the flow and permit a higher velocity before separation along the sharp ridge line occurred, but it imposed formidable obstacles on the actual measurement of velocities in the space between the "inversion" and the surface of the model, not to mention the question of the propriety of using such a physical barrier in a situation where similitude is so important. The attempt was abandoned.

Dry ice was placed on the floor of the tunnel upstream of the model to produce a cold, dense layer of "atmosphere" and reduce the tendency for separation along the ridge line. Using dry ice slabs measuring about 10 x 10 x 1 in., an area of about 36 sq ft was covered and the tunnel started. Improvement was noted and, to thicken the cold layer, the dry ice slabs were stood on edge. Further improvement was noted, and it was immediately seen that the edge positioning allowed the frost, which continually forms on the surface of the dry ice, to drop off, thus reducing the tendency for this frost layer to inhibit the release of the CO_2. It was observed that there was a good flow down the test section without the fan running, so a dam was placed upstream of the dry ice bank and the fan shut off. The "fog" of dense, cold air and CO_2 mixed moved down the tunnel at about 1 ft/sec. The final configuration used 500 lbs of dry ice cut into slabs 10 x 10 x 2 in. and stood on edge on wooden planks studded with upright nails to assist in holding the dry ice up. Four planks were used, with the two nearest the model being on the tunnel floor, the next raised about 6 in. and the last raised about 12 in. (see Fig. 5). This arrangement was found to give velocities of about 1 ft/sec and the flow over and around the model of the mountain seemed to duplicate the field conditions so well that density flow induced by gravity alone and without the use of the wind tunnel fan was used for all the stably stratified flows.

In order to obtain the elevated inversion characteristics desired, the floor was heated slightly and the resultant temperature profile developed as shown in Fig. 6. This final configuration gave the desired flow over models of both scales and largely eliminated the bypassing of a major part of the cold vapor around the end of the model, a condition particularly marked with the 1:3000 model.

During work with the dry ice, an exploratory effort was made to obtain CO_2 concentrations at various elevations by drawing a sample from the tunnel 6 in. upstream from the model. The sample of atmosphere was passed through an absorption tube and then weighed. The apparatus used was primitive, slow to operate and the probability of cumulative error large, but the general trend agreed with our prediction. This CO_2 concentration distribution and temperature distribution are shown together in Fig. 7 . A more refined method of determining CO_2 concentrations is clearly indicated by these data.

It should be noted that this effort with the dry ice technique was an exploratory effort undertaken after the start of this project and that it involved an unproven, hitherto untried method. Hence, flow information obtained by this technique represents a step forward in modeling techniques as well as an aid to the study of this particular problem.

E. Visualization Techniques

Since the wind velocity for the density flow regimes was so low, difficulty was experienced in obtaining quantitative values at any given point. However, visualization with smoke proved both simple and effective. Three types of smoke were tried. The first was an oil smoke obtained by heating a heavy oil and injecting it into the tunnel by means of a stream of air. It proved difficult to get enough dense smoke into the tunnel without having the speed of injection rather greater than the tunnel air speed. This, of course, disturbed the air flow conditions. In addition, the oil quickly condensed on the surfaces of the model and tunnel and produced an objectionable atmosphere within the tunnel, and to some degree outside the tunnel as well. Liquid $TiCl_4$ was also used. By dipping the end of a dowel rod in the solution and thrusting it through a hole in the side of the tunnel, the smoke could be accurately located. This method has great utility for spot checking a given location, but has some limitations since the HCl produced is corrosive to the model and to the mechanisms in the tunnel and produces an uncomfortable atmosphere in the tunnel for the experimenter. The third method used required pairs of pins placed at strategic spots on the model. Swabs of cotton were fixed upon the pin heads and one swab innoculated with a drop of concentrated NH_4OH and the other with a drop of concentrated HCl. The resultant plume of NH_4Cl smoke was highly visible for a time and did not contaminate the atmosphere as did the two previous methods. Motion pictures of these plumes were taken from above and the velocities obtained from examination of the films. One serious limitation of this method lies in the time required for the flow conditions to stabilize after being disturbed by the experimenter entering the tunnel to innoculate the swabs. If the motion pictures are taken too soon, the results could be misleading and if the pictures are taken too long a period after innoculation, the plume could be very difficult to see and analyze for its velocity. An additional disadvantage lies in the exothermic nature of the reaction which causes the plumes to tend to rise.

Tufts were used for visualizing the higher velocity neutral flows. The first models were made by glueing a 3/4 in. long piece of white yarn on a glass bead mounted on a pin and held from beneath with a small disk of acetate through which the pin was pushed. These, particularly after being exposed to the oil smoke, developed excessive resistance to turning for many of the locations. The second model used a fine glass tubing cut into about 1/2 in. length, closed at one end and drawn into a conical bearing at the top. The bottom was heated just enough to form a slight annular bulge around the inside of the bottom to provide a stabilizing support when the bearing was set up on a needle. A piece of white nylon thread was tied around the center of the glass and cemented in place with a quick drying cement which was then drawn out along the doubled thread to stiffen it and to prevent the end of the tuft from drooping and catching on the porous surface of the styrofoam model. The flags were cut to about 1 in. length. This produced a very sensitive tuft when mounted with the axis vertical. This took considerable care to do but was important, as gravity could play a most significant part in the interpretation of the wind direction where the winds were light. With the proper side lighting, which proved difficult for some locations because of the rugged terrain, these tufts showed clearly in the motion pictures and color slides and somewhat less clearly in the black and white Polaroid photographs.

In order to prepare the flow diagrams, the motion pictures of the area concerned were projected upon a sheet of tracing paper such that the projected image was the same scale as the 1:6000 map. As the film ran, the individual tufts were marked and the limits of their excursions indicated. Where there was a preferred direction, it was so marked and where continual or alternating circular motion was observed, this was marked also. Because the camera could not be placed so its line of sight was normal to the tunnel floor for all views, some distortions were introduced which made this part of the task most time consuming. Care was exercised in filming so that north on the model was at the top of the picture for all wind directions. These tracings were then used to produce prints on Mylar film to a scale of 1:6000 which can be used directly over the 1:6000 maps to show the location of the tufts, their motion, and the sketched in flow patterns. These overlays 1 through 32 are a part of this report.

IV. DISCUSSION

The wind-flow patterns reveal a close similarity between the 1:6000 and 1:3000 scale models for all three configurations. However, the velocity ratios do not show this same agreement. It is felt that the 1:3000 scale model, because of its significant tunnel blockage and its close proximity to the walls which cause it to behave almost like a two-dimensional model, is generally less reliable for the purposes of this study than the 1:6000 model, and therefore the major effort was put into the collection and reduction of data for the 1:6000 scale model. The configurations modeled and the actual data collected are indicated in Table 1. Inversion flow figures are included in Table 2.

The oroginal plan called for construction of 4.1, 4.2 and 4.3 models of excavation proposals which cut into the ridge line to various degrees and separate the mountain into two parts as well as the 4.0 model of the existing mountain. It was agreed to consider first the 4.0 and 4.3 models as the latter represented the most radical proposal. The 4.3 model was built in the two scales and placed in the tunnel. It was immediately apparent that with wind in the direction range from northwest to south under inversion conditions, that there would be a massive flow of dense air through the gap in the ridge created by the 4.3 excavation and thence down over Brisbane. It was decided to discontinue all work on this model 4.3 in accordance with Dr. Perkins' letter of 18 September. By that time wind tunnel work had been completed on the 4.0, E and the 4.3 models in the 1:6000 scale and velocities had been taken for eight points (See Fig. 8) at a scale elevation of 100 ft for wind directions at 45° intervals around the compass. A copy of these velocities and directions at these points is included in Table 3.

Figures 11 through 29 show the ratio of velocity at any given elevation to the free stream velocity above that point vs elevation for the various locations and for the wind from the north, west and south. These give the best indication of the scale of change to be expected in the wind profiles from the proposed topographic changes. The greatest uncertainty, unfortunately, is at, or very near, the surface of the model. Independence of Reynolds number was verified by taking velocity profiles at location A at different wind speeds and for wind from the south and from the north. See Figures 9 and 10.

The following comments are made about the neutral flow condition and are taken in order counterclockwise from the wind position at North, and will compare models E and I to the 4.0 model of the existing terrain. Differences in identified locations will then be mentioned.

With the wind from the north, little difference can be seen in either E or I , except for some evidence of turbulence in the excavated portion of the I model on the south side of the mountain.

With a northwest wind, the E model shows less upslope wind in the great excavated area, presumably because the finger ridges that cause the channeling have been removed.

With the wind from the west, the conditions at the west end of the I excavation on the south side of the mountain are turbulent and sheltered, while the flow in the east end of this excavation is more clearly defined and of a higher velocity.

With the wind from the southwest, there is little difference between the models except that turbulence in the great excavation of the E model is clearly seen, increasing as positions near the base of the mountain are investigated. Some turbulence is also seen in the I excavation on the south side of the mountain and a possible suggestion of vortex formation toward the west end of this excavation.

With the wind from the south, there is little change evident for model E or I when compared to the 4.0, though there appears to be slightly more turbulence in the I excavation on the south side of the mountain.

With the wind from the southeast, again there seems to be little or no change in the flow patterns.

In the Brisbane area, there seems to be little change in flow pattern for I or E models compared to 4.0. Velocities seem to be changed, however, as follows: with the wind from the north in the E and I models, the velocity seems about 6% higher; with the wind from the west in the E model, it is about 40% lower; with the wind from the south for the E model, the velocity is approximately 48% lower and in the I model approximately 18% higher.

In the Guadalupe Valley, with the wind from the north in the E model, the wind is only 50% and in the I model 80% of the velocity seen in the 4.0 model. With the wind from the west in the E model, the velocity is only 20% and in the I model is substantially unchanged. With the wind from the south, the velocity in the E model is 23% greater than that seen in the 4.0 model and for I is unchanged.

Because of excessive turbulence with some pronounced vertical components, it is felt that measurements made at the Quarry location are of little value.

At KNBC and location A , the velocities and patterns are substantially the same with all models in all the testing, as was hoped for when these locations were chosen.

At location B with the wind from the north in the I model, the velocity is found to be 50% that of the 4.0 model. With the wind from the south, the velocity is found to be 80% greater than that seen in the 4.0 model.

At location C , with the wind from the north in the I model, the velocity is found to be only 10% that seen in the 4.0 model.

Bearing in mind that coupled to the uncertainty of the actual determination of velocity at any given point is the difficulty of finding with accuracy the elevation above that point and this in a region where the velocity changes rapidly with elevation, the reader will realize that the foregoing figures represent little until they exceed at least 25%, and even then represent trends only, not absolute values.

More information can be gained about the elevated inversion flow from repeated viewings of the movies than from anything written. However, there are some statements that can be made.

This "density" flow behaves somewhat as water would in flowing over rough terrain. The cold, dense gas builds up against the dam formed by the mountain, with some finding its way around the ends, comes over the lower areas of the ridges and pours down the far side, following the gulleys and impacting on the outside of curved restraints and even simulates the hydraulic jump when the flow exceeds a certain minimum. With the first viewing, it would appear that in the E model with this elevated inversion flow approaching from the west, there is a tremendous "waterfall" effect down the slope of the excavation with a well-defined "hydraulic" jump a short way out from the bottom of the slope. However, by examining the films repeatedly for the 4.0 model under the same conditions, a very similar pattern is seen, although the rough terrain tends to hide much of it and the lighting is far more difficult. No doubt the flow in the E model down the slope, being virtually unimpeded, is somewhat faster than that seen in the 4.0, but the difference is not as large as was first thought.

On a quantitative basis, it does appear that the excavation of the E model for the elevated inversion regime does increase the velocities slightly at Guadalupe and Brisbane with the flow from the northwest and west. The I model seems to show little change in any flow direction. See Table 2.

V. SUMMARY OF FINDINGS

1. Sufficiently good similarity was achieved with the 1:6000 scale model for both the neutral and elevated inversion flows to give accurate mean flow distributions for the different topographic modifications considered.

2. For both neutral flows and elevated inversion flows the mean flow patterns are substantially unmodified relative to flows over the existing topography (model 4.0) for all configurations in which the ridge line is unaltered excepting within regions where excavations are made.

3. For neutral flows within the wind-direction range southeast to west, flow velocities within the E excavation are less intense than for the I excavation.

4. Elevated-inversion flows within the wind-direction range south to west cause flows within the E excavation which are not substantially different than those for the unmodified topography over the region where the E excavation is made.

TABLE 1 CONFIGURATIONS TESTED AND TYPE OF DATA OBTAINED

Model Configuration			Type of Data					
			Density flow Movie	Neutral Flow				
				Velocity Profiles	U/U_o	Tufts		
Model	Scale	Wind Dir.				Movie	Stills	Overlay
4.0	1:6000	360°		x	x	x	x	x
		315°	x	x		x	x	x
		270°	x	x	x	x	x	x
		225°	x	x		x	x	x
		180°		x	x	x	x	x
		135°		x		x	x	x
E	1:6000	360°		x	x	x	x	x
		315°	x	x		x	x	x
		270°	x	x	x	x	x	x
		225°	x	x		x	x	x
		180°		x	x	x	x	x
		135°		x		x	x	x
I	1:6000	360°		x	x	x	x	x
		315°	x	x		x	x	x
		270°	x	x		x	x	x
		225°	x	x		x	x	x
		180°		x	x	x	x	x
		135°		x		x	x	x
4.0	1:3000	360°		x	x	x	x	x
		315°		x		x	x	x
		270°	x	x		x	x	x
		225°		x		x	x	x
		180°		x	x	x	x	x
		135°		x		x	x	x
E	1:3000	360°		x	x	x	x	x
		315°						
		270°	x					
		225°						
		180°		x	x	x	x	x
		135°						
I	1:3000	360°		x	x	x	x	x
		315°		x		x	x	x
		270°	x	x		x	x	x
		225°		x		x	x	x
		180°		x	x	x	x	x
		135°		x		x	x	x

TABLE 2 ELEVATED INVERSION FLOW VELOCITIES - 7 LOCATIONS

Model	Wind (Azimuth)	A	B	C	KNBC	Guad.	Quarry	Brisbane
		Locations / Velocities in ft/sec*						
4.0	315°	0.8			0.7	0.5	0.6	0.5
4.0	315°	0.9			0.5			
E	315°	0.6			0.3	0.4	0.4	0.4
E	315°	0.8			0.7	0.8	1.0	0.8
4.0	315°	0.5	0.4	0.3				
I	315°	0.7	0.5	0.4				0.3
4.0	270°	0.5			1.0	0.5	0.3	0.5
E	270°	0.5			0.7	0.6	0.4	0.4
E	270°	0.5			0.6	0.5	0.5	0.2
4.0	270°	0.5	0.4	0.4				
4.0	270°	0.7	0.7	0.8				0.7
I	270°	0.6	0.5	0.5				0.6
4.0	225°	0.5			0.9	0.6	--	0.6
E	225°	0.5			0.9	0.6	--	0.3
E	225°	0.3			0.4	0.4	--	0.4
4.0	225°	0.5	0.4	0.7				
I	225°	0.4	0.5	0.5				0.7

* The reference wind speed U_o (at a height of 1300 ft) is approximately 1 ft/sec.

TABLE 3 LOCAL WIND DIRECTIONS AND VELOCITIES - MODELS 4.0, 4.3 AND E - 8 LOCATIONS

Point	Wind	Tunnel Speed - 44 ft/sec Model 4.0 Dir.	4.0 Vel.	4.3 Dir.	4.3 Vel.	E Dir.	E Vel.
1	360°	360°	44	360°	44	360°	43
	315	315	40	315	41	315	39
	270	270	37	270	38	270	37
	225	225	39	225	37	225	38
	180	180	45	180	42	180	43
	135	135	46	135	42	135	23
	090	090	27	090	35	090	34
	045	045	44	045	43	045	41
2	360	345	12	360	16	345	13
	315	285	23	300	23	285	20
	270	285	28	300	30	300	32
	225	300	25	270	21	315	27
	180	360	18	105	12	030	9
	135	120	36	135	31	135	42
	090	090	25	095	33	105	33
	045	135	19	135	12	135	13
3	360	045	41	360	32	360	32
	315	315	33	315	31	330	32
	270	270	24	270	24	270	27
	225	285	12	315	5	315	11
	180	075	10	180	23	135	9
	135	145	32	150	35	160	31
	090	090	19	090	20	090	19
	045	045	32	045	32	045	31
4	360	225	7	300	8	225	10
	315	315	9	320	10	315	9
	270	300	28	315	18	315	13
	225	360	12	-	6	030	12
	180	090	20	045	7	090	19
	135	135	24	135	25	135	22
	090	090	23	100	24	090	22
	045	090	12	090	13	075	14
5	360	360	14	315	14	360	17
	315	315	18	315	22	315	20
	270	315	18	315	22	315	15
	225	145	8	315	9	045	13
	180	090	17	100	12	105	13
	135	135	27	135	22	150	29
	090	270	12	255	8	270	13
	045	045	16	145	18	045	15

TABLE 3 LOCAL WIND DIRECTIONS AND VELOCITIES - MODELS 4.0, 4.3 AND E - 8 LOCATIONS - Cont'd.

Point	Wind	Tunnel Speed - 44 ft/sec Model 4.0 Dir.	4.0 Vel.	4.3 Dir.	4.3 Vel.	E Dir.	E Vel.
6	360°	360	34	315	11	360	34
	315	330	31	360	13	330	25
	270	270	39	090	9	270	34
	225	225	36	180	27	225	35
	180	180	35	180	21	210	34
	135	135	35	105	8	045	5
	090	075	34	090	19	075	37
	045	015	30	240	30	045	37
7	360	360	40	360	30	360	42
	315	330	21	315	9	330	14
	270	220	32	270	38	225	32
	225	225	41	225	37	225	40
	180	180	38	180	45	210	40
	135	135	29	135	26	150	19
	090	045	27	090	43	075	39
	045	045	38	045	41	045	40
8	360	360	26	360	24	330	26
	315	315	29	315	29	315	32
	270	285	22	285	22	300	22
	225	225	21	225	22	225	19
	180	165	23	165	19	180	23
	135	135	23	135	29	135	30
	090	090	22	090	22	100	22
	045	360	16	360	11	330	17

Note: These readings were taken at a height of 100 scale feet (1/4 in.) above the surface of the model at the eight points given. The pitot tube was oriented with the local wind as tested by a tuft at the point. The tuft was removed while readings were made so as not to interfere with the air flow.

Fig. 1 Topographic Map of existing terrain

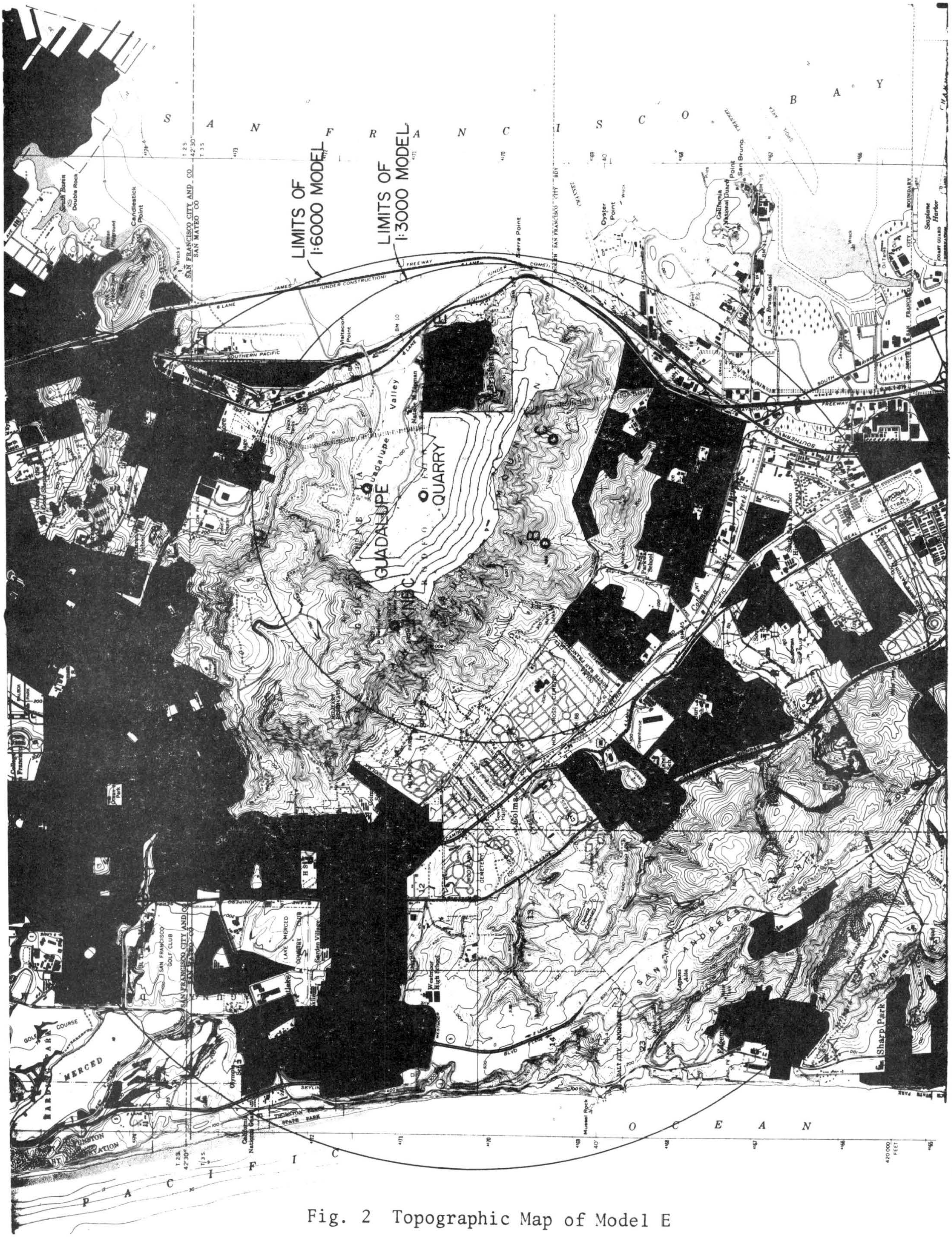

Fig. 2 Topographic Map of Model E

Fig. 3 Topographic Map of Model I

Fig. 4 Topographic Map of area covered

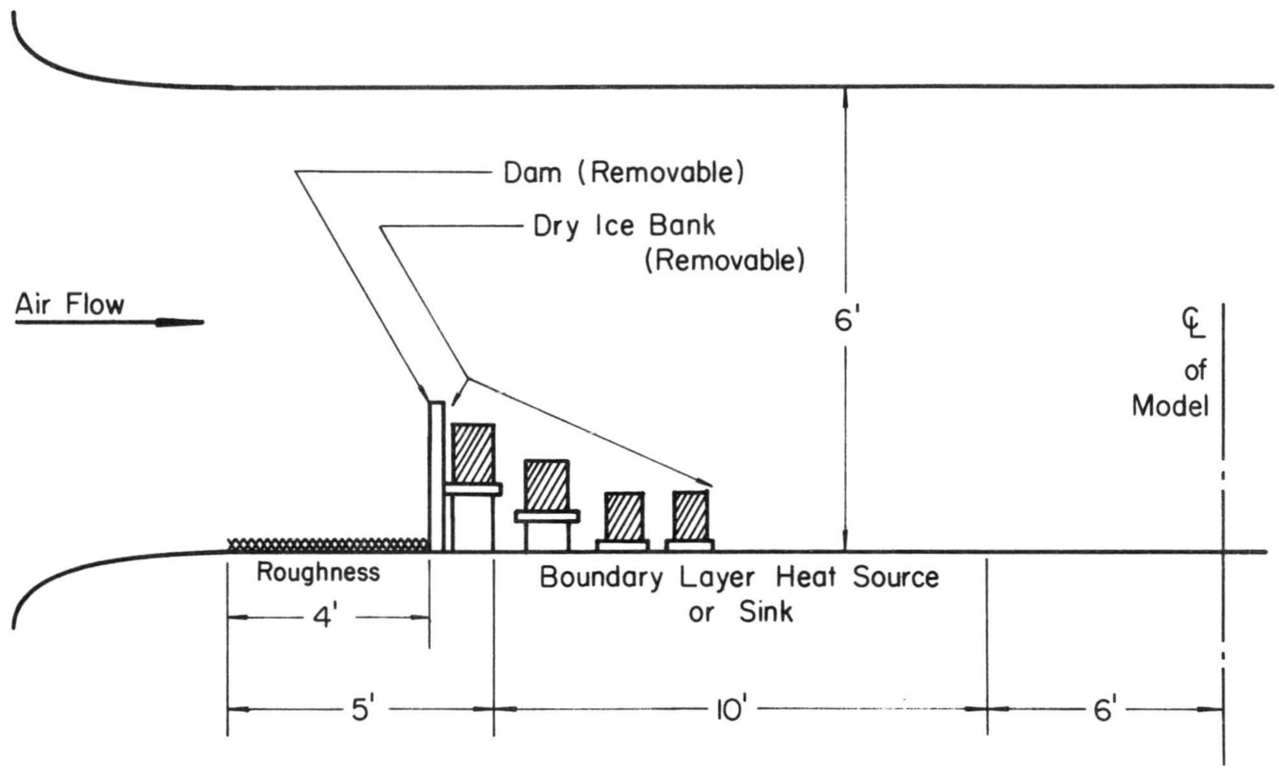

Fig. 5 Arrangement of model in tunnel

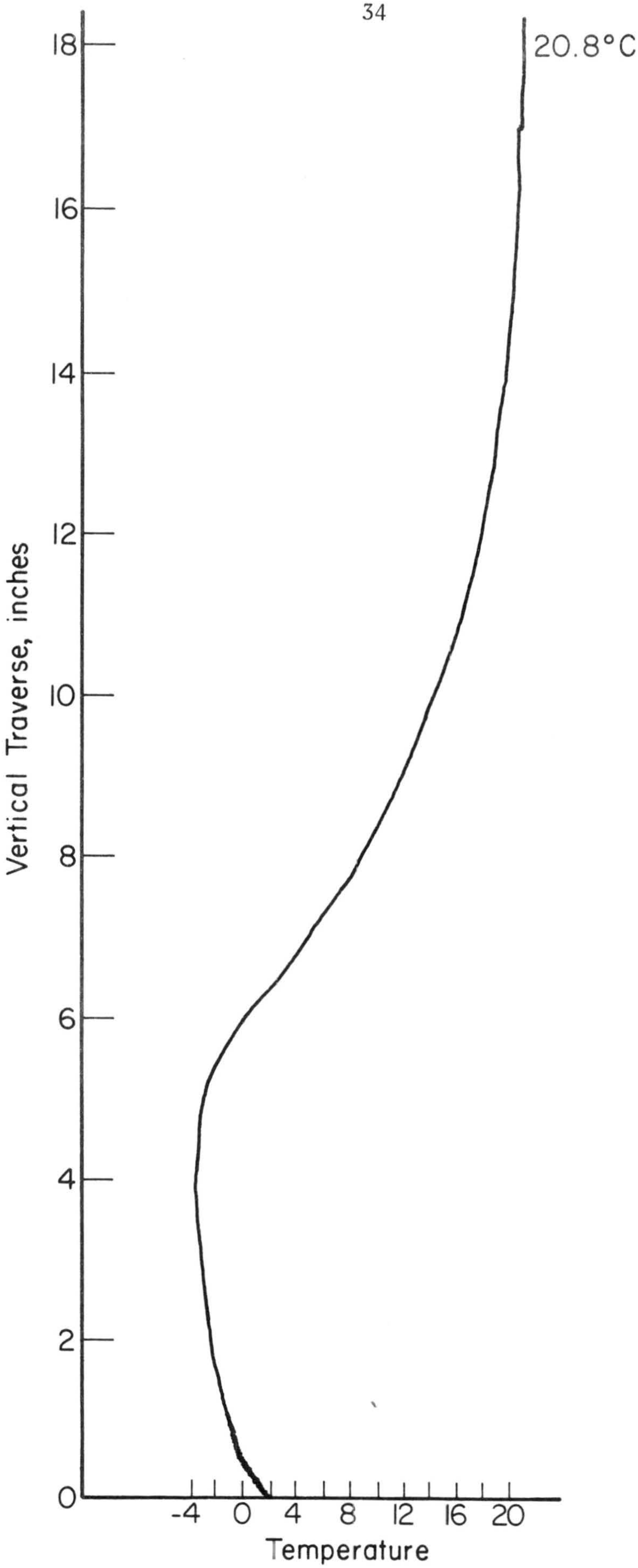

Fig. 6 Temperature profile

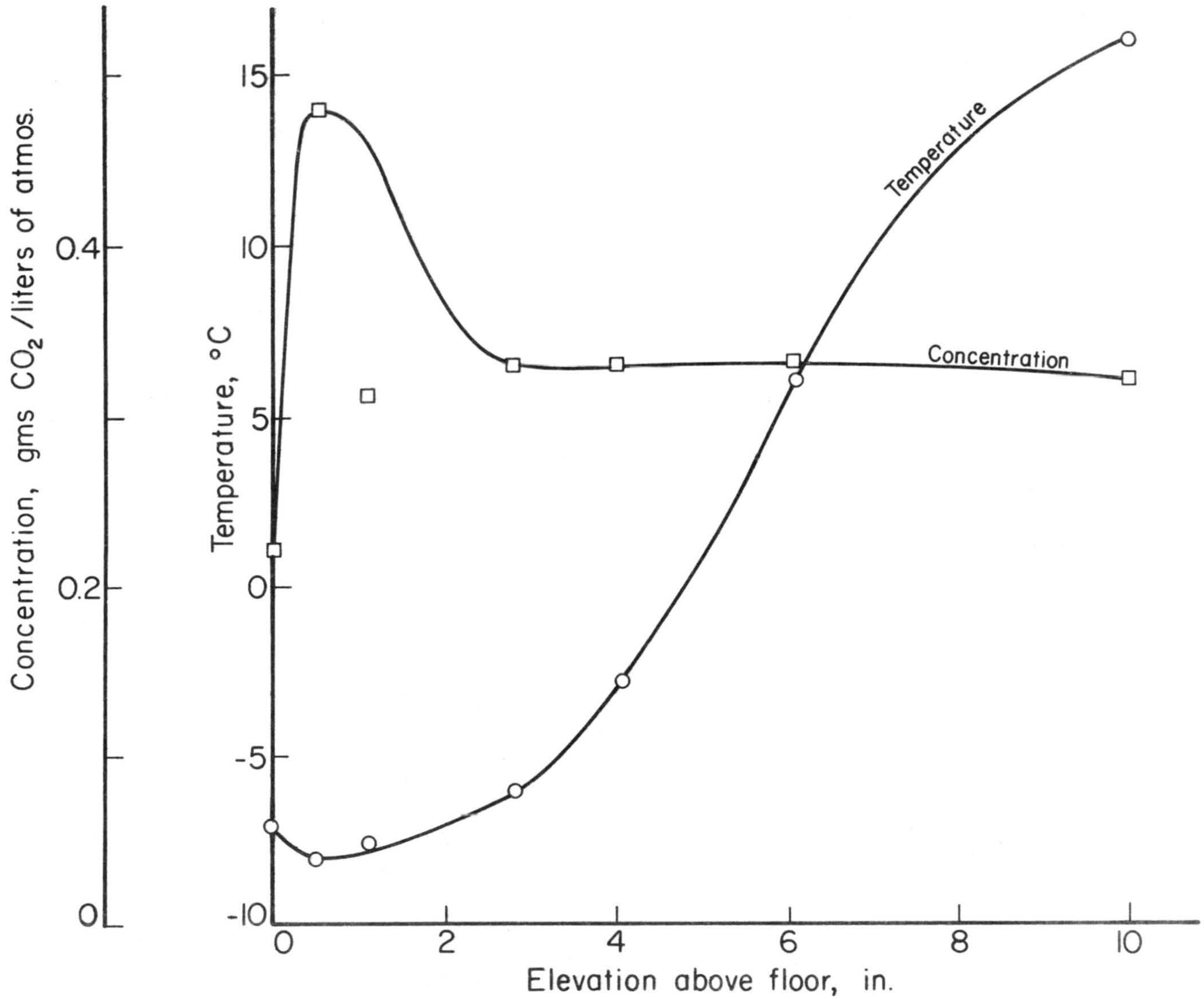

Fig. 7 CO_2 concentration profile

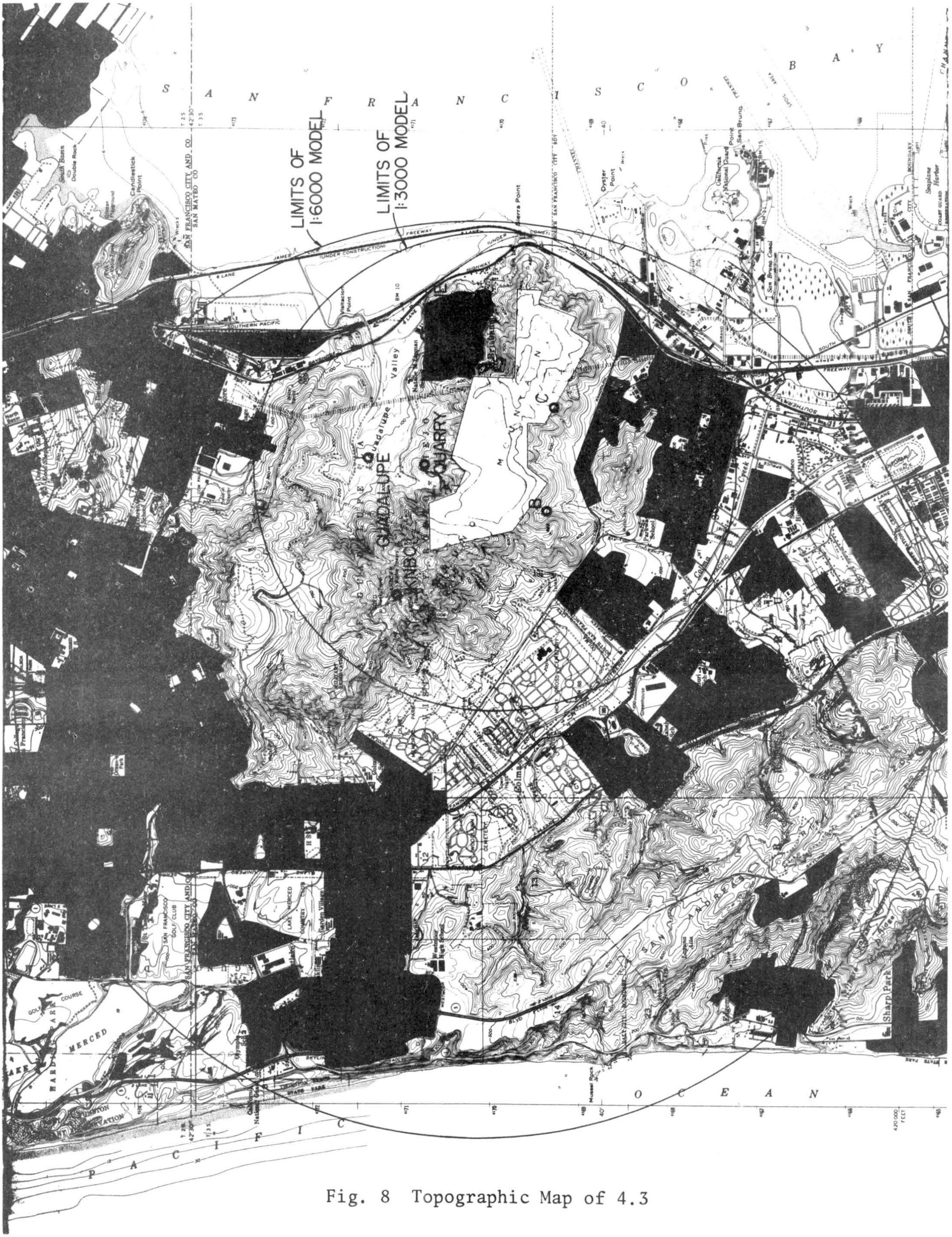

Fig. 8 Topographic Map of 4.3

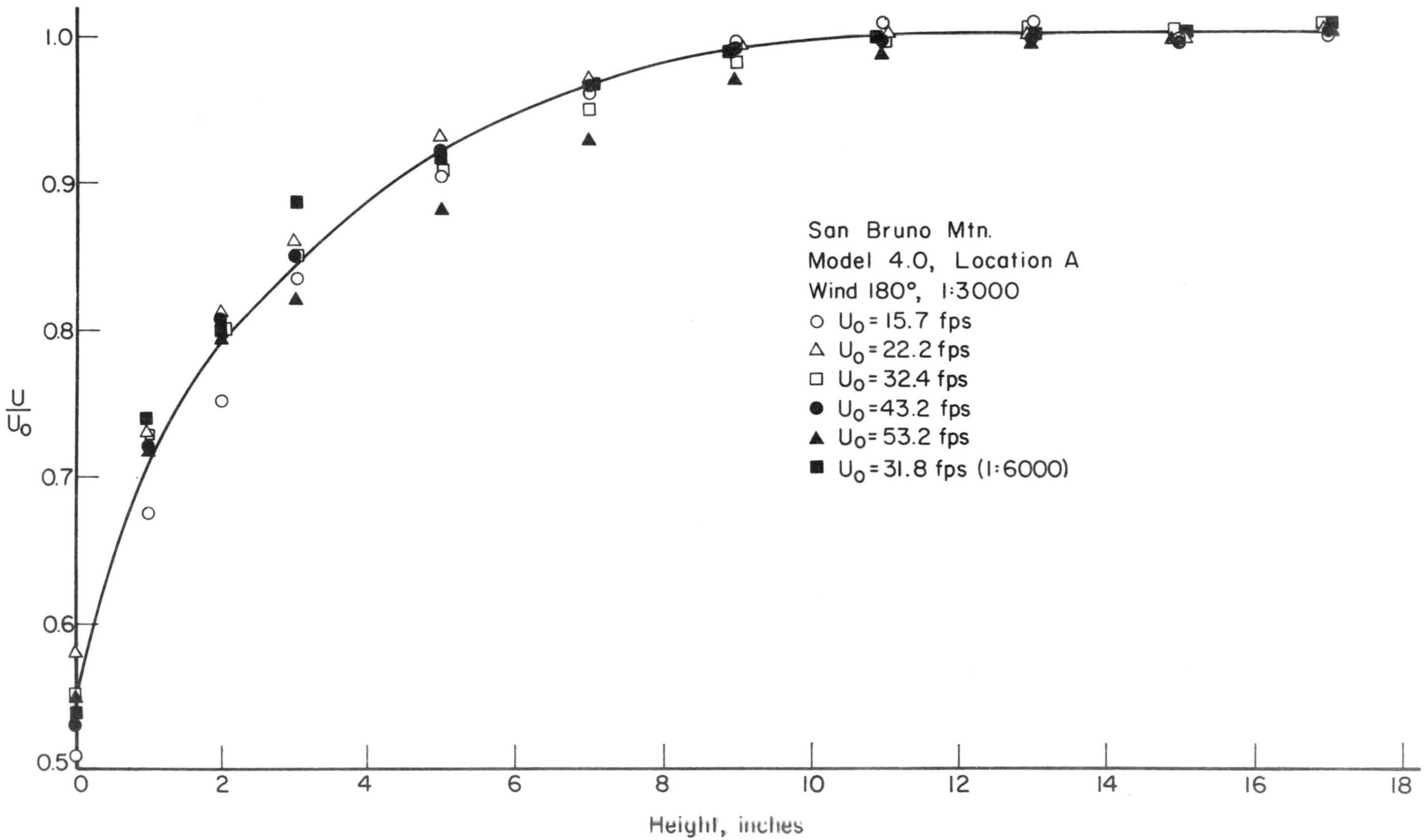

Fig. 9 Independence of Reynolds Number - wind 180°

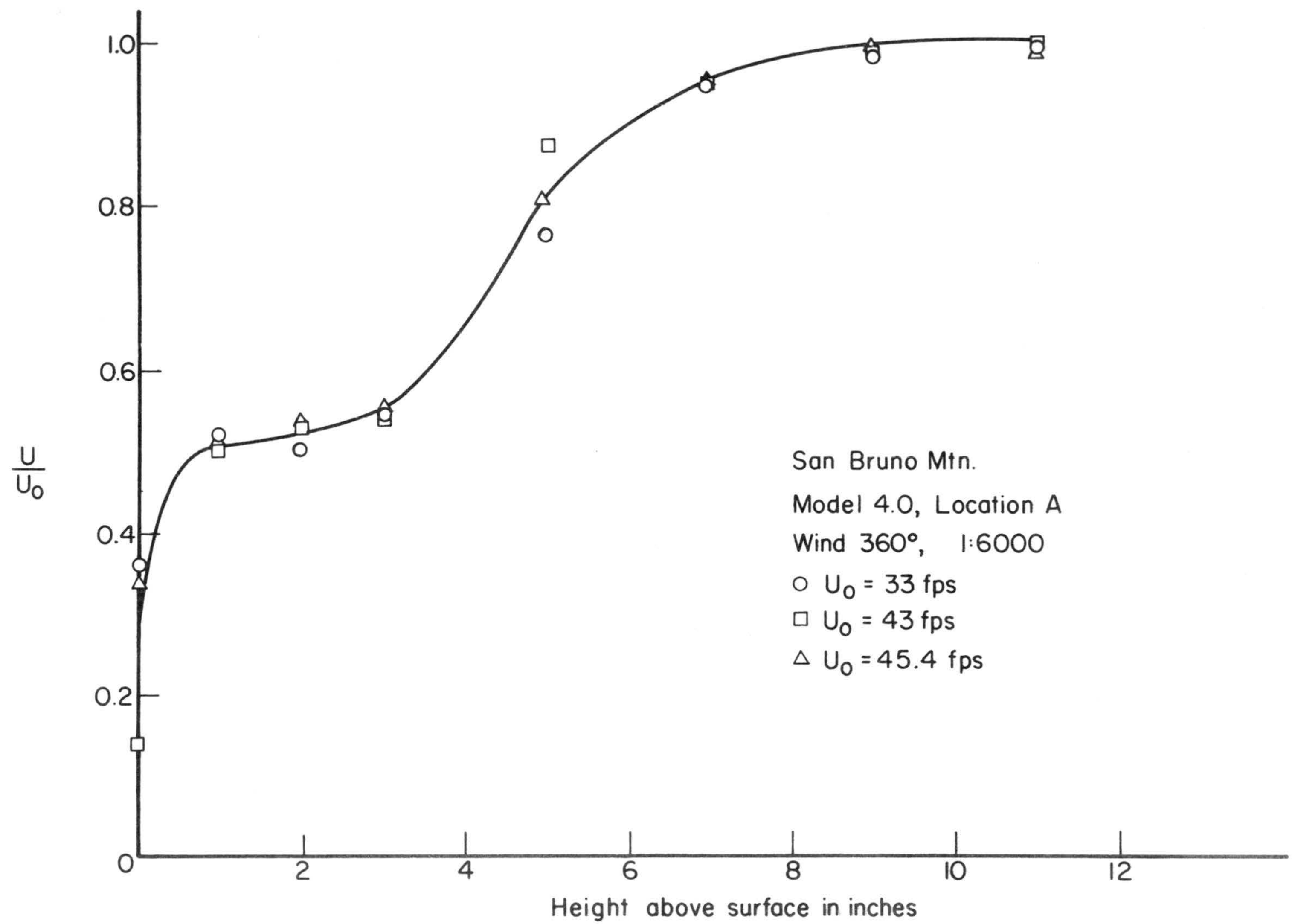

Fig. 10 Independence of Reynolds Number - wind 360°

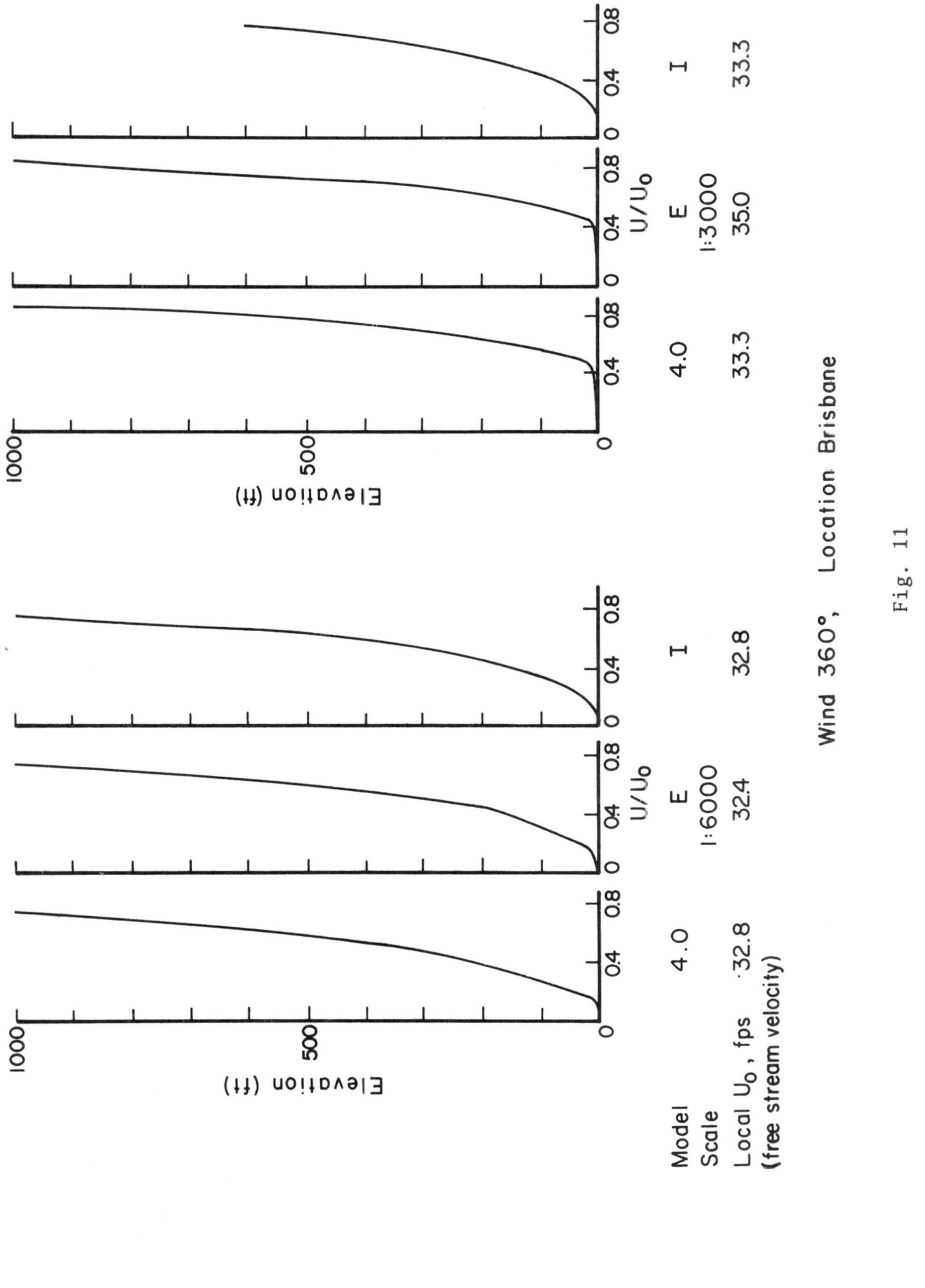
Elevation (ft)
1000
500
0
0.4
0.8
U/U$_0$
Model
Scale
Local U$_0$, fps
(free stream velocity)
4.0
E
1:6000
I
32.8
32.4
32.8
4.0
E
1:3000
I
33.3
35.0
33.3
Wind 360°, Location Brisbane

Fig. 11

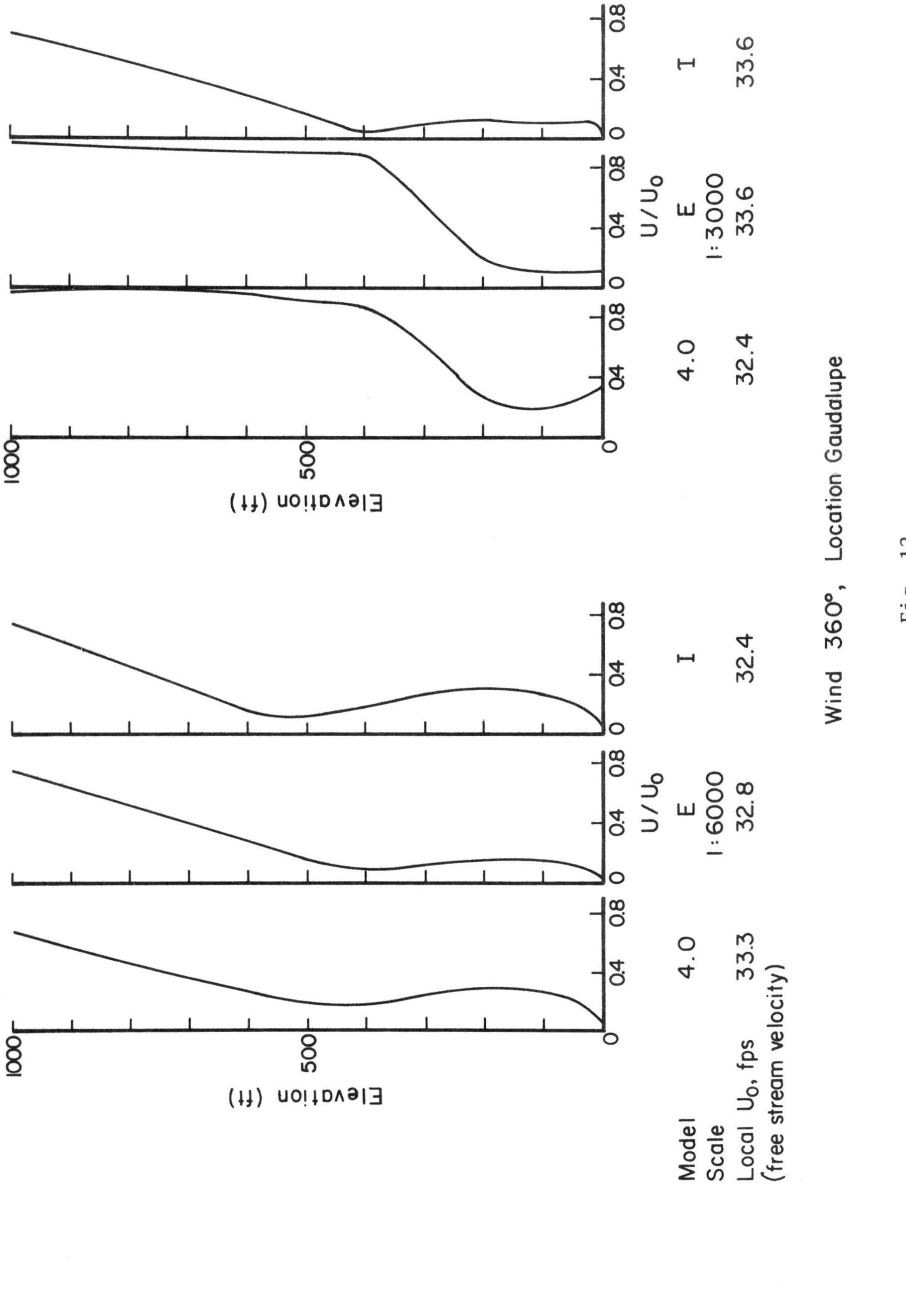

Wind 360°, Location Gaudalupe

Fig. 12

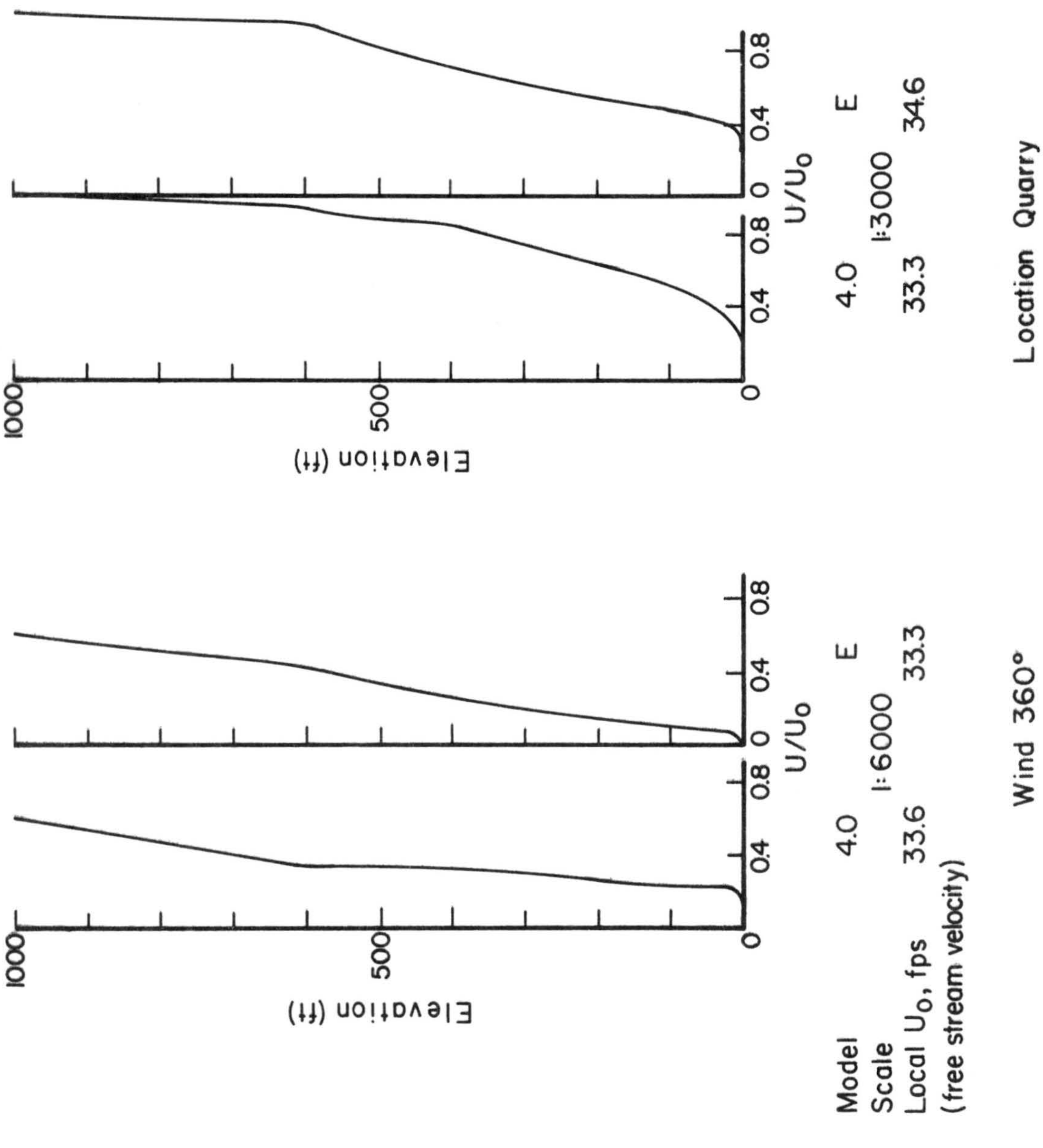
Elevation (ft)
1000
500
0
0.4
0.8
U/Uo
Model 4.0 E
Scale 1:6000
Local Uo, fps 33.6 33.3
(free stream velocity)
Wind 360°
4.0 E
1:3000
33.3 34.6
Location Quarry

Fig. 13

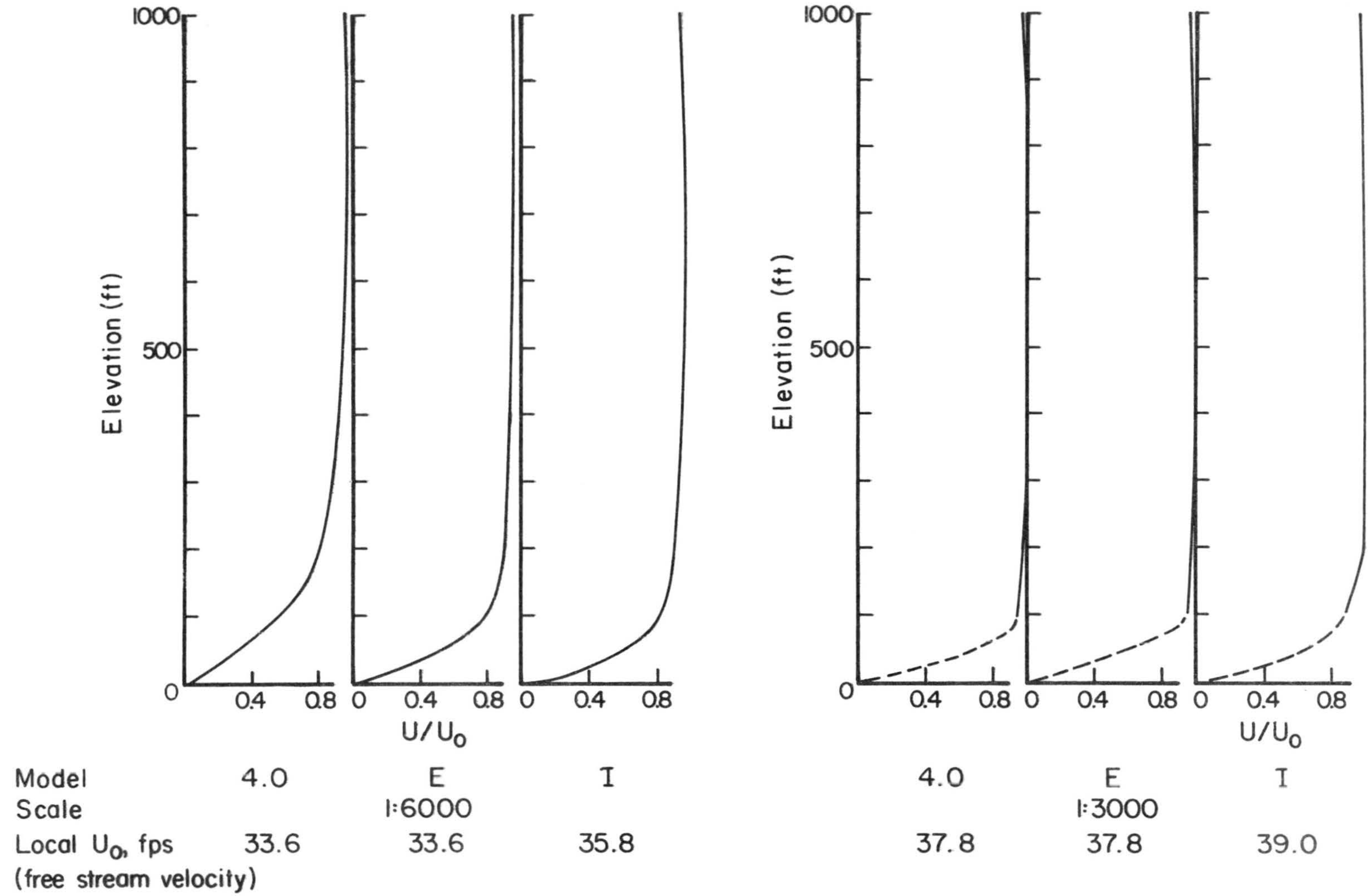

Wind 360°, Location KNBC

Fig. 14

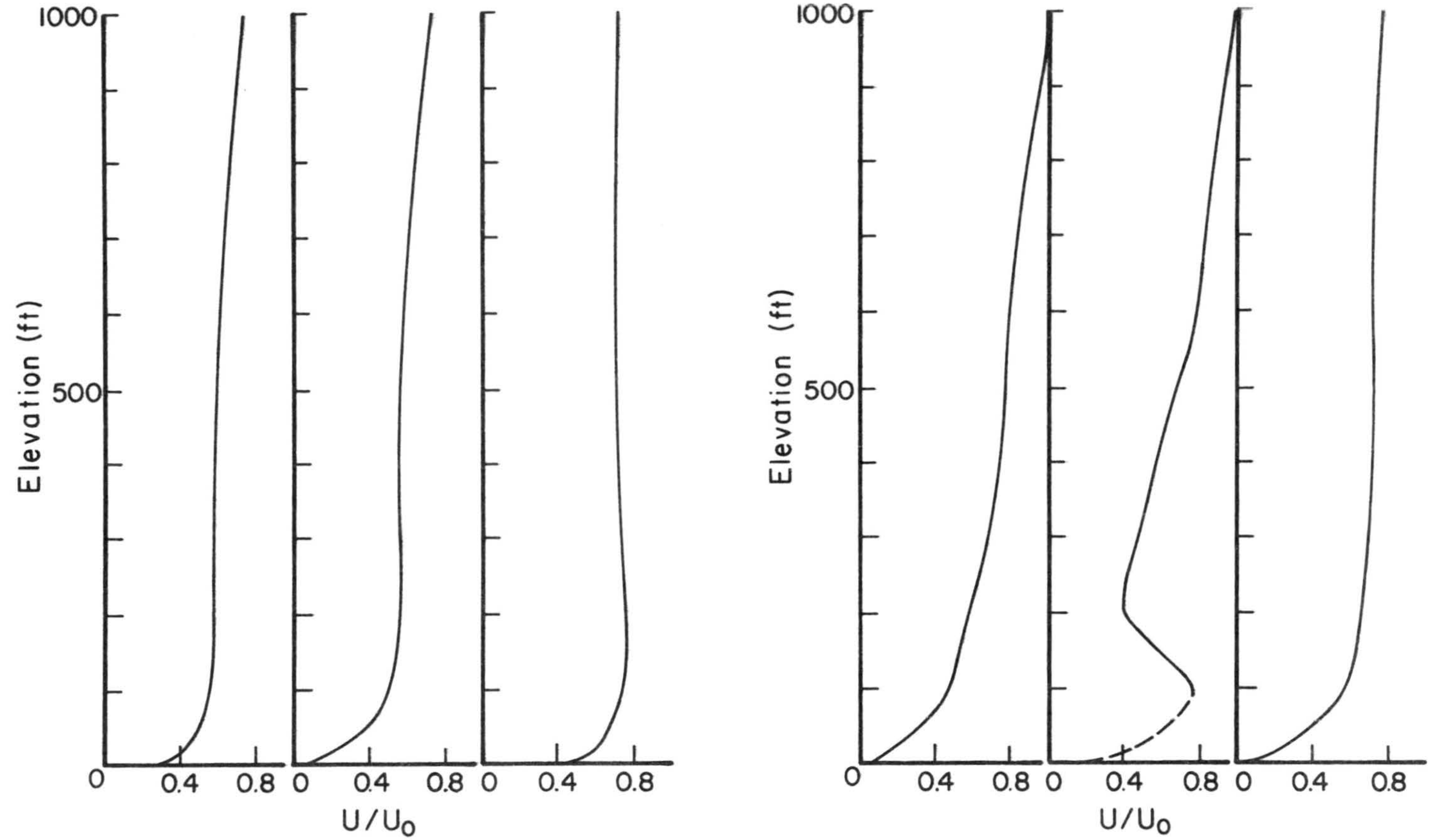

Model	4.0	E	I	4.0	E	I
Scale		1:6000			1:3000	
Local U_0, fps (free stream velocity)	33.3	33.3	33.3	35.8	35.4	35.8

Wind 360° Location A

Fig. 15

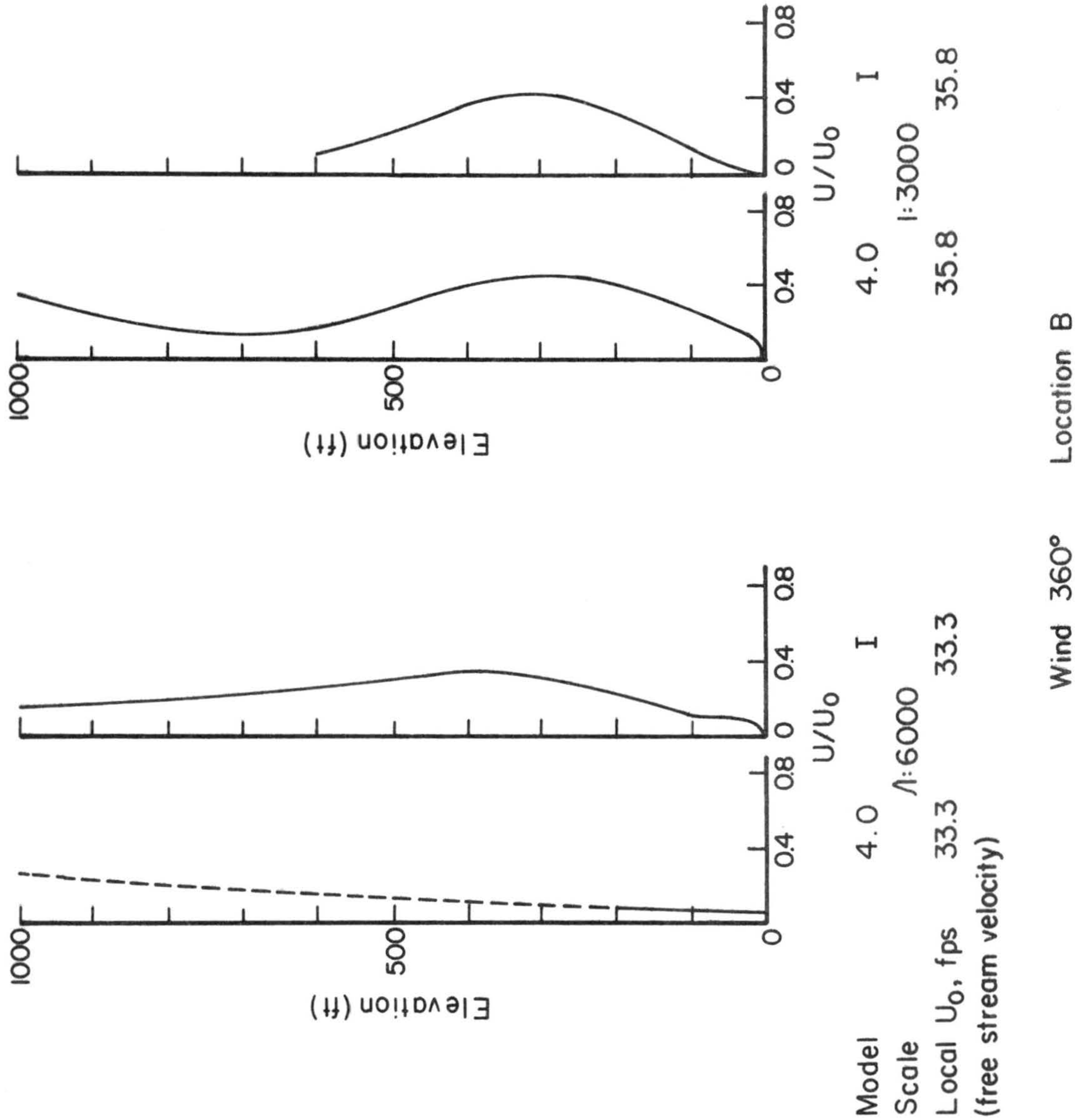
Elevation (ft)
1000
500
0
0.4
0.8
U/U0
Model 4.0 I
Scale 1:6000
Local U0, fps 33.3 33.3
(free stream velocity)
4.0 I
1:3000
35.8 35.8
Wind 360° Location B

Fig. 16

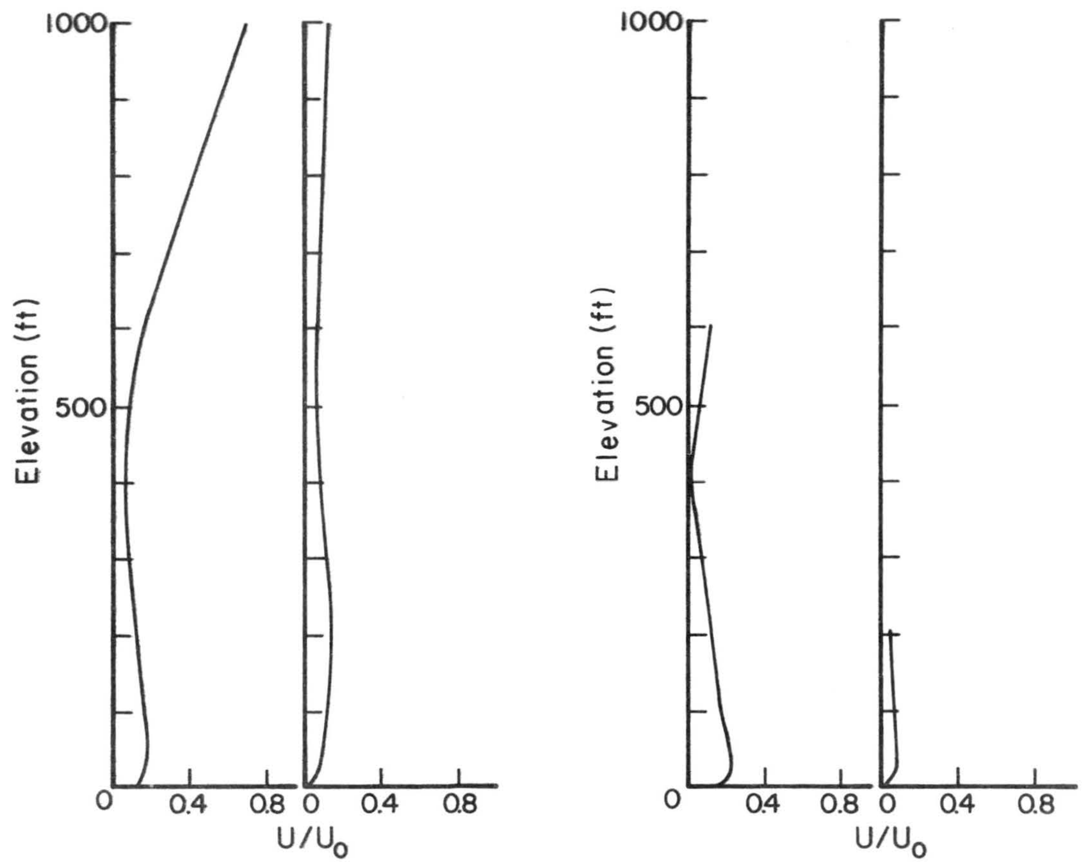

Model	4.0	I	4.0	I
Scale	1:6000		1:3000	
Local U_o, fps (free stream velocity)	33.3	33.3	35.8	35.8

Wind 360° Location C

Fig. 17

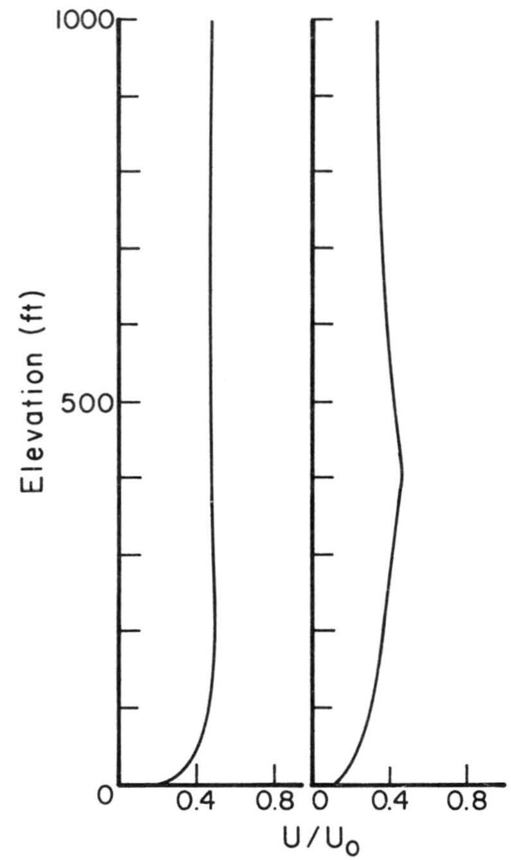

Model	4.0		E
Scale		1:6000	
Local U_0, fps	32.8		31.9
(free stream velocity)			

Wind 270°, Location Brisbane

Fig. 18

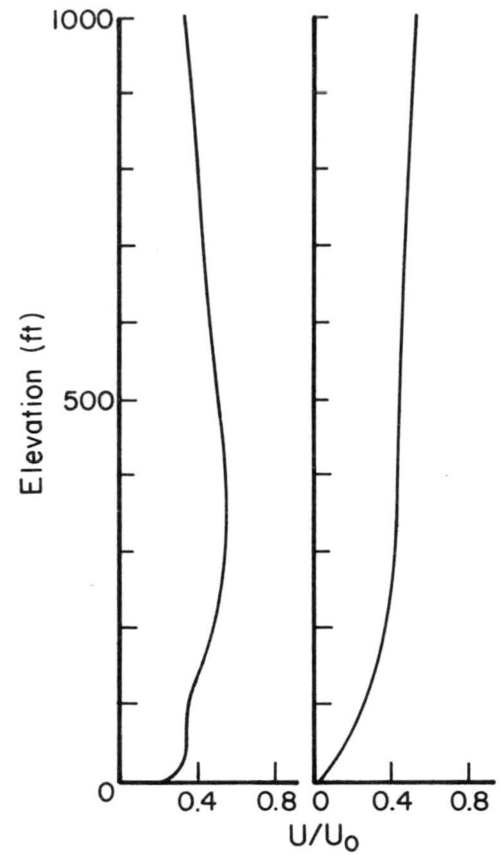

Model	4.0	E
Scale	1:6000	
Local U_0, fps (free stream velocity)	33.3	33.3

Wind 270°, Location Guadalupe

Fig. 19

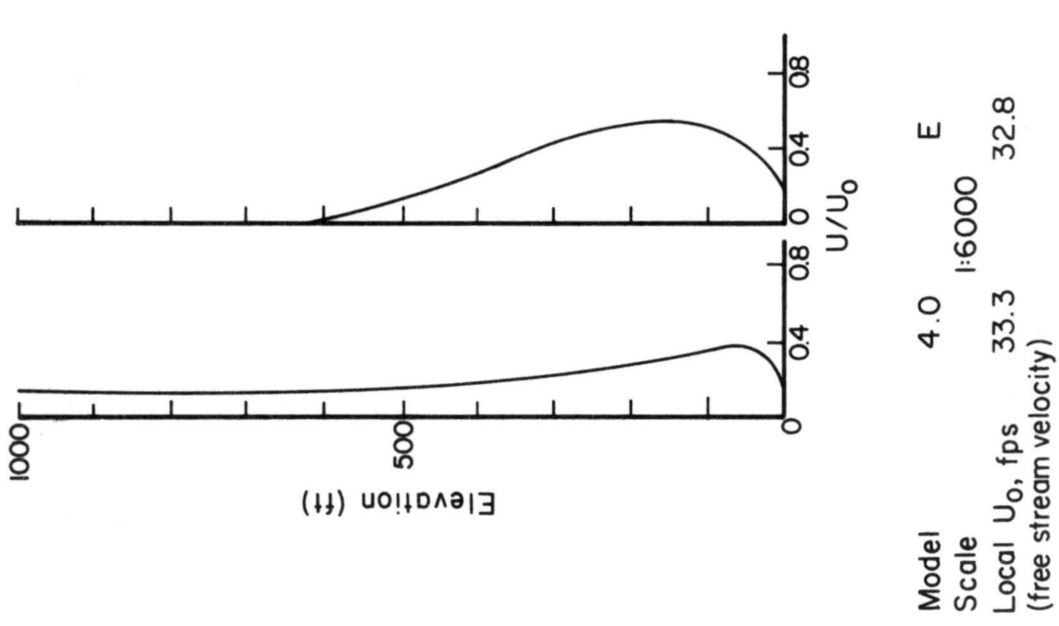

Wind 270°, Location Quarry

Fig. 20

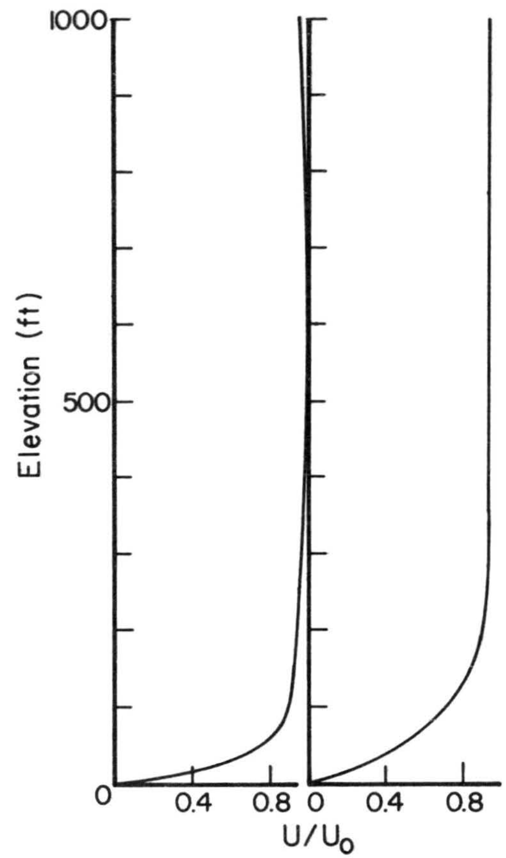

Model	4.0	E
Scale	1:6000	
Local U_0, fps (free stream velocity)	33.3	33.3

Wind 270°, Location KNBC

Fig. 21

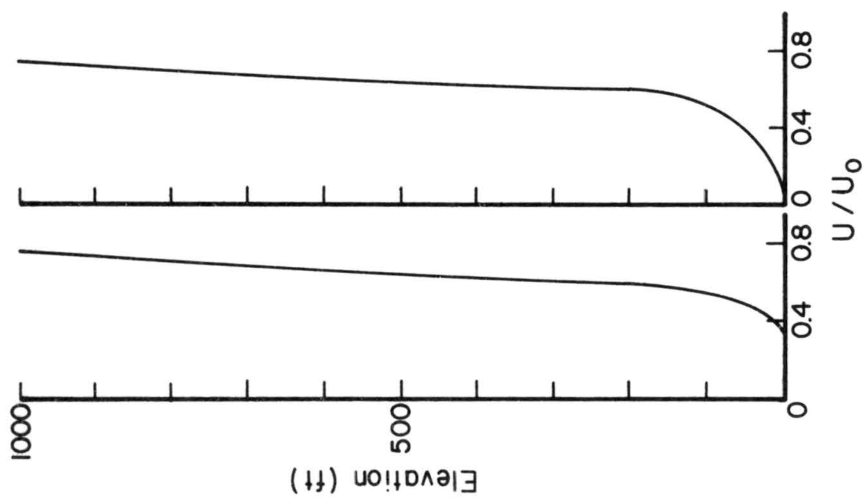

Model	4.0	E
Scale	1:6000	
Local U_0, fps (free stream velocity)	32.8	32.4

Wind 270°, Location A

Fig. 22

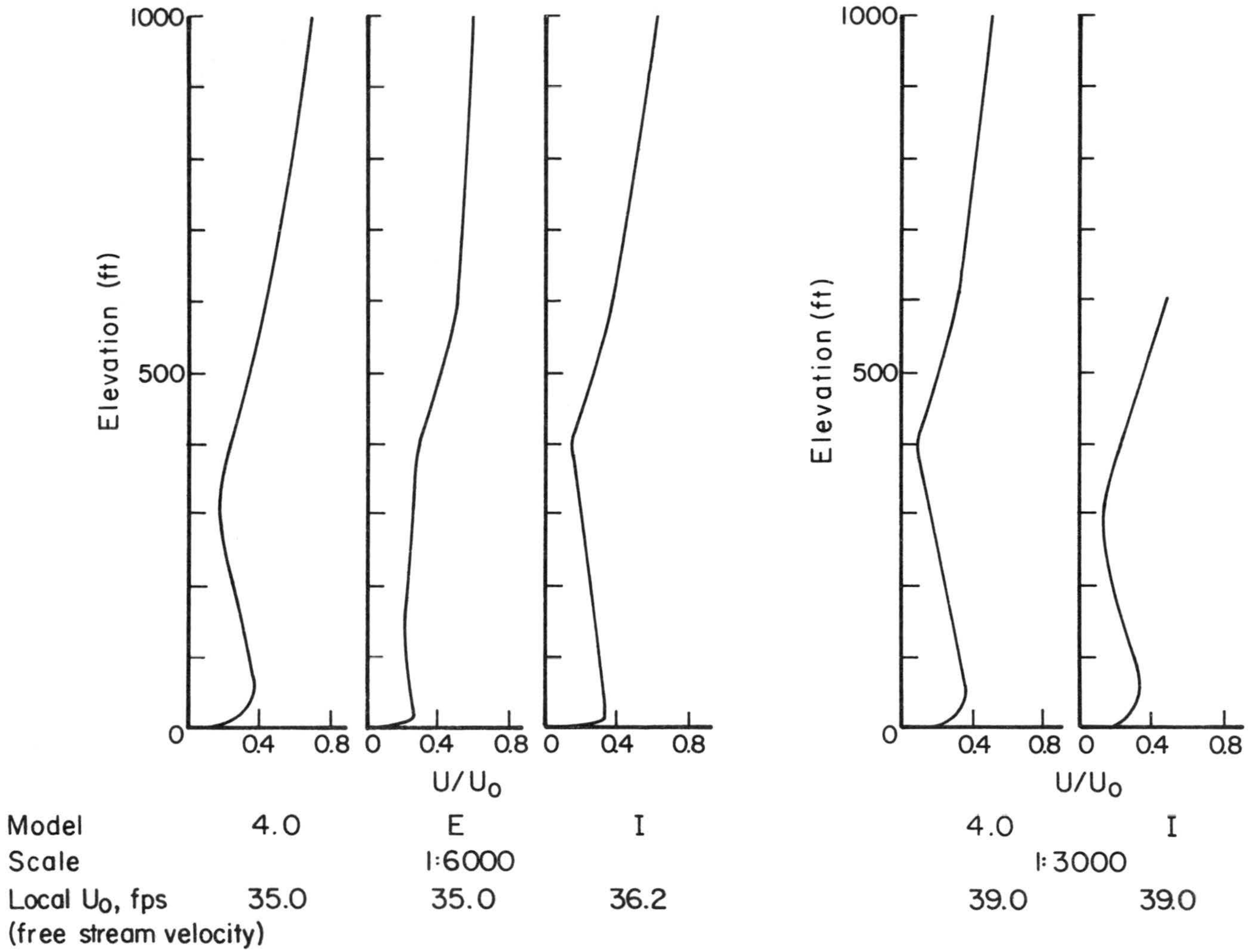

Wind 180°, Location Brisbane

Fig. 23

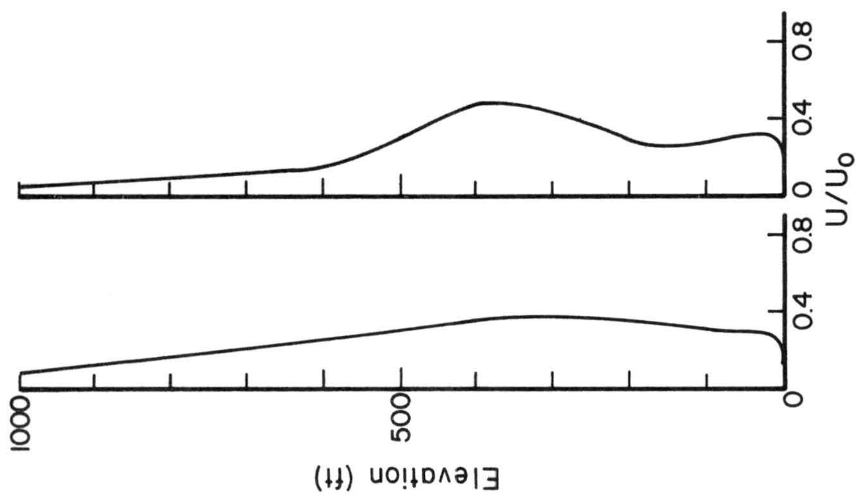

Model	4.0	E
Scale	1:6000	
Local U_o, fps (free stream velocity)	35.0	34.6

Wind 180°, Location Guadalupe

Fig. 24

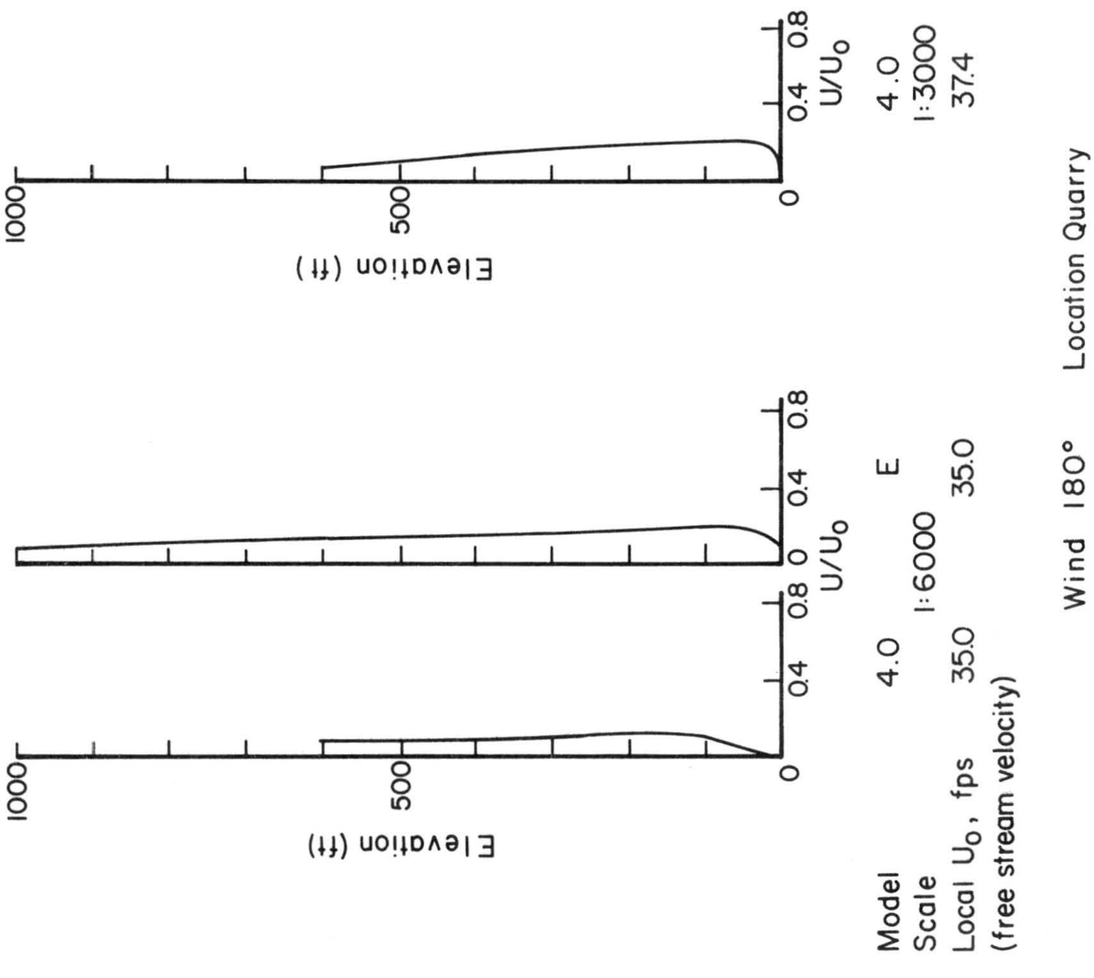
Elevation (ft)
1000
500
0
0.4
0.8
U/U$_o$
Elevation (ft)
1000
500
0
0.4
0.8
U/U$_o$
Model 4.0 E 4.0
Scale 1:6000 1:3000
Local U$_o$, fps 35.0 35.0 37.4
(free stream velocity)
Wind 180° Location Quarry

Fig. 25

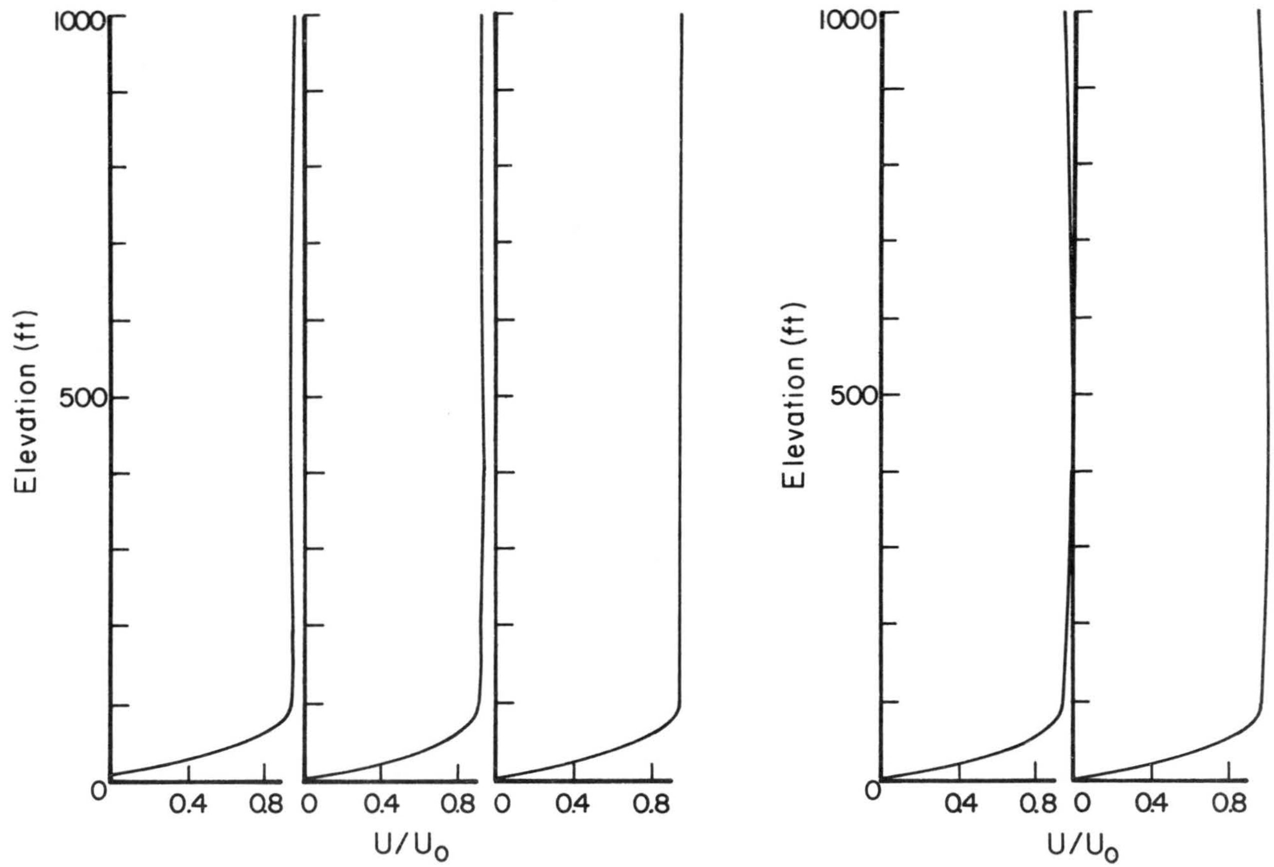

Model	4.0	E	I	4.0	I
Scale		1:6000		1:3000	
Local U_0, fps (free stream velocity)	33.6	33.3	34.2	36.6	37.4

Wind 180° Location KNBC

Fig. 26

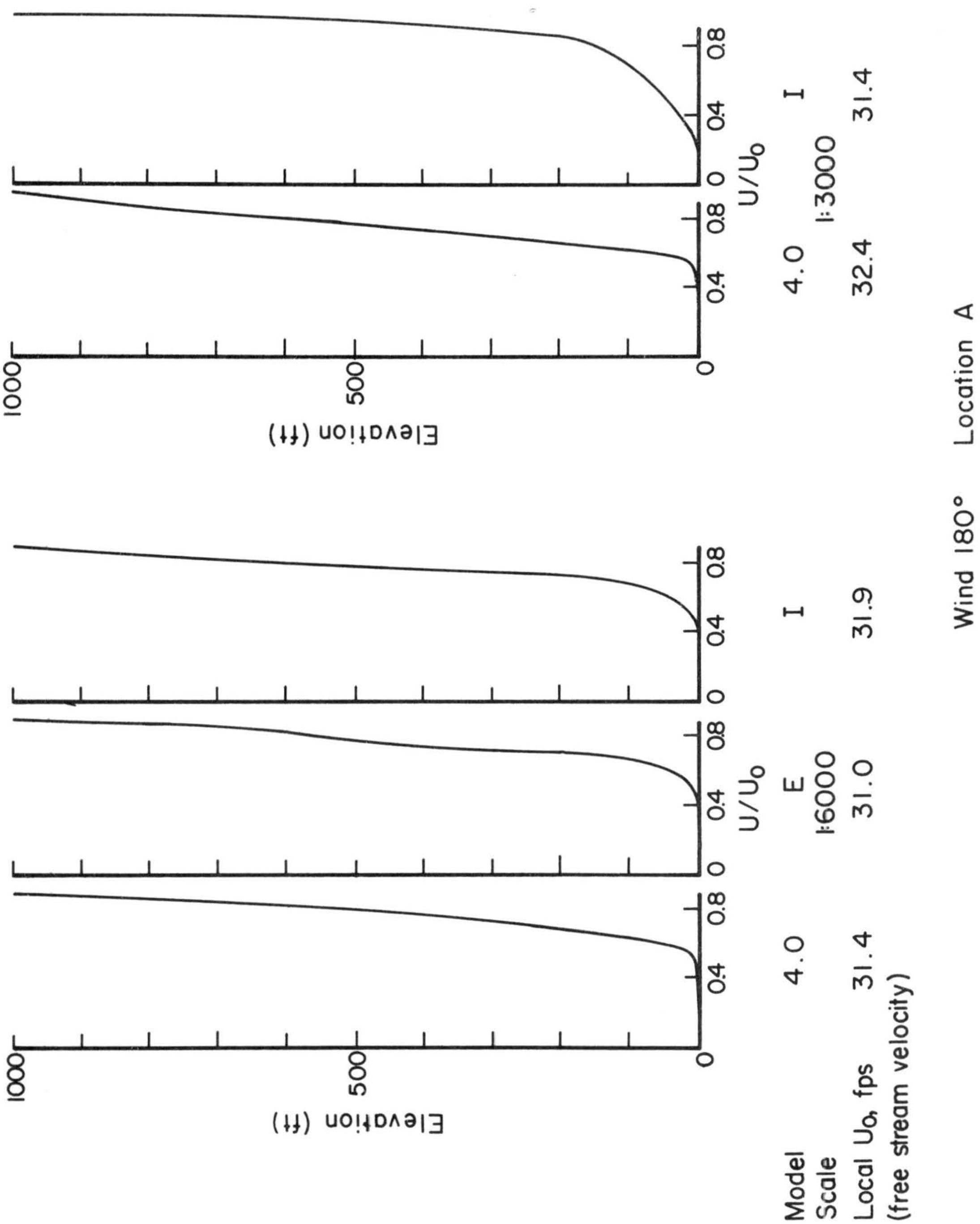
Elevation (ft)
1000
500
0
0
0.4
0.8
U/Uo
Model
4.0
E
I
4.0
I
Scale
1:6000
1:3000
Local Uo, fps
(free stream velocity)
31.4
31.0
31.9
32.4
31.4
Wind 180°
Location A

Fig. 27

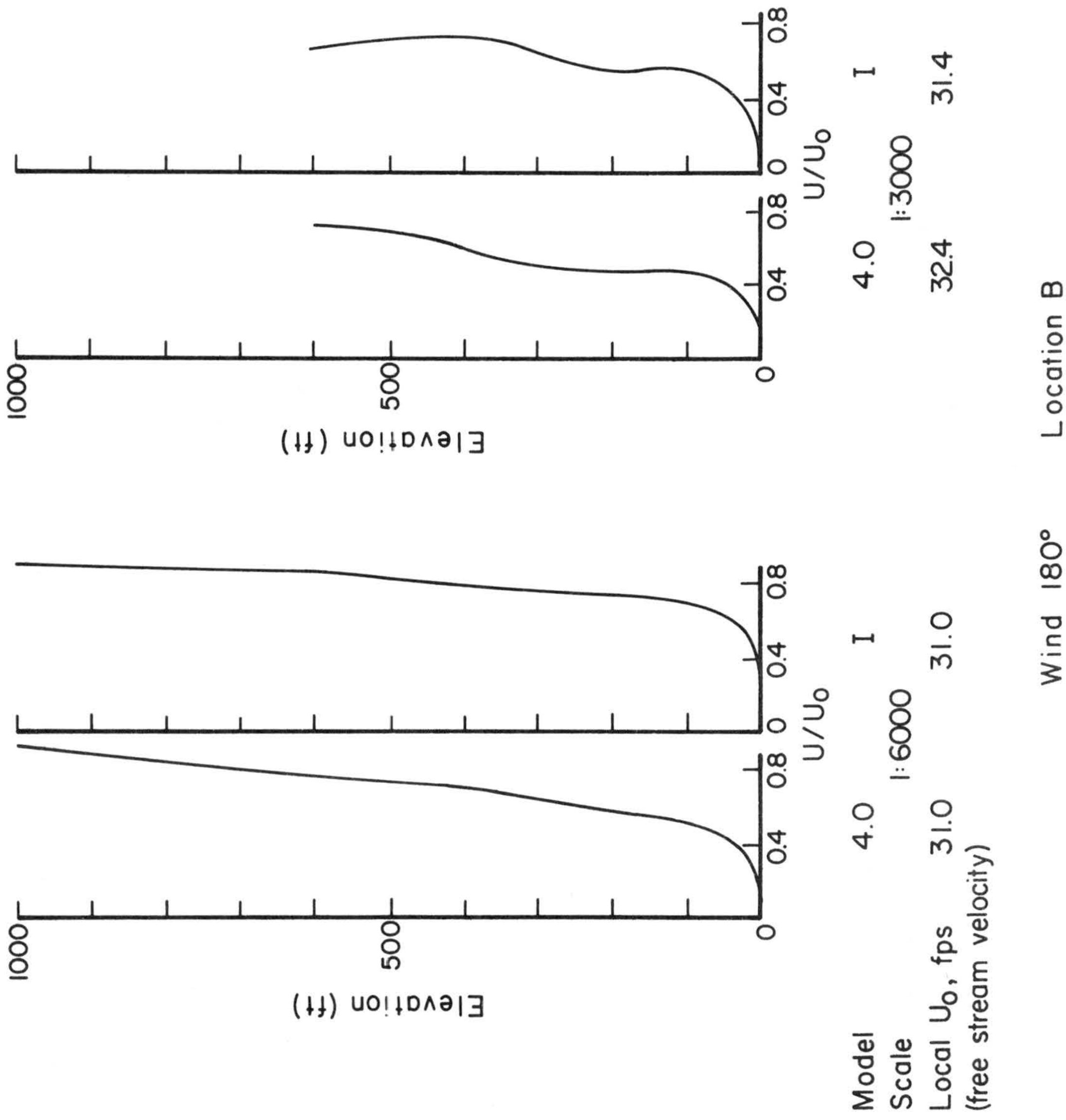
Elevation (ft)
1000
500
0
0.4
0.8
U/U$_o$
Model 4.0 I 4.0 I
Scale 1:6000 1:3000
Local U$_o$, fps 31.0 31.0 32.4 31.4
(free stream velocity)
Wind 180°
Location B

Fig. 28

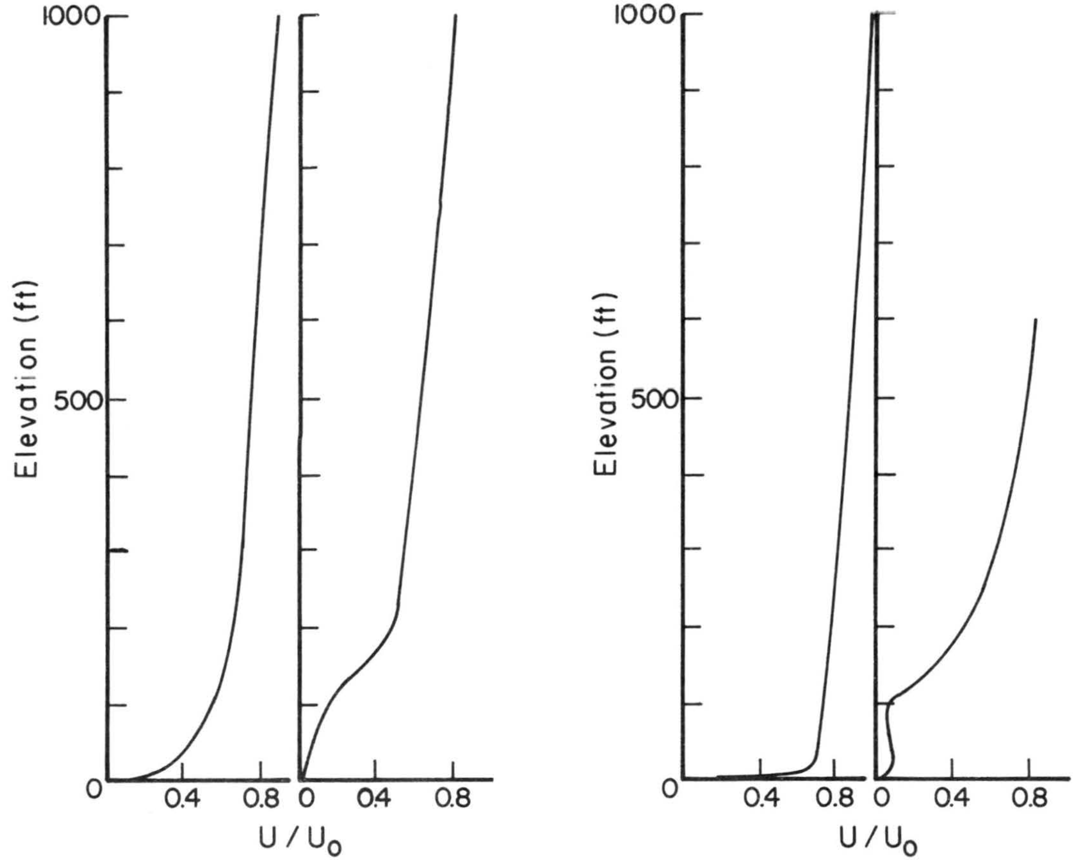

Model	4.0	I	4.0	I
Scale	1:6000		1:3000	
Local U_0, fps (free stream velocity)	33.3	33.3	31.4	31.4

Wind 180° Location C

Fig. 29

0-1

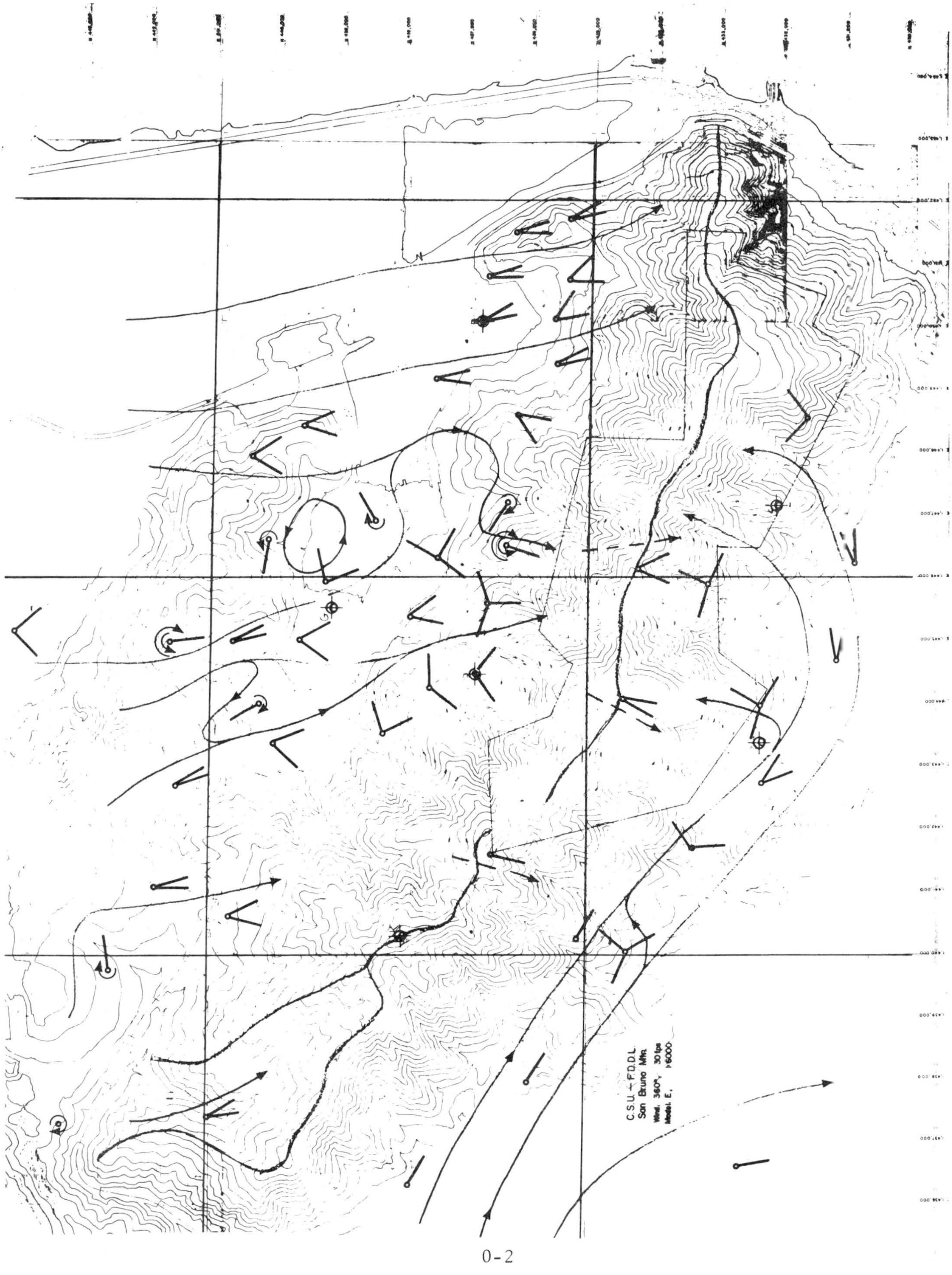

0-2

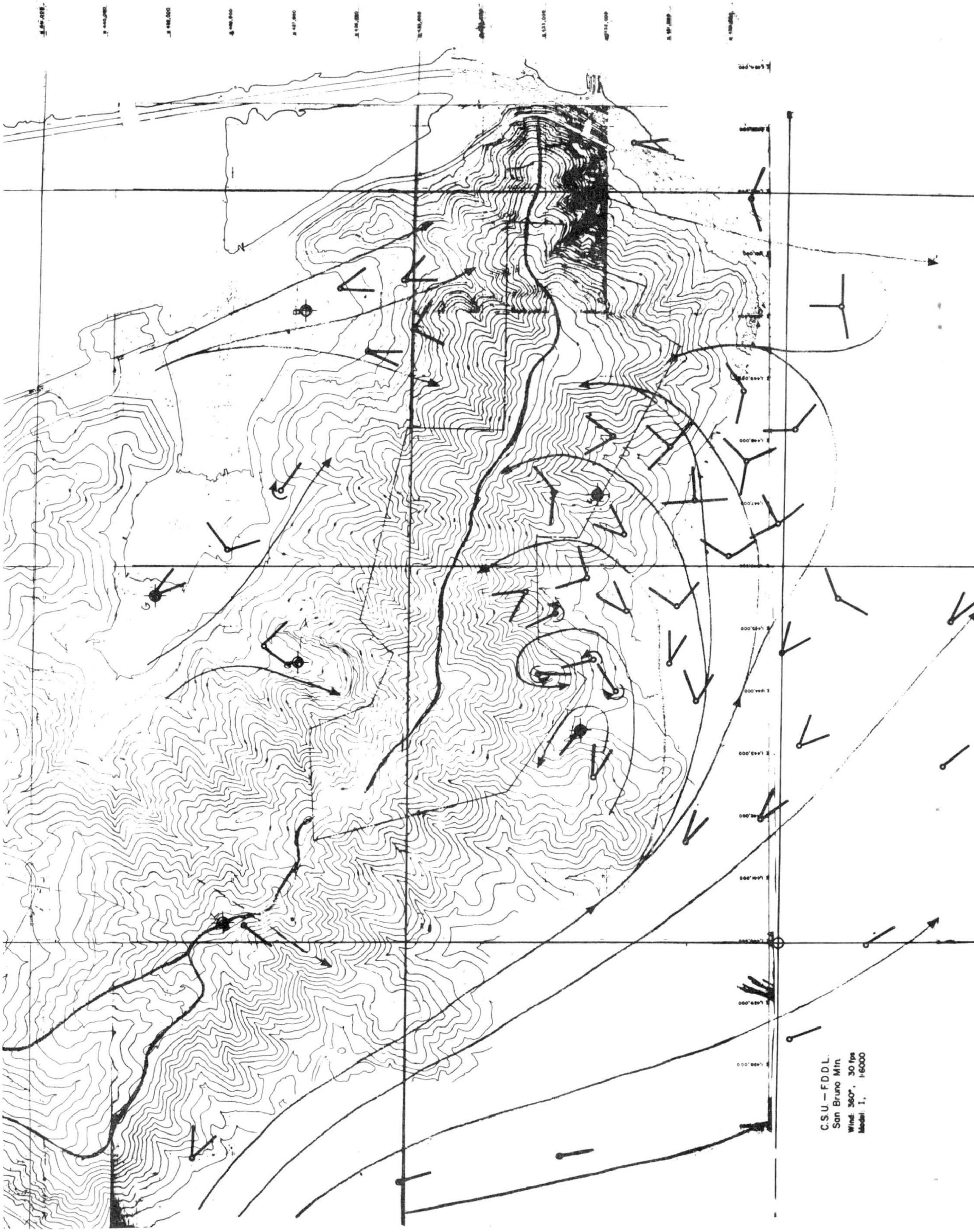

0-3

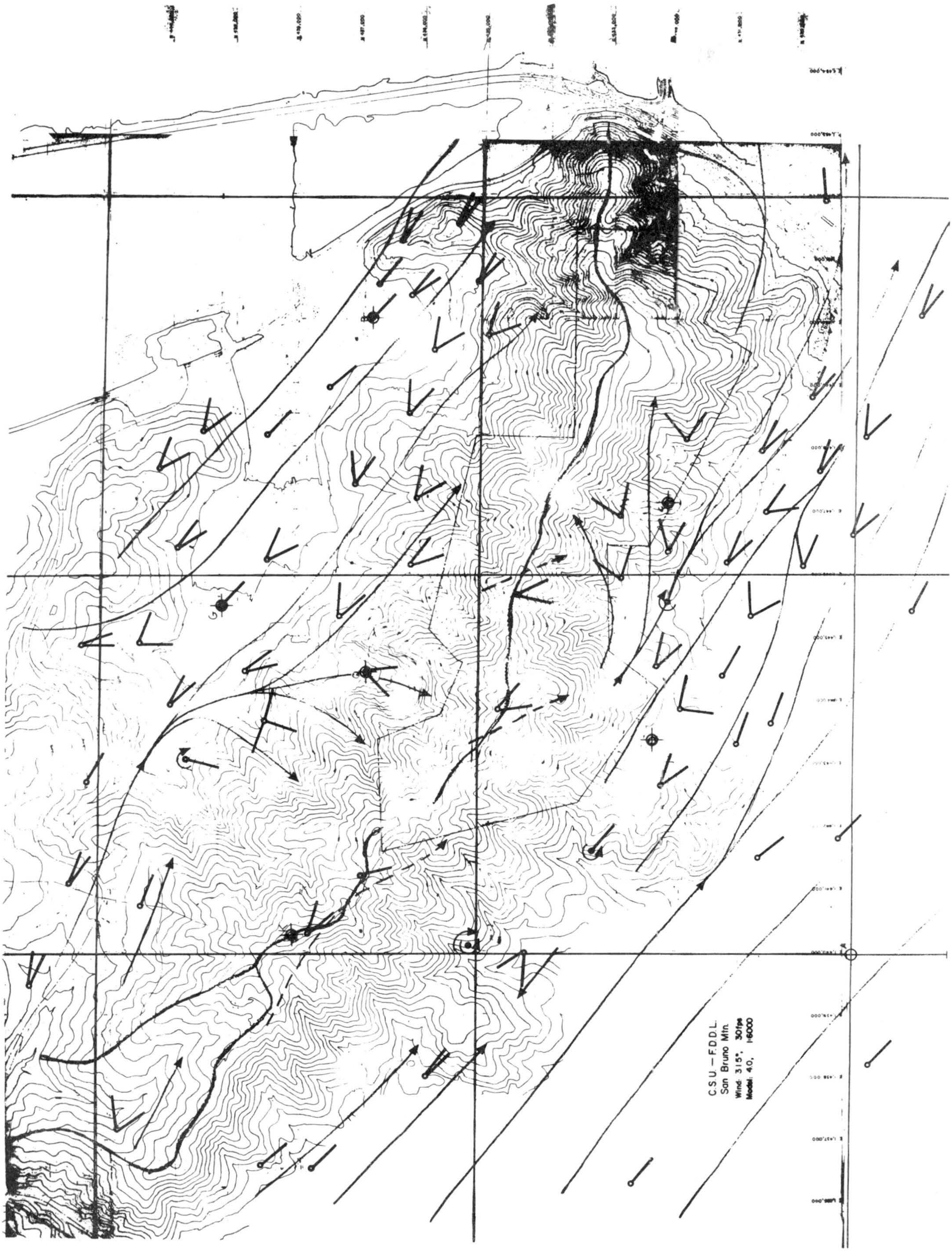
C.S.U.—F.D.D.L.
San Bruno Mtn.
Wind: 315°, 30fps
Model: 4.0, 1:6000

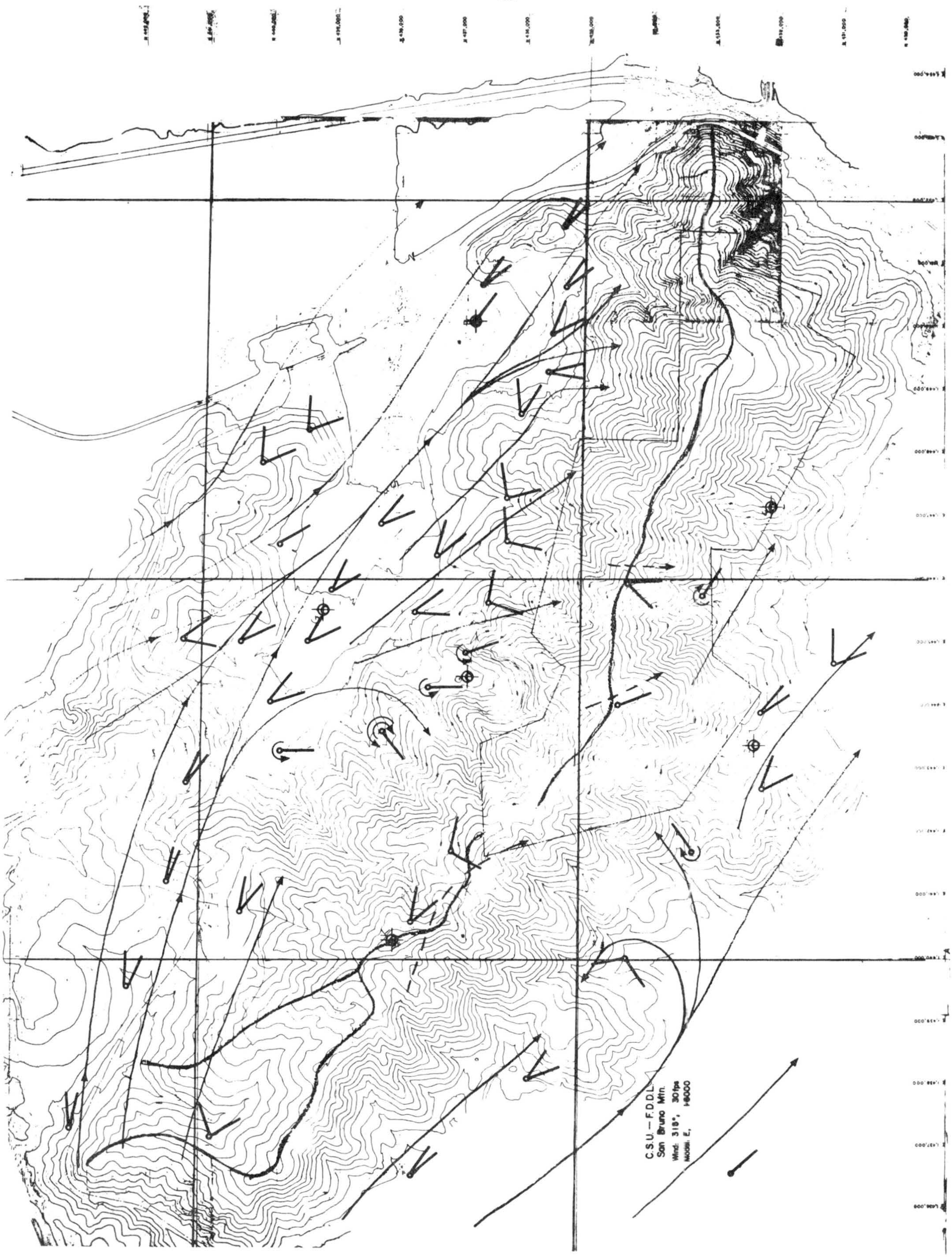
C.S.U.—F.D.D.L.
San Bruno Mtn.
Wind: 315°, 30fps
Model: E, 1:6000

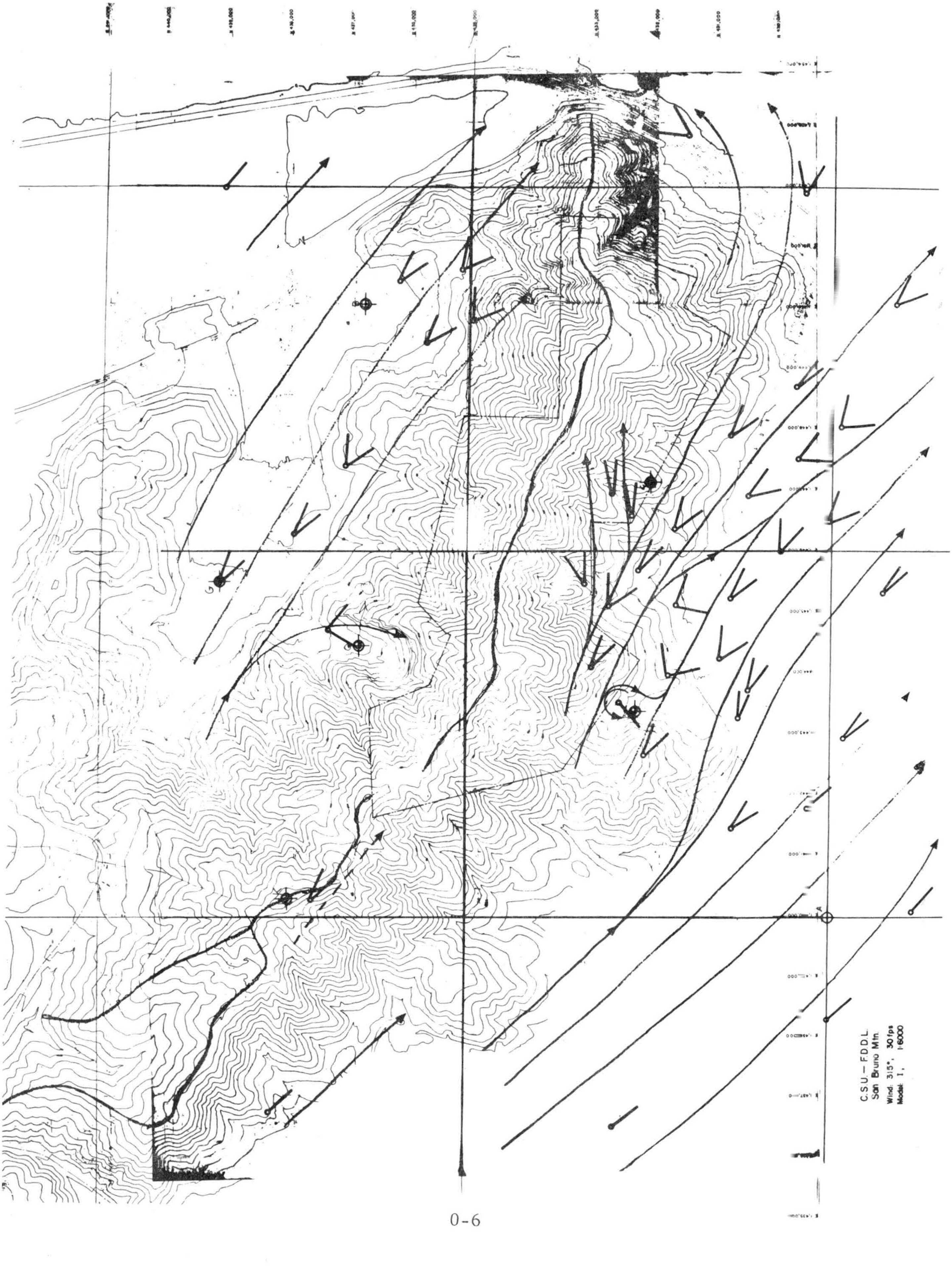
C.S.U. – F.D.D.L.
San Bruno Mtn.
Wind: 315°, 30 fps
Model I, 1:6000

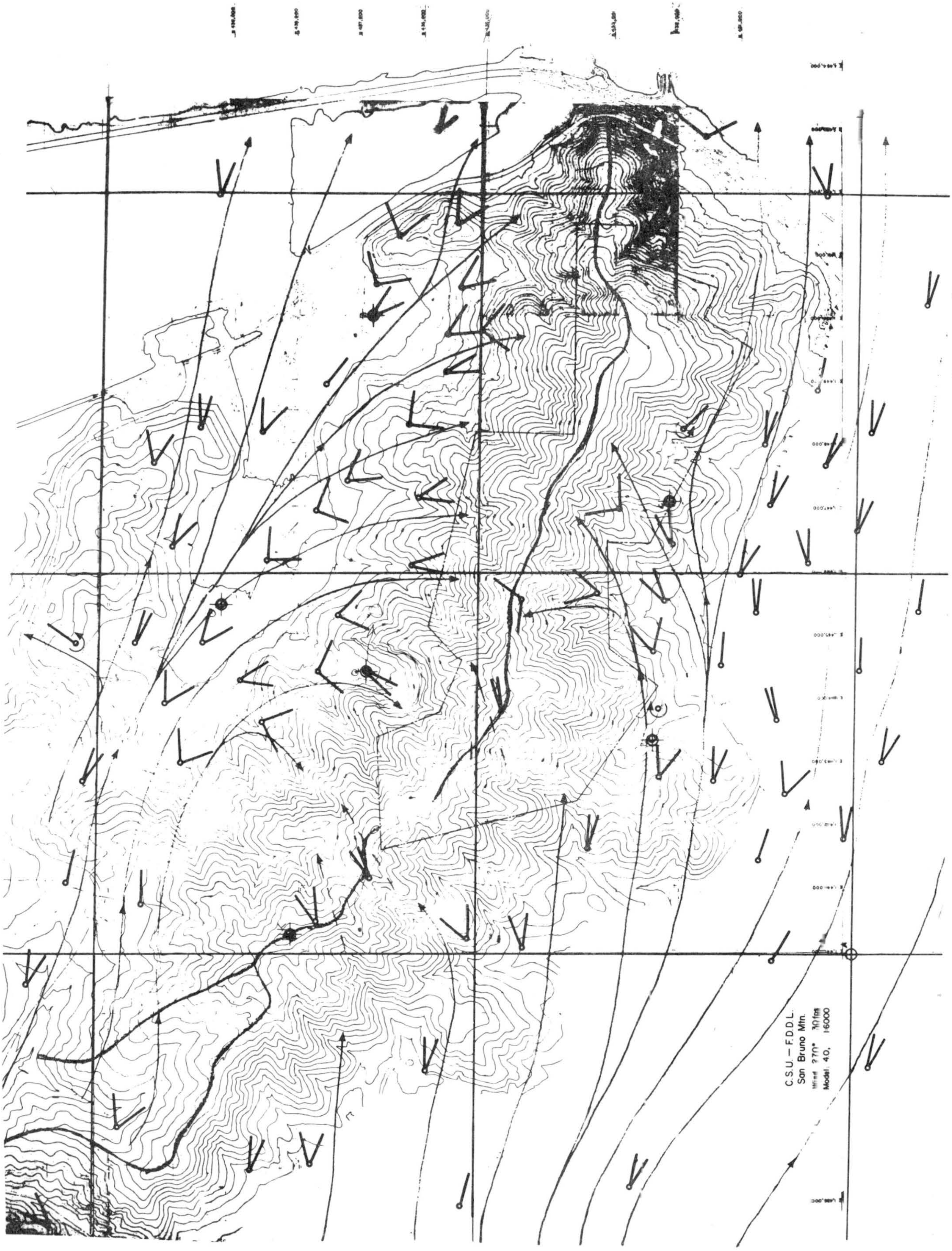

0-7


C.S.U.—F.D.D.L.
San Bruno Mtn.
Wind 270°, 30fps
Model E, 1:6000

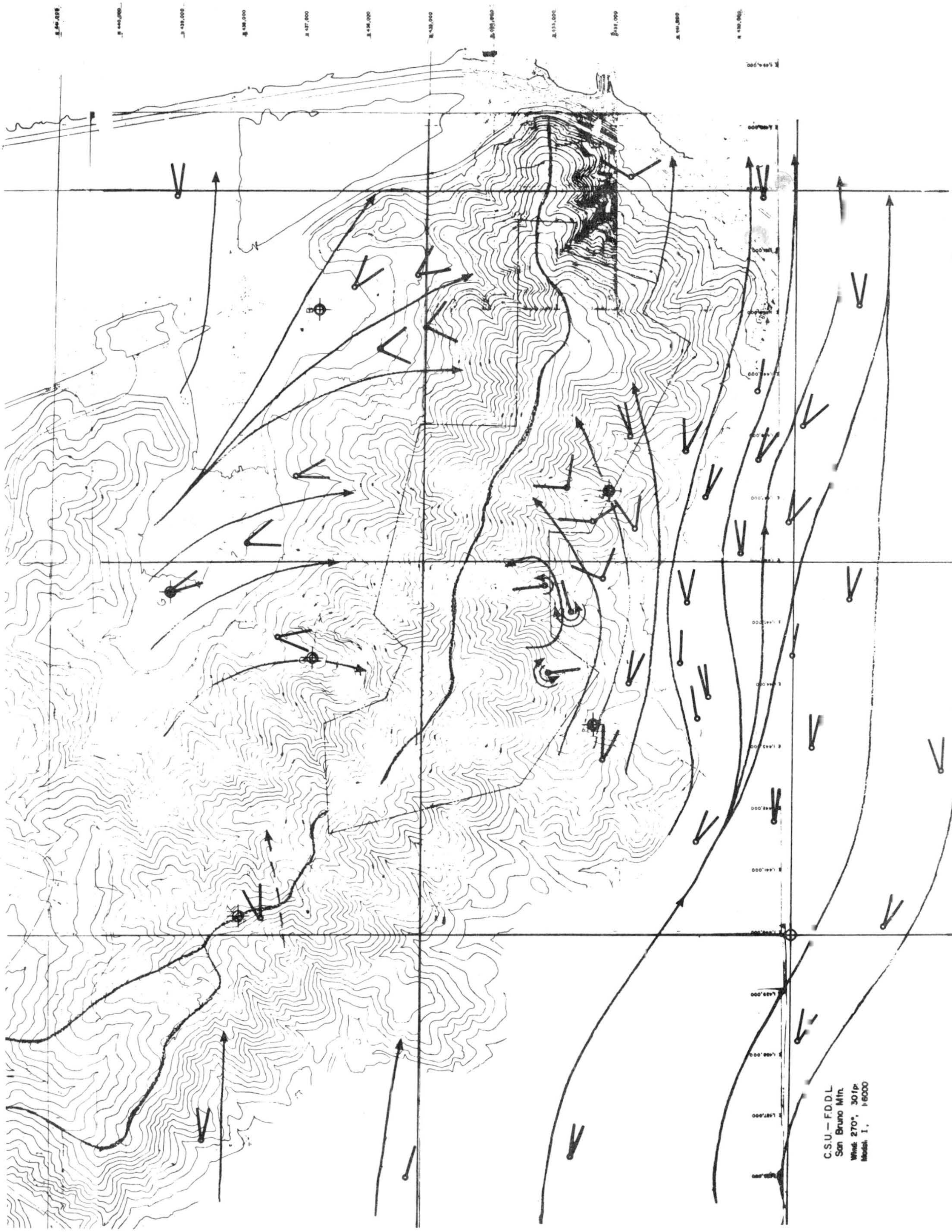
C.S.U. — F.D.D.L
San Bruno Mtn.
Wind: 270°, 30 fps
Model I, 1:6000

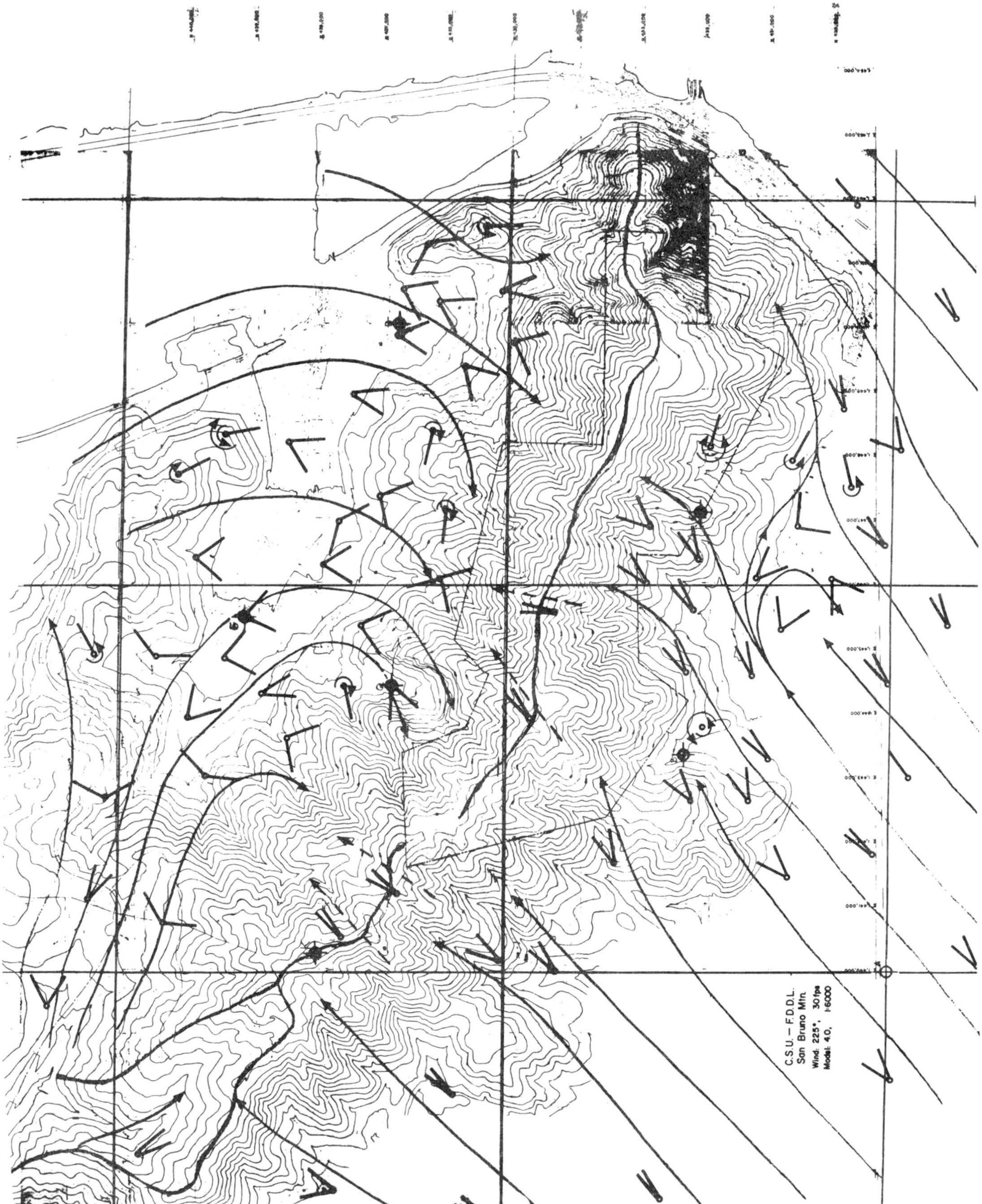

0-10


C.S.U.—F.D.D.L.
San Bruno Mtn.
225°, 30fps
E, t6000

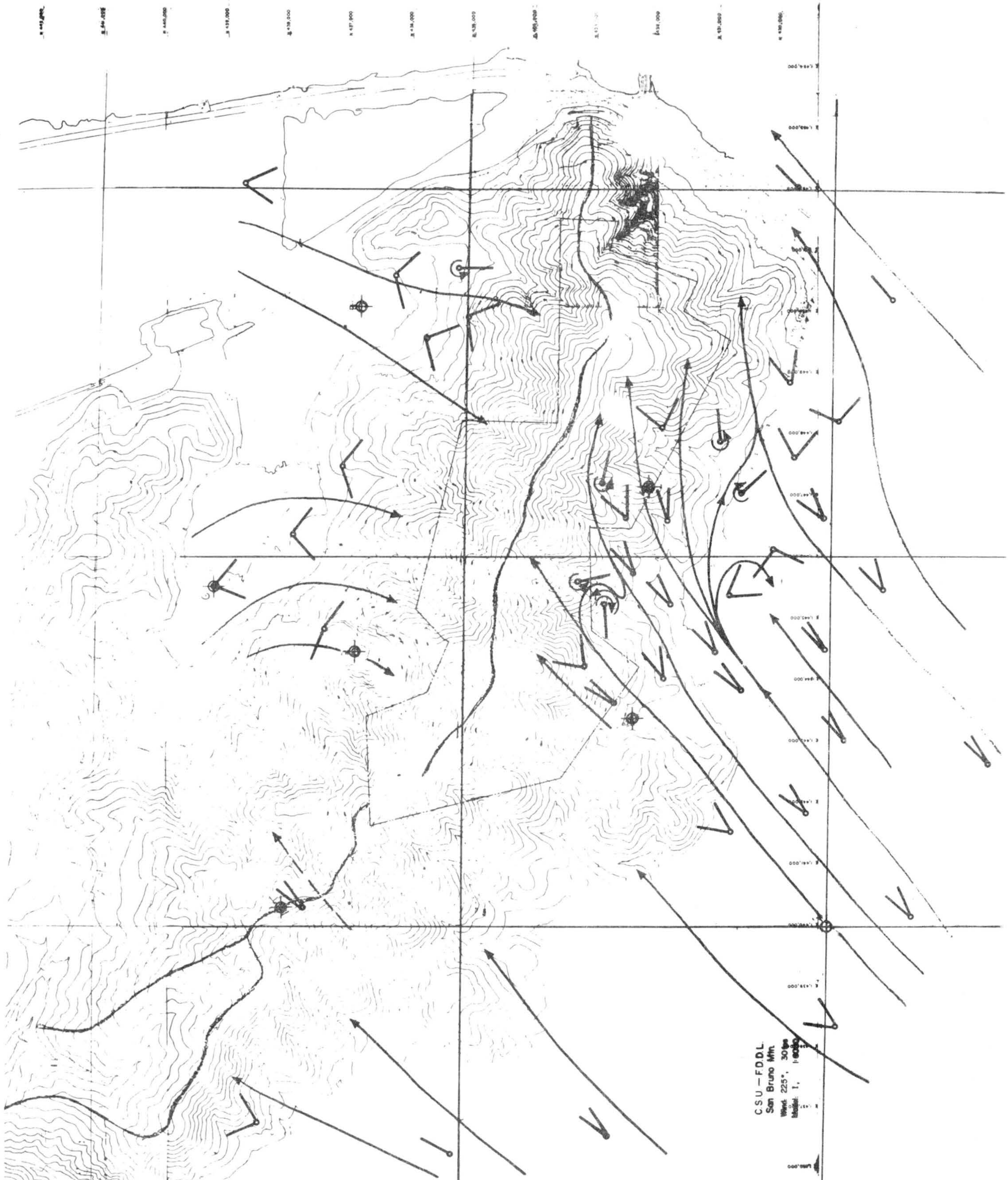
C.S.U. — F.D.D.L.
San Bruno Mtn.

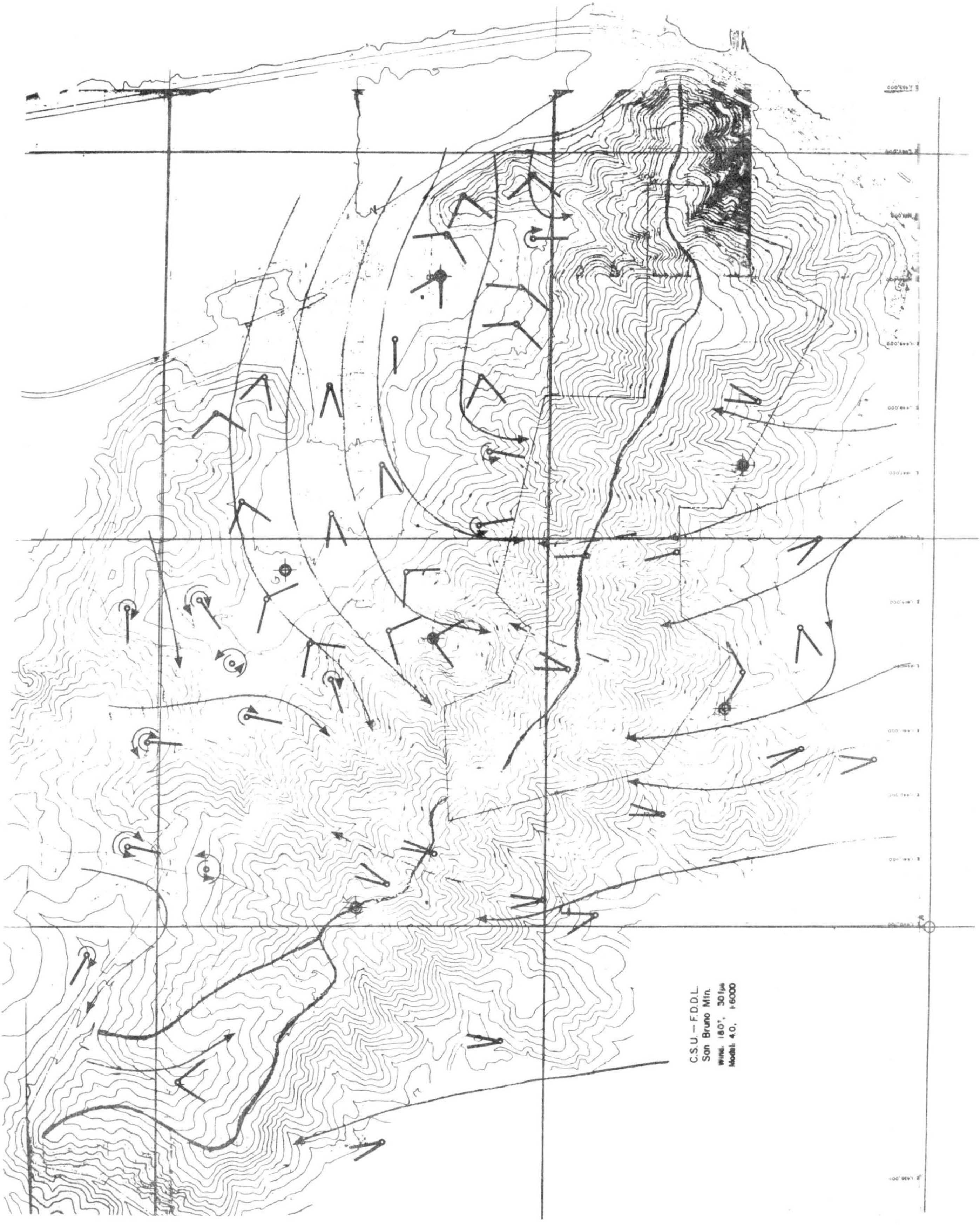
C.S.U. – F.D.D.L.
San Bruno Mtn.
Wind. 180°, 30 fps
Model: 4.0, 1:6000

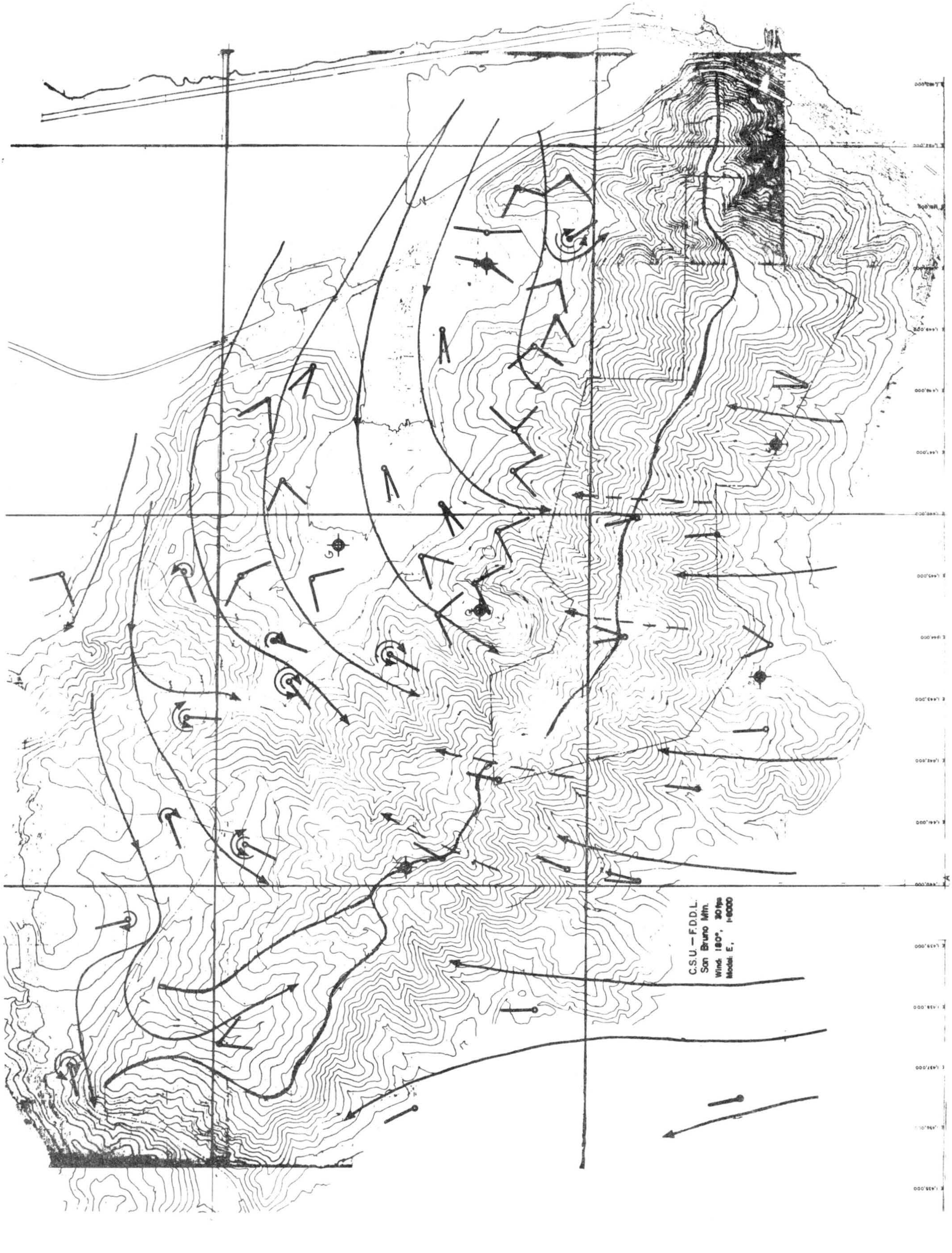
C.S.U. — F.D.D.L.
San Bruno Mtn.
Wind: 180°, 30 fps
Model: E, 1:6000

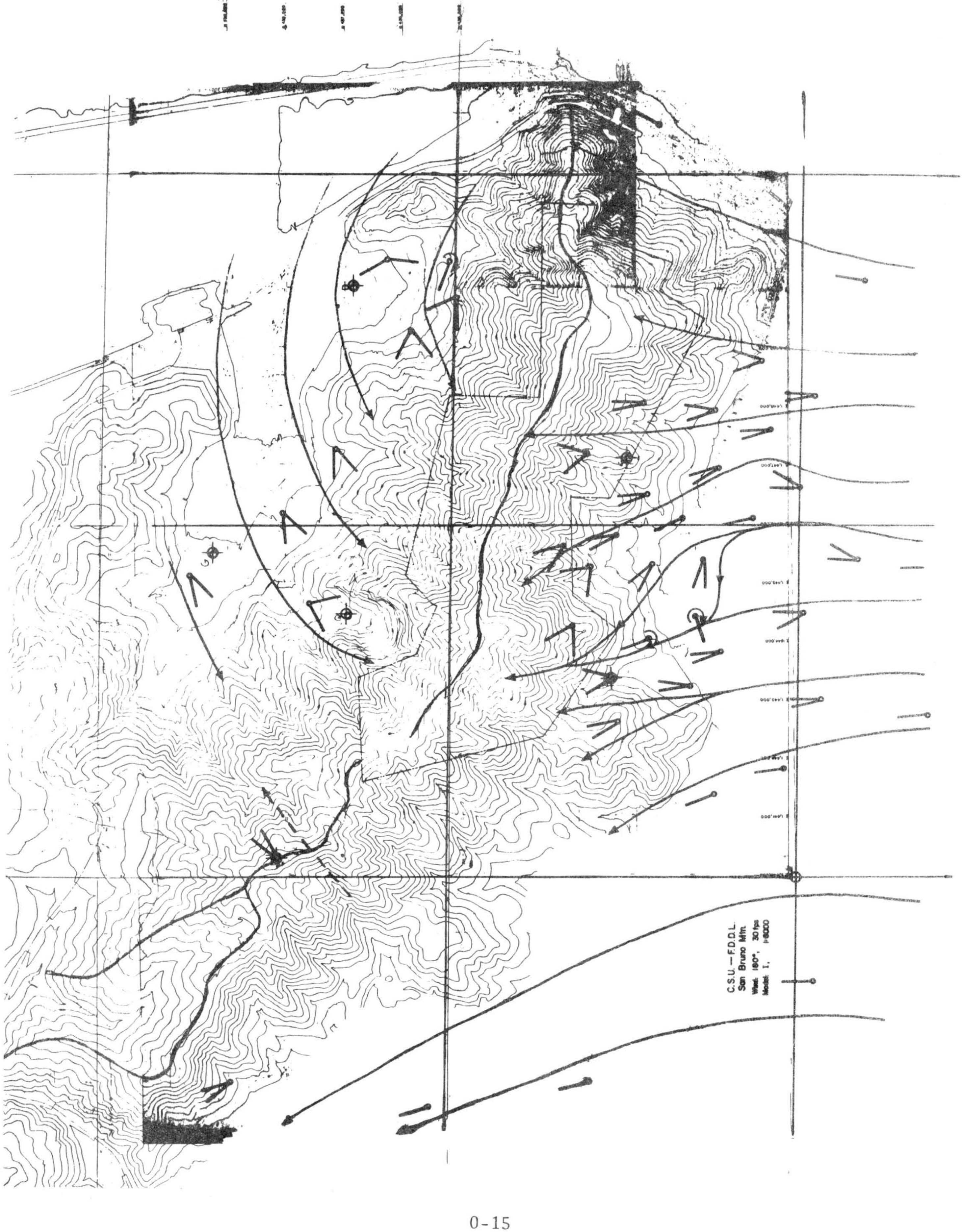
C.S.U. — F.D.D.L.
San Bruno Mtn.

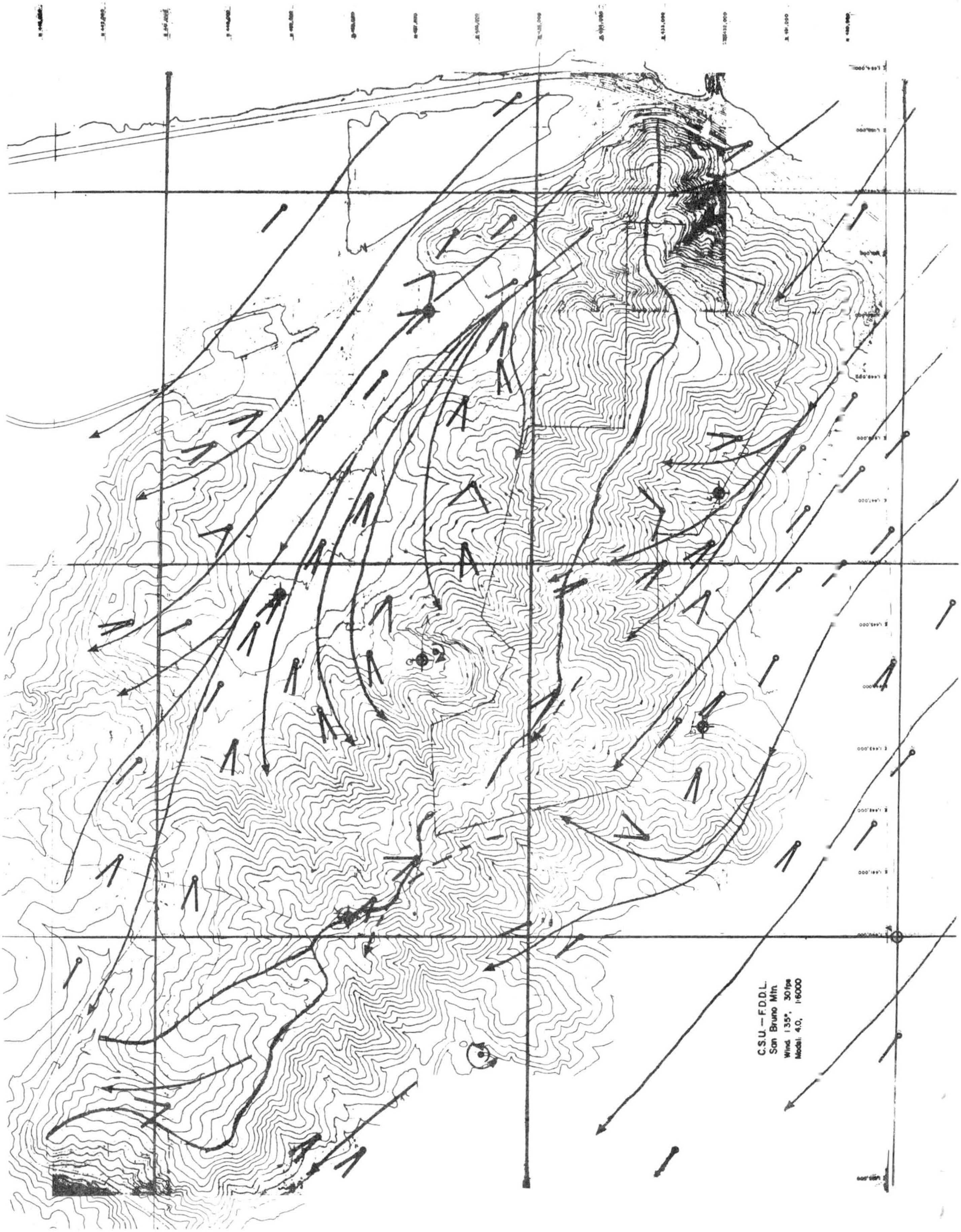
C.S.U. — F.D.D.L.
San Bruno Mtn.
Wind 135°, 30fps
Model 4.0, 1:6000

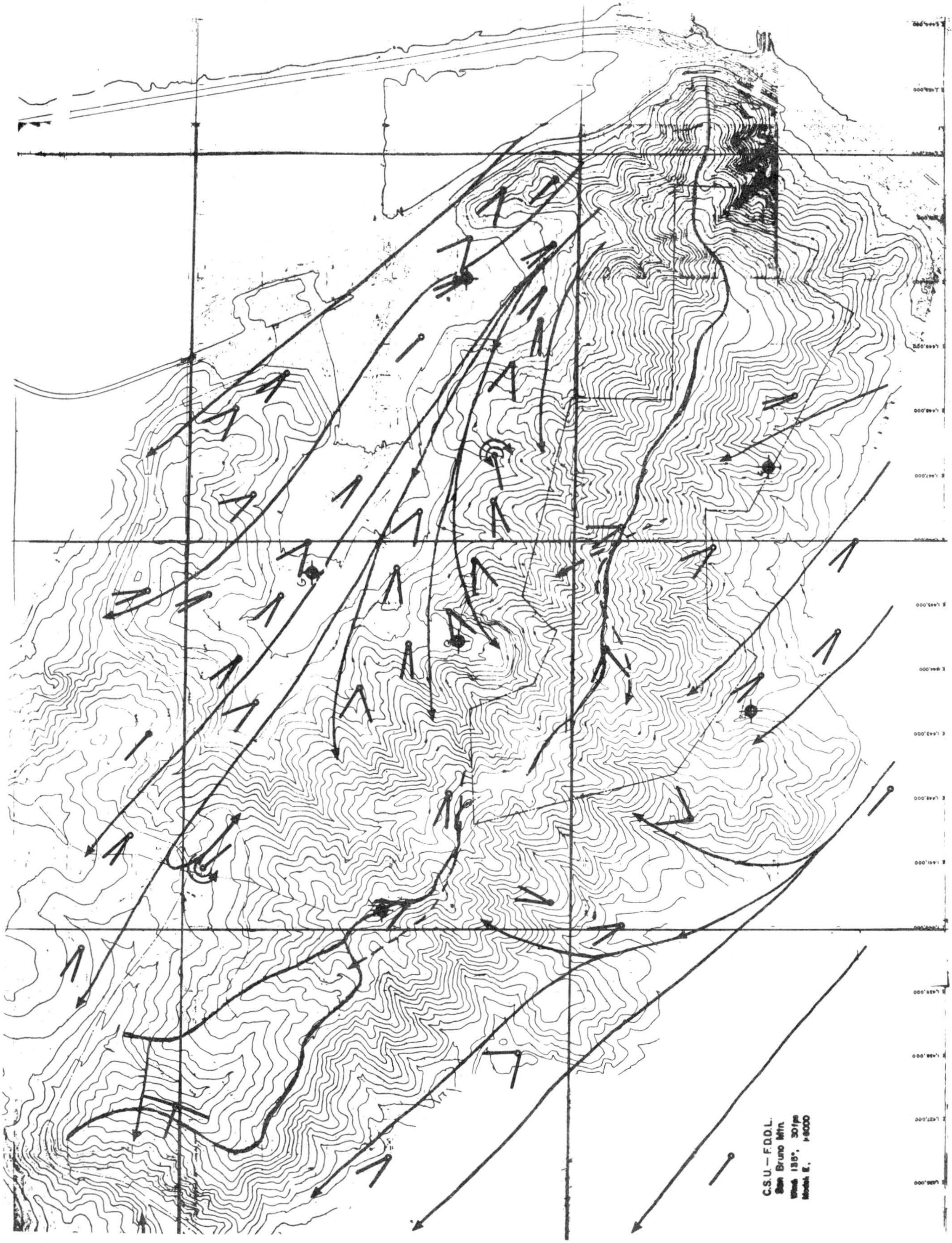
C.S.U. — F.D.D.L.
San Bruno Mtn.
Wind 135°, 30fps
Model E, 1:6000

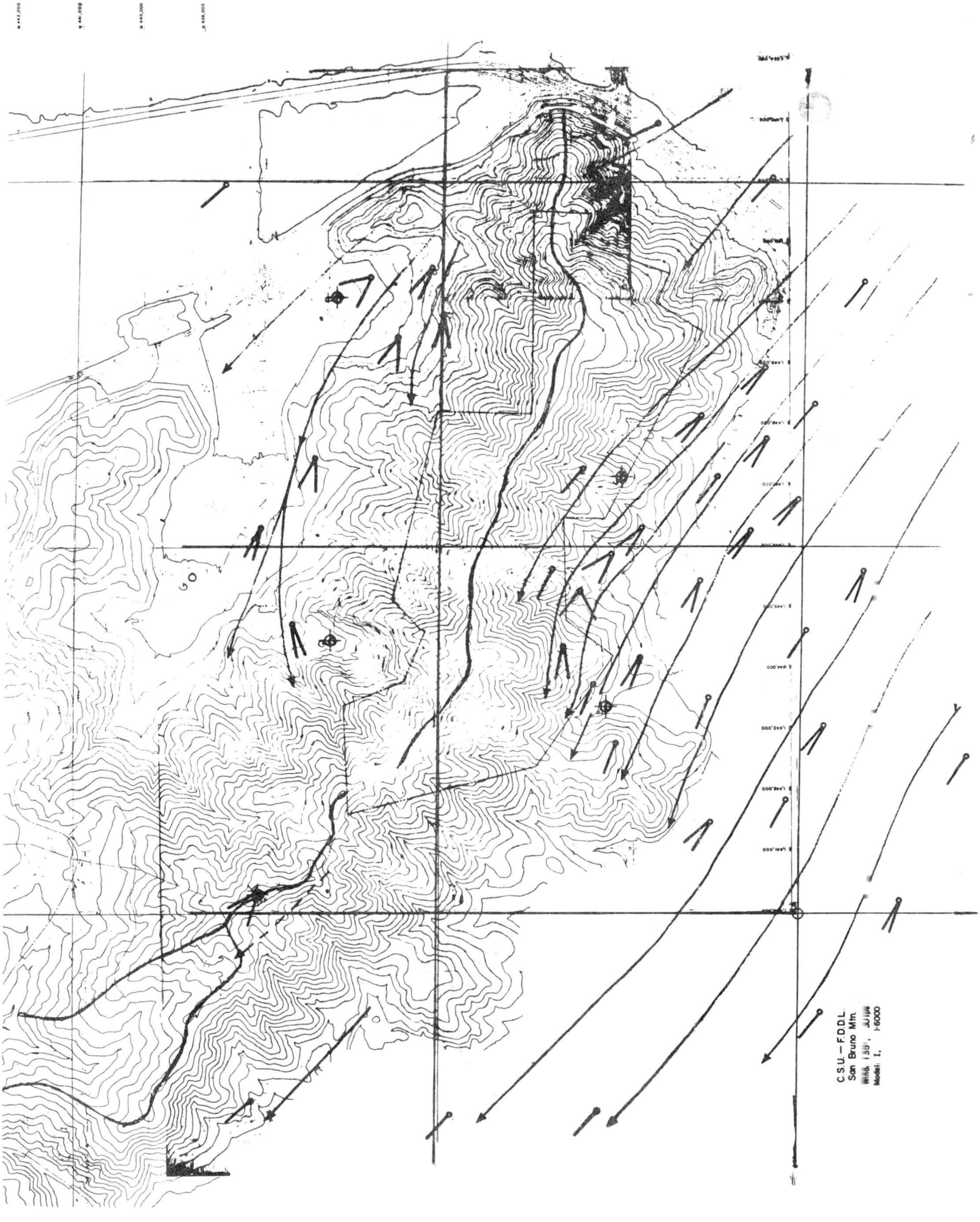
C.S.U.—F.D.D.L.
San Bruno Mtn.

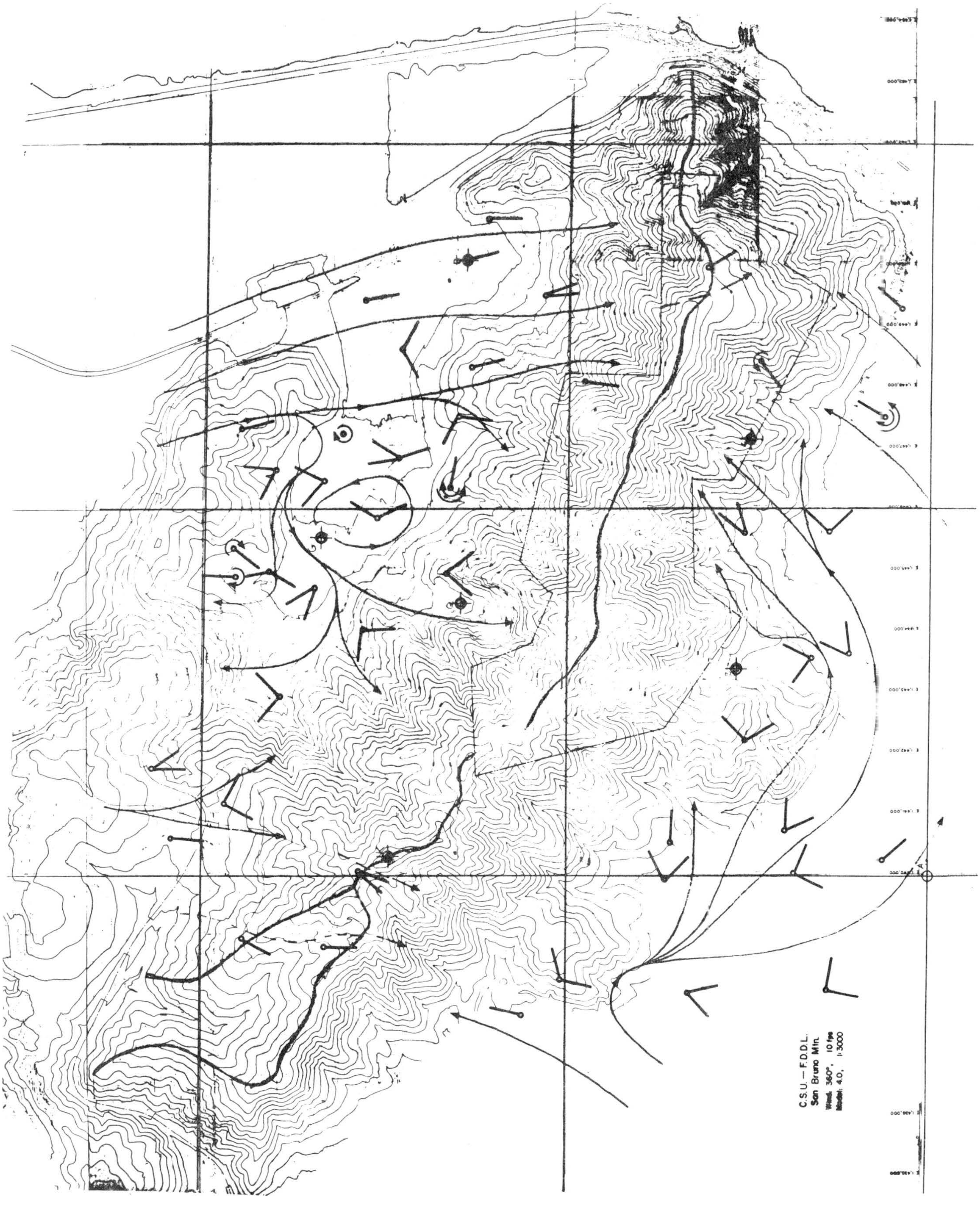
C.S.U. — F.D.D.L.
San Bruno Mtn.
Wind: 360°, 10 fps
Model: 4.0, 1:3000

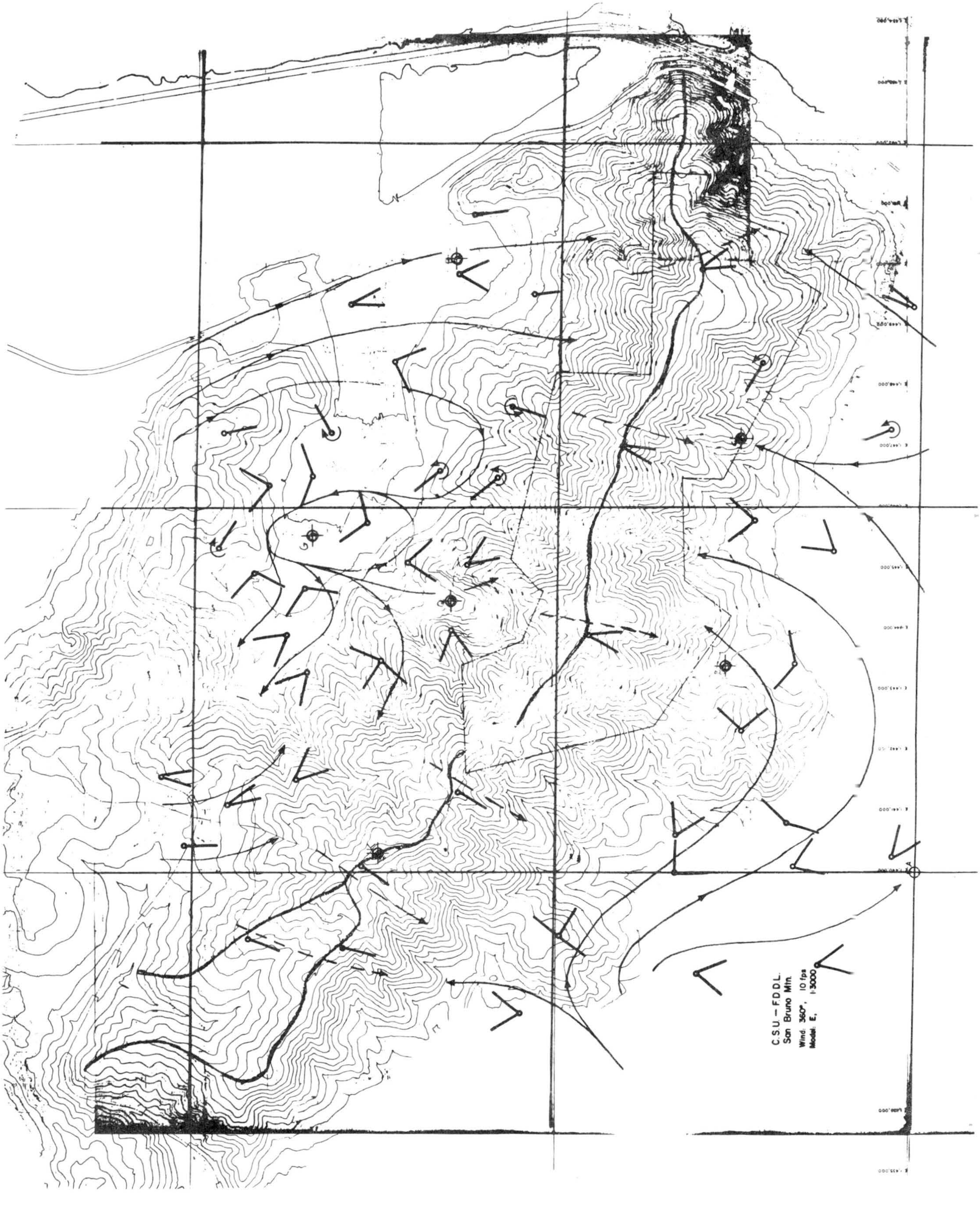
C.S.U. – F.D.D.L.
San Bruno Mtn.
Wind: 360°, 10 fps
Model: E, 1:3000

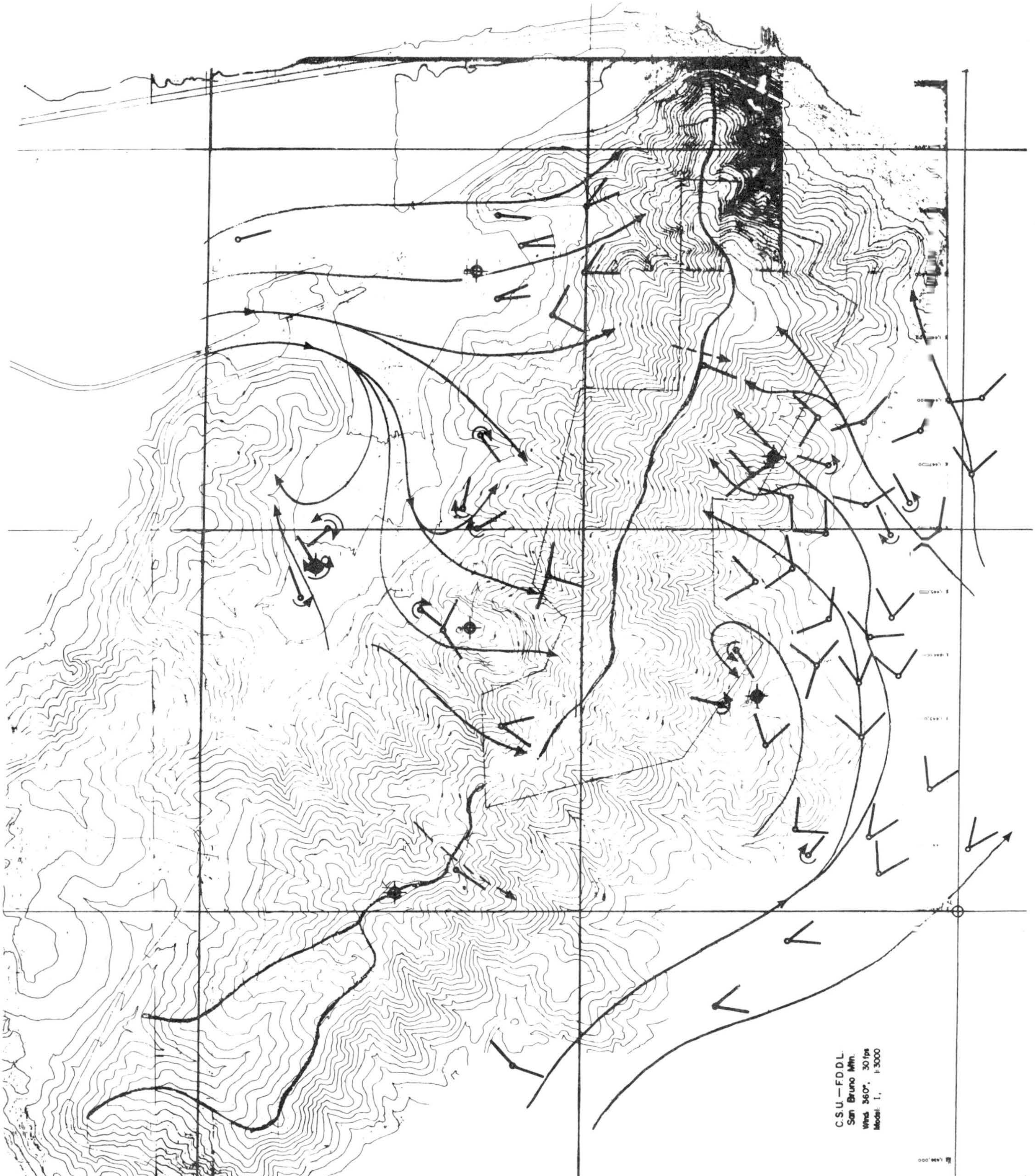
C.S.U.—F.D.D.L.
San Bruno Mtn.
Wind 360°, 30 fps
Model I, 1:3000

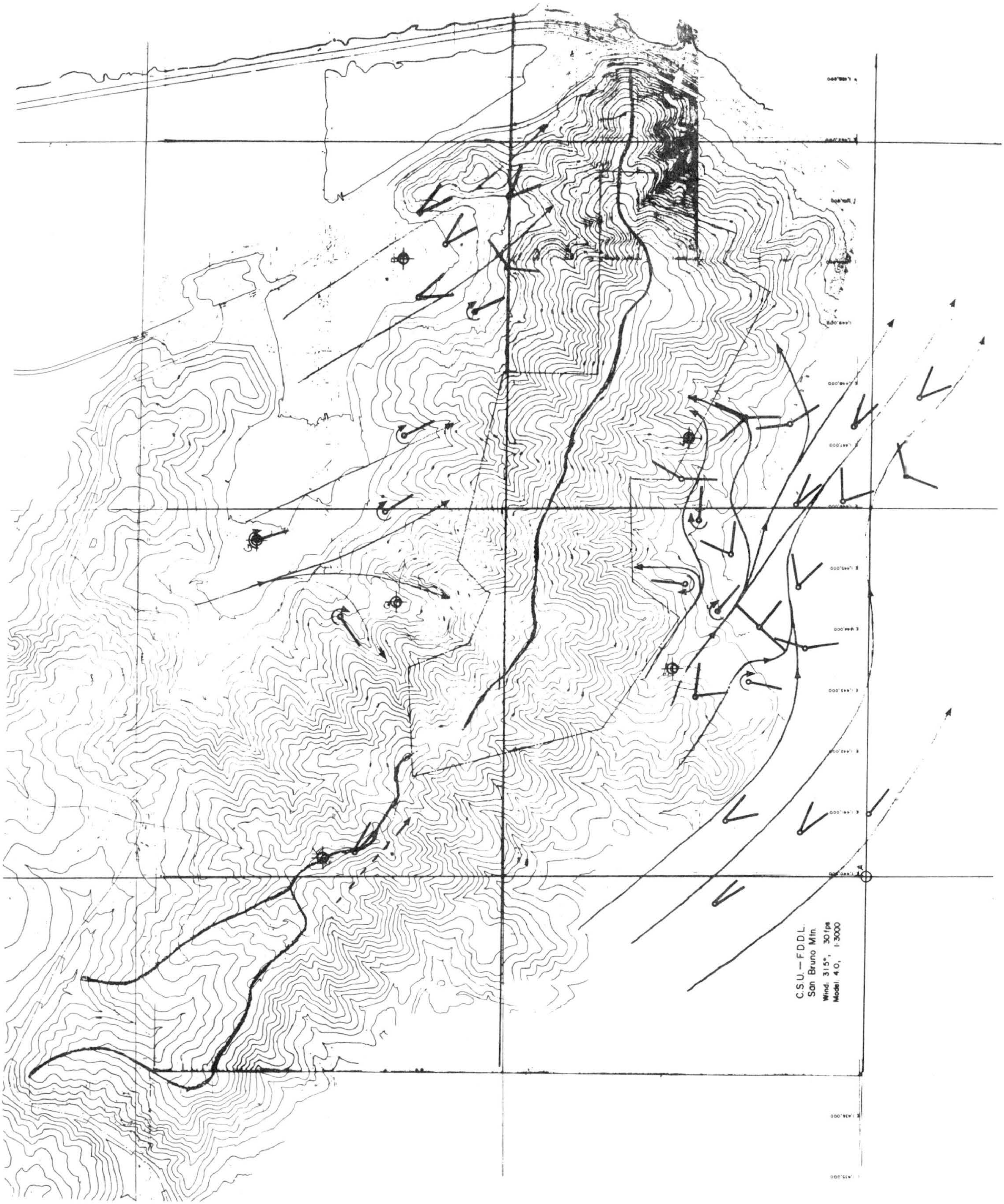
C.S.U.—F.D.D.L.
San Bruno Mtn.
Wind: 315°, 30 fps
Model: 4.0, 1:3000

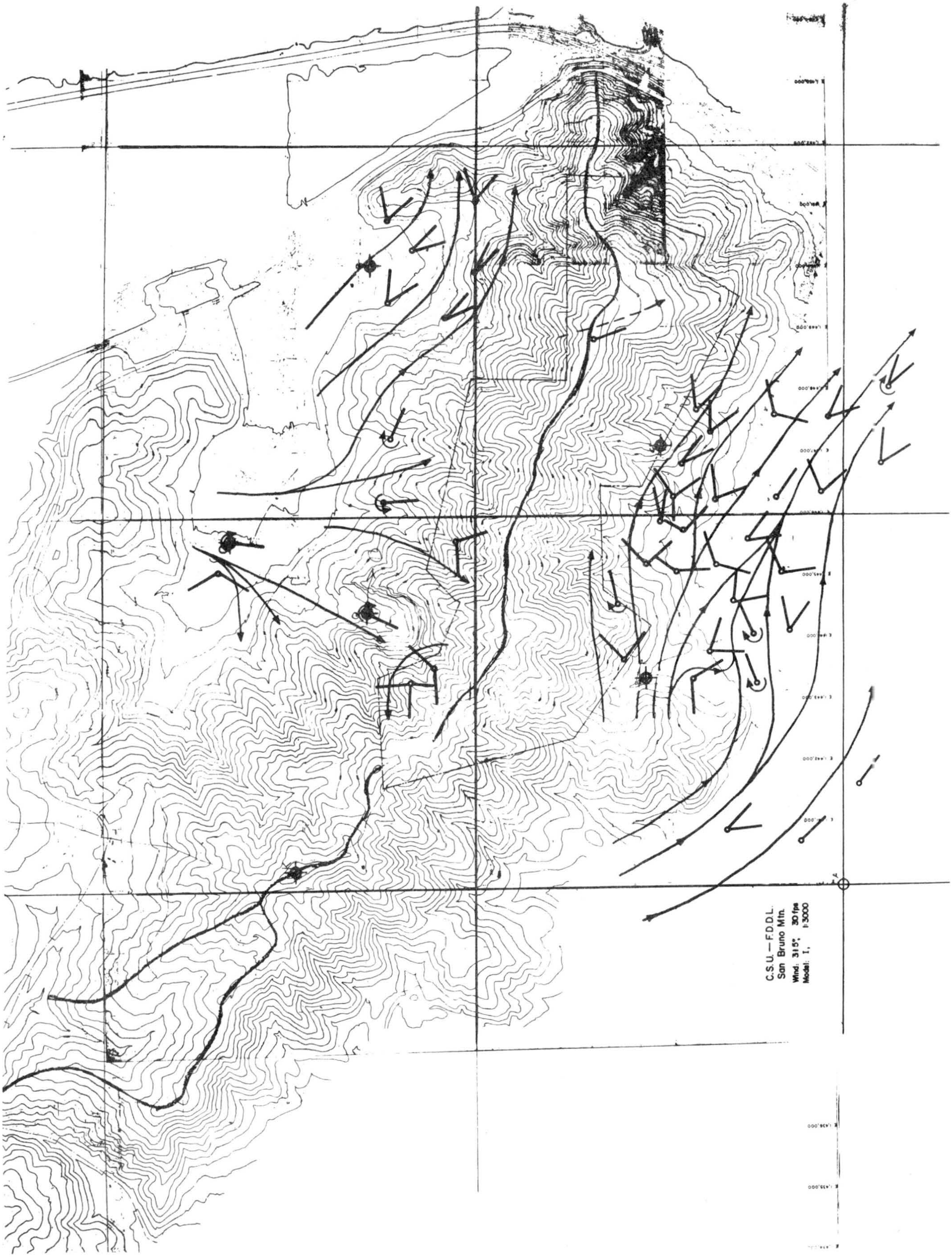
C.S.U.—F.D.D.L.
San Bruno Mtn.
Wind: 315°, 30 fps
Model: I, 1:3000

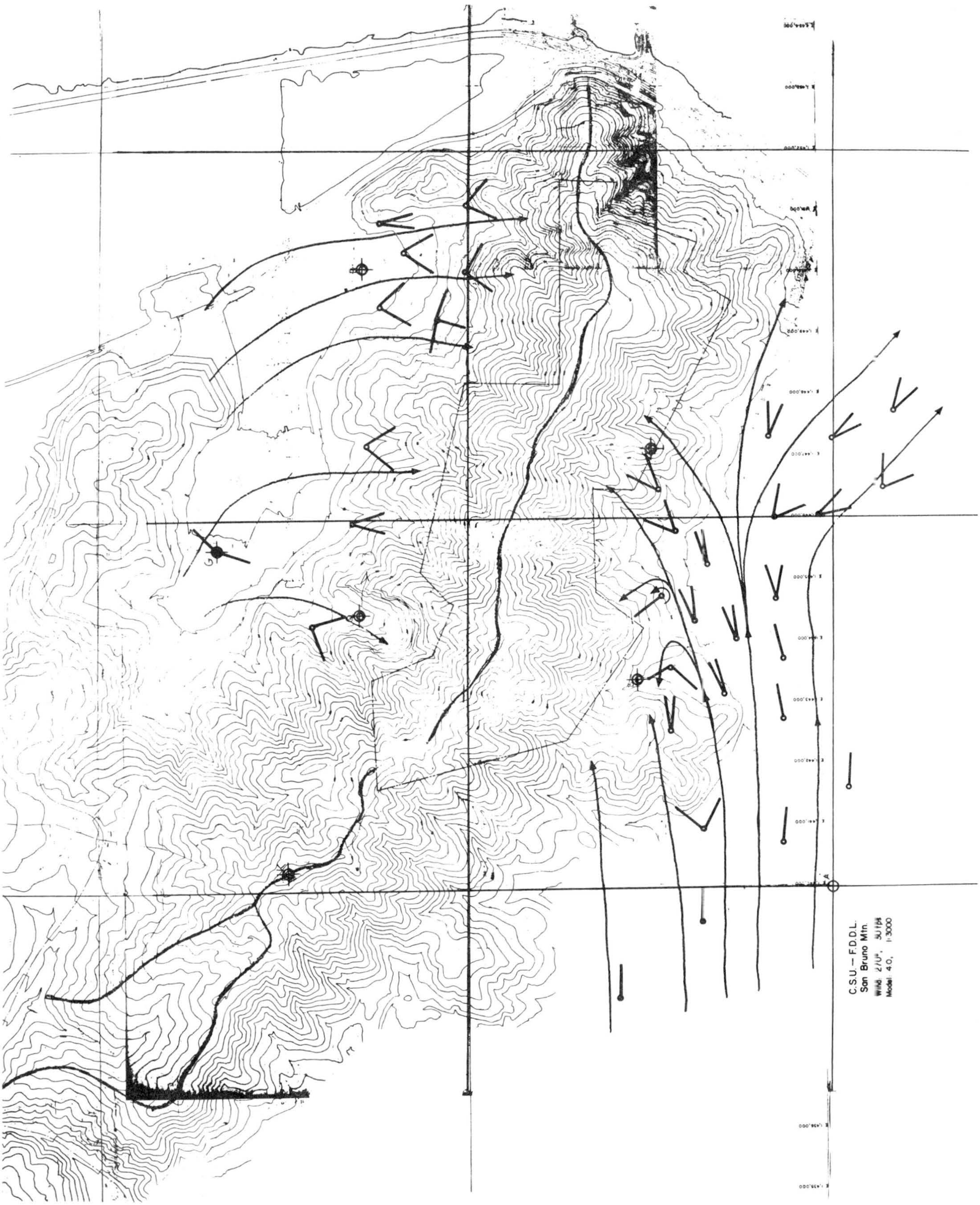
C.S.U. – F.D.D.L.
San Bruno Mtn.
Wind 270°, 30 fps
Model 4.0, 1:3000

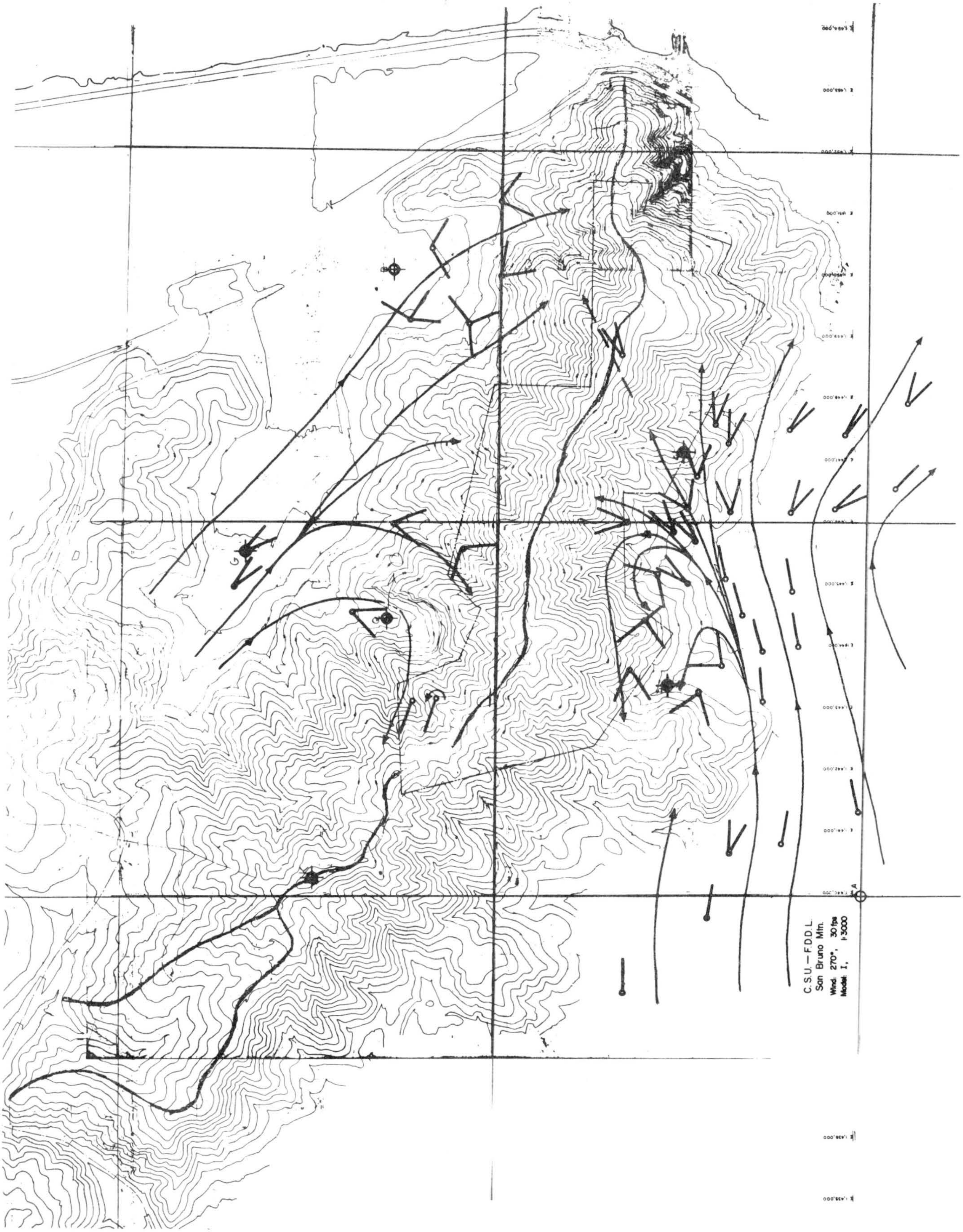
C.S.U.—F.D.D.L.
San Bruno Mtn.
Wind: 270°, 30 fps
Model: I, 1:3000

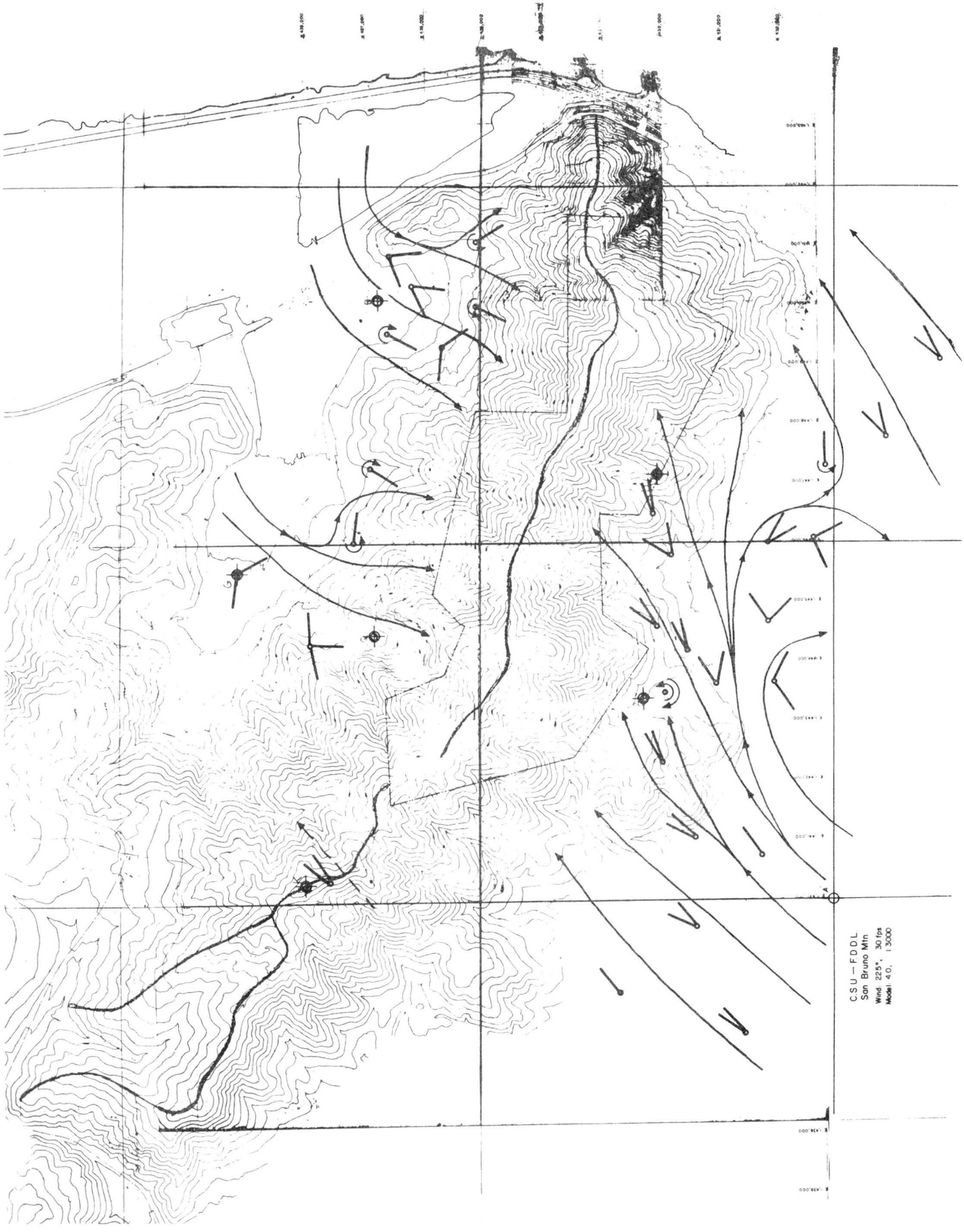
C.S.U. — F.D.D.L.
San Bruno Mtn
Wind: 225°, 30 fps
Model: 4.0, 1:3000

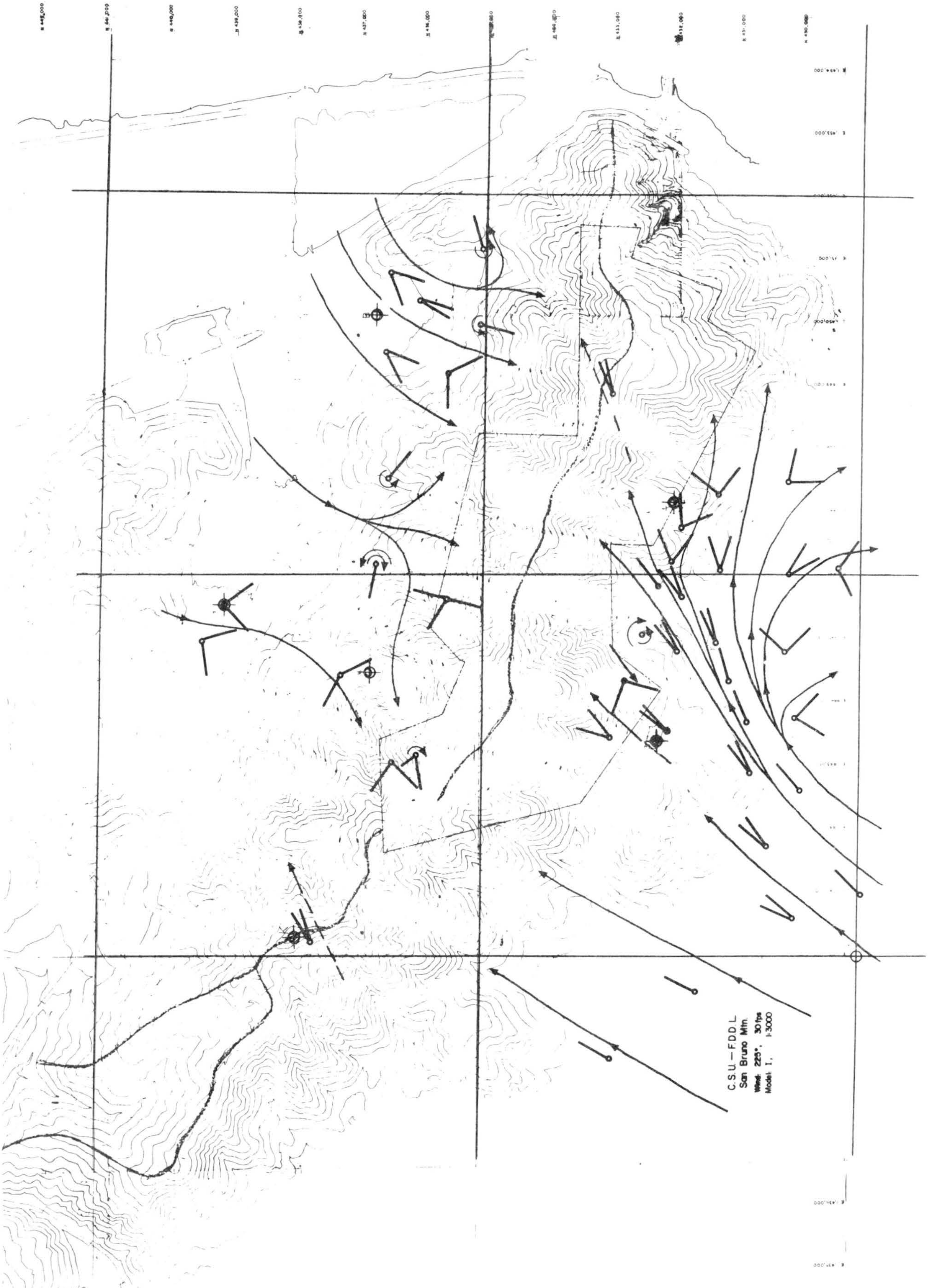
C.S.U.—F.D.D.L.
San Bruno Mtn.
Wind: 225°, 30 fps
Model: I, 1:3000

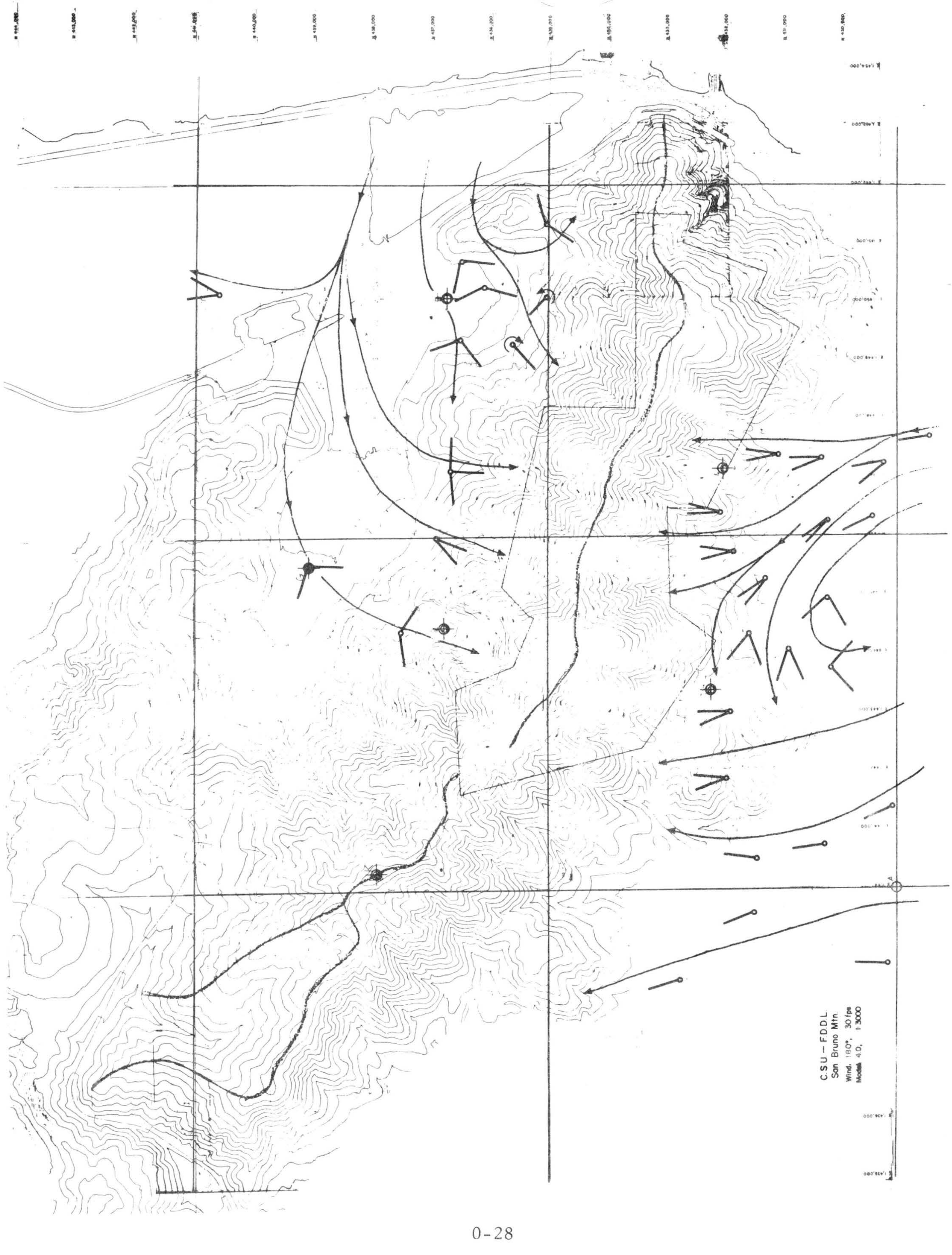
C.S.U. – F.D.D.L.
San Bruno Mtn.
Wind. 180°, 30 fps
Model 4.0, 1:3000

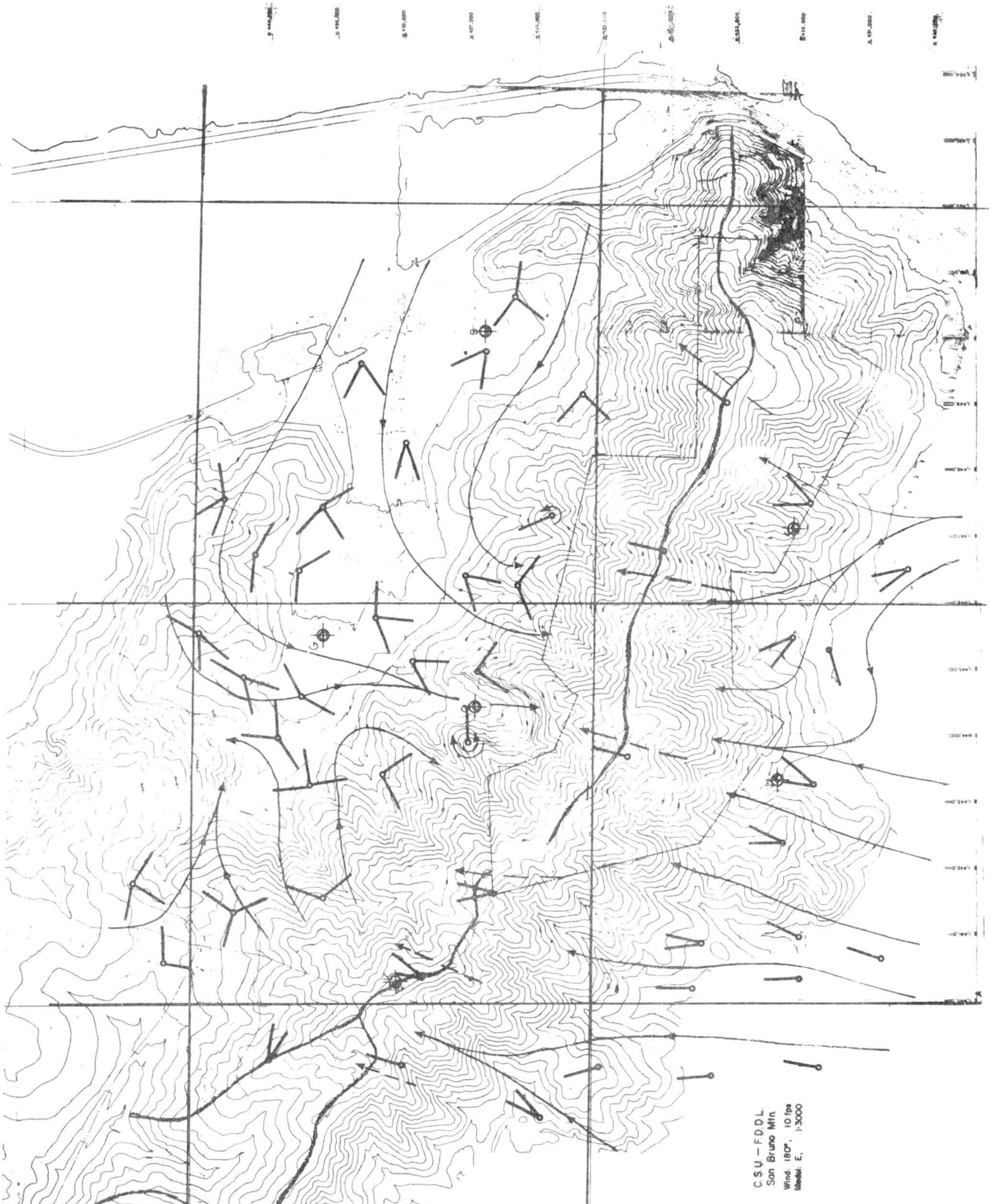
C.S.U. – F.D.D.L.
San Bruno Mtn.
Wind: 180°, 10 fps
Model: E, 1:3000

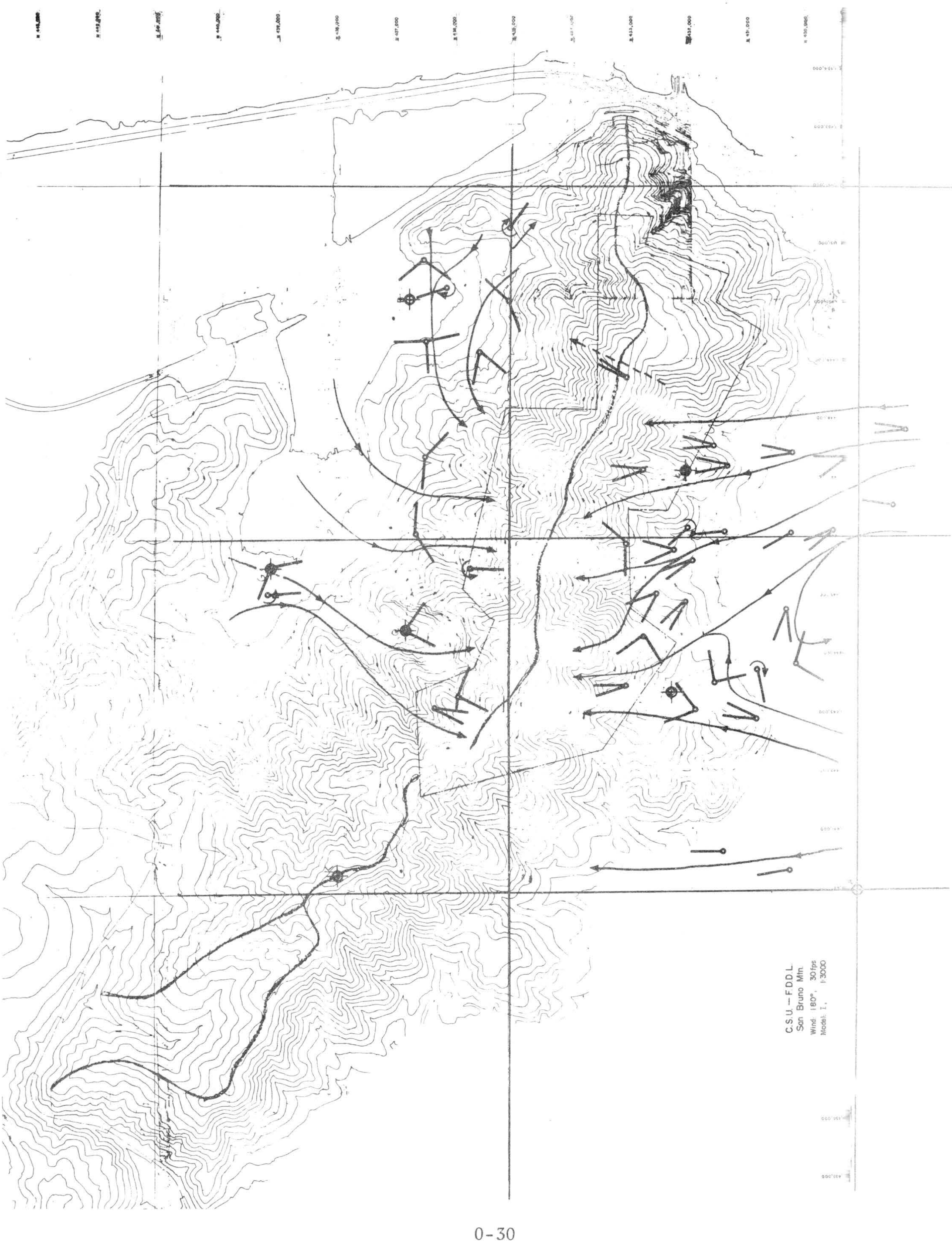
C.S.U. — F.D.D.L.
San Bruno Mtn.
Wind: 180°, 30 fps
Model: I, 1:3000

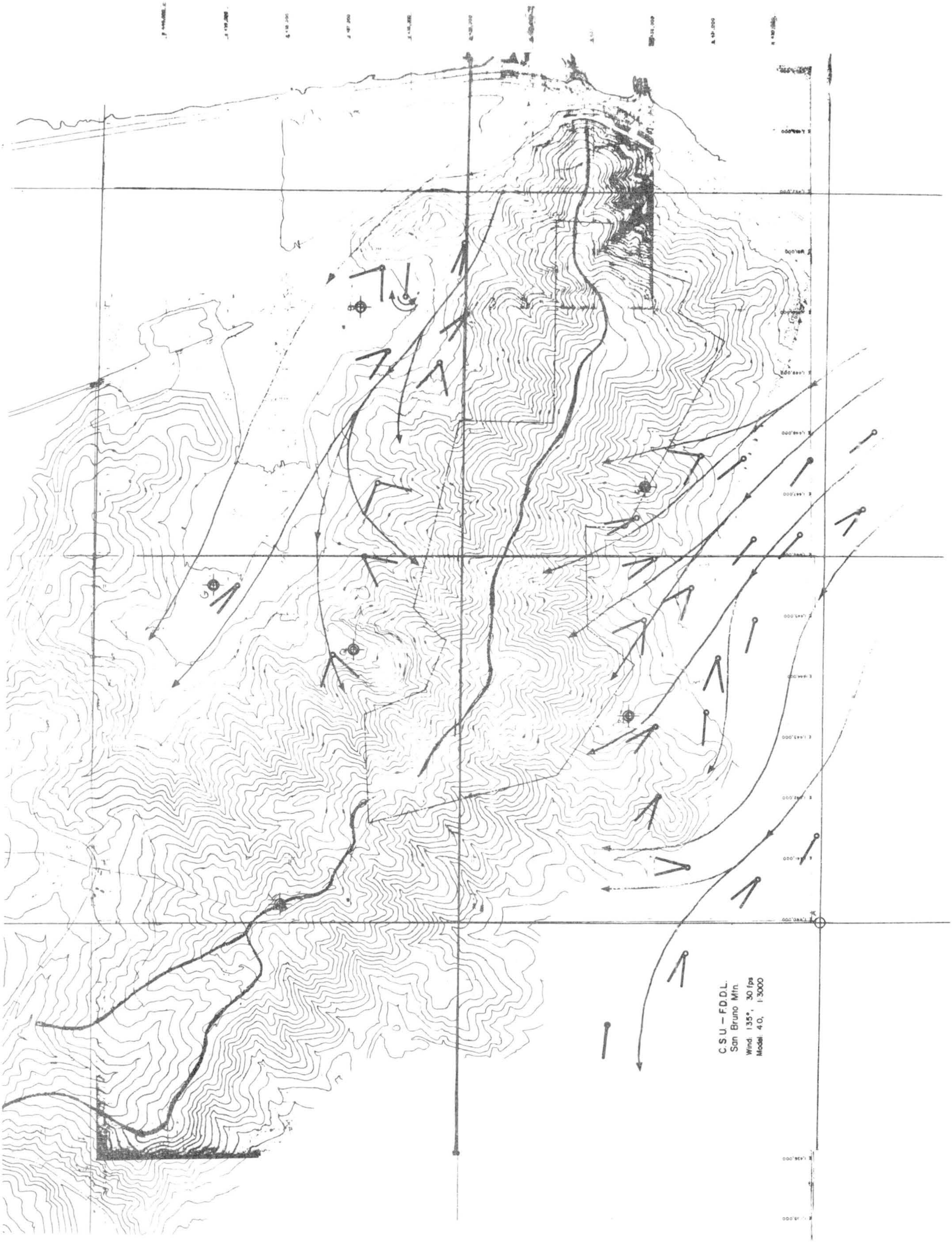
C.S.U. – F.D.D.L.
San Bruno Mtn.
Wind: 135°, 30 fps
Model: 4.0, 1:3000

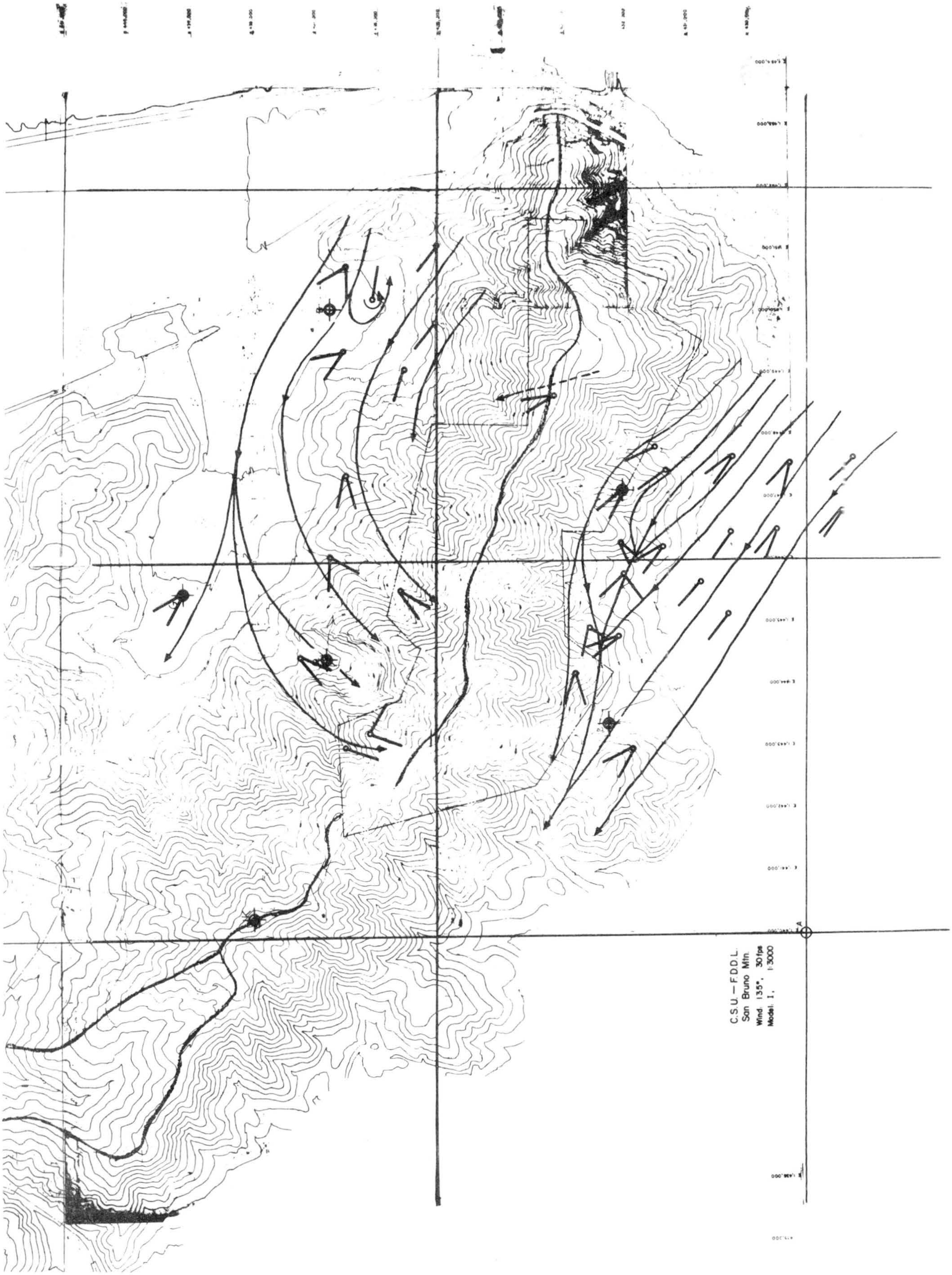
C.S.U.—F.D.D.L.
San Bruno Mtn.
Wind 135°, 30fps
Model I, 1:3000

ERRATA

Page v.	Fig. 4 should read "Eight point locations used during the period prior to 18 September, 1967."
12.	In the fourth line of the text, substitute Fig. 1 for Fig. 4.
20.	Three lines from the bottom the statement in parenthesis should read "(See Fig. 4 and Fig. 8)."
32.	Fig. 4 should read "Eight point locations used during the period prior to 18 September, 1967."
29 - 31 and 36.	Location of point "A" on these maps is lost in a black area inadvertently produced during the reproduction process. "A" can be readily estimated as 1 in. southwest of "B". More precisely, it can be found at the intersection of the eastward extension of the Daly City south boundary line from where it intersects the Pacific Coast and a line drawn south from Radio Station KQED.
32.	Location of point 5 is in the black area (Brisbane) and will be found on the North-South line drawn midway on the north boundary of Brisbane and 1/8 in. south of that boundary.
All Overlays	Location of KNBC was inadvertently shown at KQED, though all data was taken at KNBC.
	Location of Quarry was similarly misplaced and is shown in the actual quarry, when in fact, all readings were taken due east of the location shown approximately 1 in. on the full size overlays and 1/4 in. on the reproduced copies.